약학박사학위논문

Design and therapeutic evaluation of heparin based bioconjugate for oral delivery and antiangiogenic therapy

경구전달 및 신생혈관생성 억제 항암효과를 위한 헤파린 유도체의 설계 및 활성 평가

2016년 2월

서울대학교 대학원

약학과 약제과학전공

박 주 호

Abstract

Design and therapeutic evaluation of heparin based bioconjugate for oral delivery and antiangiogenic therapy

Jooho Park
College of Pharmacy
Seoul National University

Bioconjugate techniques have been improved with the growth of the bio-pharmaceutical industry. Highly functional biomaterials were modified by various chemical and biological methods for drug delivery and development. Therapeutic agents including carbohydrate, gene, peptide, protein and drug have been improved as a new pharmaceutical composition which is finally applied to human. Among therapeutic polysaccharides, heparin is the one of the unique biomimetic molecules which has potentials of an effective and safe drug.

Heparin is a highly sulfated and linear polysaccharide which is clinically used as an anticoagulant. However, the low bioavailablity of heparin has restricted wide use of it. Heparin and LMWHs have been the drug of choice for the treatment or the prevention of thromboembolic diseases, in other way, their uses were limited by parenteral injection. To overcome this problem, tetraDOCA was conjugated at the end of heparin via chemical glycation. This conjugation increased the bioavailability of low molecular weight heparin named enoxaparin, and it showed therapeutic effects in DVT and bleeding animal models. In addition, we designed heparin based orally available nanocomplex using heparin, bile acid and protamine. Positively charged protamine could form a stable nanocomplex with heparin and other polysaccharides through electrostatic interactions. The study about oral

delivery using bile acids and heparin basd nanocomplex indicated that the macromolecule could be delivered by interacting with ASBT in the ileum.

In other way, it has been known that heparin and heparin conjugates can inhibit tumor activity by interacting with tumor related to proteins such as VEGF and bFGF. But the use of LMWH for tumor inhibition effect has been limited because heparin is a strong anticoagulant. To expand the clinical use of heparin and heparin derivatives, in this study, LMWH was conjugated with highly functional fragments that have a binding affinity to the heparin-binding site. The chemical conjugate of LMWH and suramin fragments showed tumor inhibition effect on various experiments including VEGF-mediated HUVEC assay. In addition, orally available heparin fragment-deoxyholic acid conjugates were designed to confirm the size related the effects of heparin. Heparin fragment-deoxycholic acid conjugates were also able to have cancer effects by inhibiting the angiogenic activity of growth factors depending on its molecular size. When we use highly functional heparin conjugates such heparin-suramine or heparin fragment-deoxycholic acid conjugates, PEG-protamine based nanocomplex could be an attractive approach to optimize the therapeutic effect and delivery of heparin conjugates. PEG-protamine could increase the targeting effect of heparin-suramin conjugate with increased anticancer effect. PEG-protamine nanocomplex showed potentials for a novel drug carrier for functional anticancer polysaccharides. Finally, the study about the oral delivery and antiangiogeneic effects of heparin conjugates would open a new prospect in the field of drug development and delivery.

Keywords: Heparin, bile acid, bioconjugate, oral delivery, nanocomplex, antiangiogenesis, drug delivery, protamine
Student number: 2009-21684

Table of Contents

Part B : Development of angiogenesis inhibitor using heparin conjugates

Chapter 4. Antiangiogenic effect of orally available size-controlled heparin fragment and deoxycholic acid conjugates

Lists of Tables

Lists of Figures

in ASBT over-expressed MDCK cells (200×), Scale bar = 50 um (B) Representative confocal image of flourosence (F)-labeled materials in MDCK-ASBT cells was compared to that in the untreated cells (800×). Scale bar = 5 um (C) Cell viability was maintained in the presence of low or high dose of PATDs (n=7).

Figure S.6. Body wight and liver weight gain in high fat diet experiment model (A) The effect of PATD on body weight gain in mice. Male C57BL/6 mice were fed either a normal diet (ND) or a high-fat diet (HFD) for 13 weeks (n=7). For 9 weeks of diet feeding, PATD1 and PATD3 (10 mg/kg/day) were orally administered to mice after being fasted for 4 h (B) Changes in the liver weight. By reducing the weight of the liver, PATD inhibited body weight gain. *p<0.05 vs. the control group (HFD), **p<0.001 vs. the control group (HFD).

Figure S.7. Inhibition of liver fat accumulation by PATD (A) Oil red O staining of the liver in mice that were fed an ND, HFD or HFD with PATDs. PATD treatment significantly reduced fat accumulation in the liver (B) Analyses of oil red O staining with ImageJ software (n=5) *p<0.05 vs. the control group (HFD), **p<0.001 vs. the control group (HFD).

Figure S.8. PK study of PATD3 in rats

Figure S.9. The therapeutic effect of PATD in HFD-fed mice. (A) Plasma Triglyceride (TG) (B) Plasma Total cholesterol (TC) (C) Atherogenic index *p<0.05 vs. the control group (HFD), **p<0.001 vs. the control group (HFD).

Figure S.10. (A) Plasma fasting glucose (B) Oral glucose tolerance test (OGTT) *p<0.05 vs. the control group (HFD), **p<0.001 vs. the control group (HFD).

Abbreviations

AI	Atherosclerotic index
ANOVA	Analysis of variance
aPTT	Activated partial thromboplastin time
Arg	Arginine
ASBT	Apical sodium-dependent bile acid transporter
AT	Antithrombin
AUC	Area under the concentration curve
Avg	Average
bFGF	Basic fibroblast growth factor
BID	Twice a day
CAT	Cancer associated thrombosis
CCK	Cell counting kit
CD	Cluster of differentiation
CHARMM	Chemistry at HARvard Molecular Mechanics
CL	Clearance
Co	Coperation
Cy	Cyanine
$\mathbf{C_{max}}$	Maximum concentration
DCC	N,N'-Dicyclohexylcarbodiimide
DLS	Dynamic Light Scattering
DMEM	Dulbecco's Modified Eagle's medium
DMF	Dimethyl formamide
DMSO	Dimethyl sulfoxide
DOCA	Deoxycholic acid
DOPA	3,4-dihydroxyphenylalanine
DP	Depolymerization
DVT	Deep vein thrombosis
DW	Distilled water

EBM	Endothelial basal medium
ECM	Extracellular matrix
EDAC	1-Ethyl-3-(3-imethylaminopropyl)carbodiimide
EnoxaTD	Enoxaparin-tetraDOCA conjugate
EPR	Enhanced permeability and retention
Et-DOCA	N-deoxycholylethylenediamine
EU	European union
FBS	Fetal bovine serum
FDA	Food and drug administration
FGF	Fibroblast growth factor
FGFR	Fibroblast growth factor receptor
FITC	Fluorescein isothiocyanate
FXa	Factor Xa
GI tract	Gastrointestinal tract
GPC	Gel permeation chromatography
HBD	Heparin-binding domain
HBSS	Hank's balanced salt solution
Hep	Heparin
HF	Heparin fragment
HFD	Heparin fragment-deoxycholic acid conjugate
HFD	High fat diet
HIT	Heparin-induced thrombocytopenia
HS	Heparan sulfate
HUVEC	Human Umbilical Vein Endothelial Cell
H&E	Hematoxylin and eosin
INR	International normalized ratio
I.V.	Intravenous
Kd	Equilibrium dissociation constant
LDL	Low density cholesterol
LMWH	Low molecular weight heparin

LHD	LMWH-deoxycholic acid conjugate
LHsura	LMWH-suramin fragment conjugate
Lys	Lysine
LSPP	LHsura/PEG-protamine nanocomplex
mAb	Monoclonal antibody
MALDI	Matrix assisted laser desorption/ionization
MC	Methylene chloride
MD	Molecular dynamics
MDCK	Madin-Darby canine kidney
MeOH	Methanol
MRT	Mean residence time
MS	Mass chromatography
MVD	Macrovascular density
MW	Molcuolar weight
MWCO	Molecular weight cut-off
$NaNO_2$	Sodium nitrite
NC	Nanocomplex
ND	Normal diet
NEAA	Nonessential amino acid
NHS	N-hydroxysuccinimide
NMR	Nuclear magnetic resonance
OD	Optical density
OGTT	Oral glucose tolerance test
PATD	Polyacrylic acid-tetraDOCA conjugate
PBS	Phosphate buffer
PCNA	Proliferating cell nuclear antigen
PDB	Protein data bank
PDGF	Platelet derived growth factor
PE	Pulmonary embolism
PEG	Polyethylene glycol

PT	Prothrombin time
RU	Response unit
SCC	Squamous cell carcinoma
SD	Standard deviation
SD rat	Sprague Dawley rat
SE	Standard error
SEM	Scanning electron microscope
SPR	Surface plasmon resonance
SVA	Succinimidyl valerate
TC	Total cholesterol
TCA	Taurocholic acid
TCI	Tokyo chemical industry
TD	TetraDOCA
TEM	Transmission electron microscopy
TG	Triglyceride
TOF	Time-of-flight
TT	Thrombin time
$t_{½}$	Half-life
t_{max}	Time point of maximum concentration
UFH	Unfractionated heparin
ULMWH	Ultra-low molecular weight heparin
US	United state
UV/Vis	Ultraviolet–visible
VEGF	Vascular endothelial growth factor
VKA	Vitamin K antagonist
VLMWH	Very low molecular weight heparin
VTE	Venous thromboembolism

Chapter:1

Introduction

1.1. Oral delivery of heparin and macromolecule

1.1.1. Introduction of heparin

Anticoagulants including heparin have been widely used to reduce the blood clotting preventing various diseases such as deep vein thrombosis (DVT), pulmonary embolism (PE), myocardial infarction, and ischemic stroke [1, 2]. Unpredictable changes of the blood flow in the patient body could result in the pathological event of thrombosis [3]. A patient with a high risk of coagulation requires continuous anticoagulant treatment to inhibit unwanted clot formation. It is necessary to choose the proper medication for patients considering risks and benefits because unexpected clotting leads to lethal disease. Heparin is one of the most effective anticoagulants in the world.

Heparin is a linear heterogeneous mixture of polysaccharide chains, ranging in molecular weight from about 5 to 25 kDa [4]. Because of heparin's highly functional and unique characteristics, it can be recognized by a variety of proteins, such as antithrombin, growth factors, and chemokines; the main target of heparin is antithrombin [5]. The problem of unfractionated heparin is that its size and sequence are not optimized to regulate the blood coagulation cascade. According to the molecular interaction between heparin and antithrombin, a specific pentasaccharide distributed along the heparin chains is necessary to activate antithrombin [6, 7]. Considering that, antithrombin-specific heparin and heparin derivatives have been developed during the past decades.

In order to decrease the risk of clotting in patients, heparin and warfarin have been in clinical use for decades. Warfarin is an orally administered anticoagulant mediating several vitamin K-dependent coagulation factors [8, 9]. Warfarin does not antagonize the action of vitamin K, however, it has been known as a vitamin K Antagonist (VKA) because it antagonizes vitamin K recycling [10].

Although warfarin can be administered orally, it has several problems, such as severe food effects, various drug-to-drug interactions, a narrow therapeutic window, and the necessity of frequent coagulation monitoring, hence complicating the safe use of it [3, 11]. On the other hand, heparin is a relatively safe drug, which is a negatively charged glycosaminoglycan that is extracted from animal sources [12-14]. Unfractionated heparin (UFH) and low molecular weight heparin (LMWH) have shown clinically effective results with low toxicity. In recent years, smaller heparins, such as ultra-low molecular weight heparin (ULMWH), are preferred because of a longer biological half-life and its selective antagonistic action toward the Xa coagulation factor (**Figure 1.1**) [15].

The limitations of clinically available anticoagulants have led to the development of new drugs and drug delivery systems. The ideal anticoagulant should be able to be administrated safely by an oral route. The oral delivery of anticoagulants is important in patients because the efficacy of anticoagulant agent is for the prevention and prophylaxis of blood coagulation [16]. Continuous daily dosing of anticoagulant is necessary for most patients with a high risk of clotting. Clinical demand for a safe and orally available drug has led to the development of an advanced delivery system and new anticoagulant agents.

Novel oral anticoagulants (NOACs) became available as alternatives to heparin and warfarin, thereby preventing venous thromboembolism and strokes in atrial fibrillation (**Figure 1.2**) [17, 18]. NOACs are orally available and have overcome several well-documented disadvantages of previous drugs. The three most commonly prescribed NOACs (i.e., rivaroxaban, apixaban, and dabigatran) have provided some benefits, such as predictable effects, fewer drug interactions, and no dietary restrictions compared with warfarin. Nevertheless, new anticoagulants still have unsolved clinical problems including the lack of a reversal agent and the risk of major bleeding. Even though NOACs are clinically available, there is necessary for orally available safe and effective heparins.

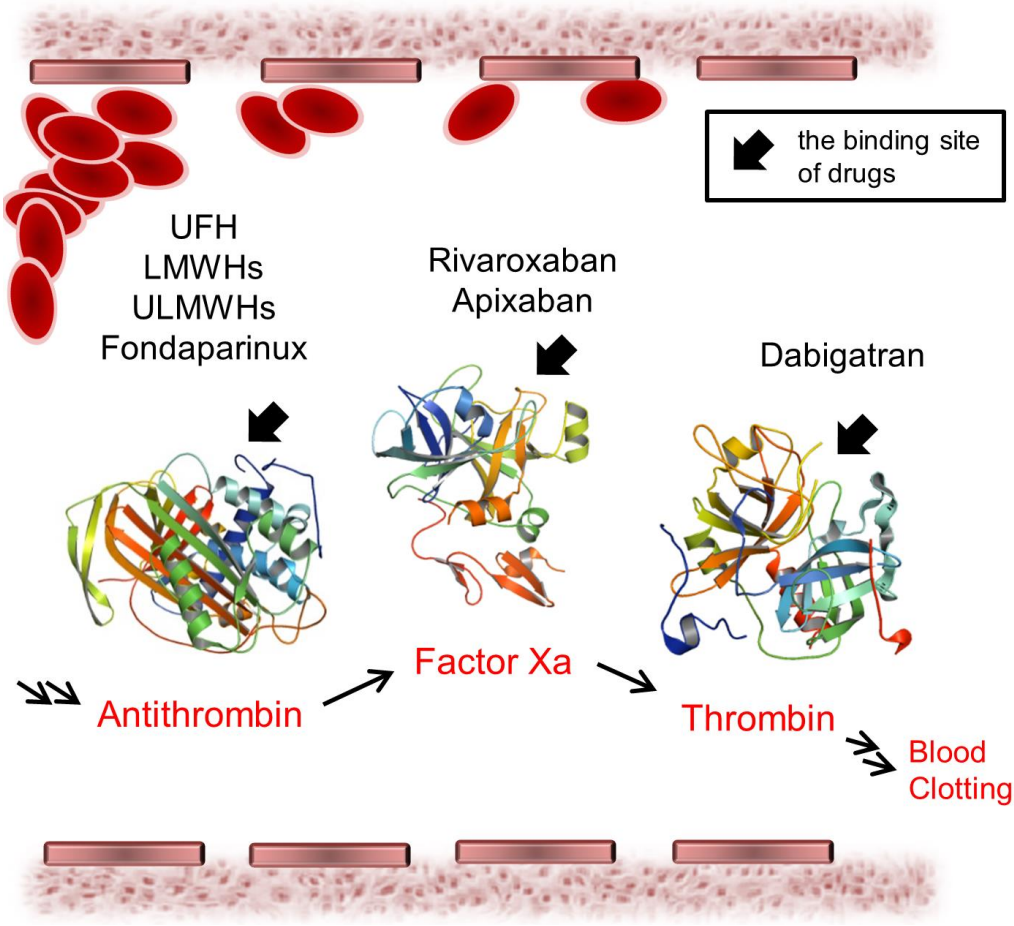

Figure 1.1. Anticoagulants and their targets in regulation of blood coagulation (PDB code: 1AZX, 1KTS and 2W26)

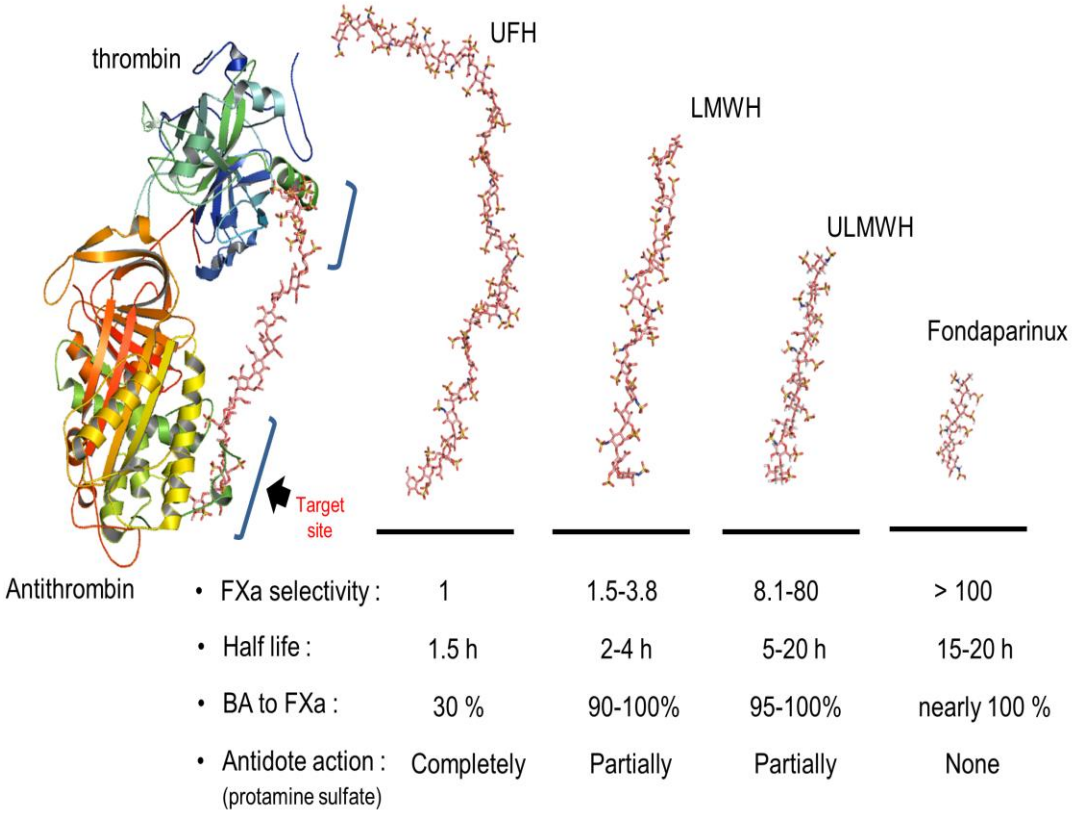

Figure 1.2. Advanced heparins and fondaparinux. The molecular size of heparin has been smaller by considering the size of the target site in antithrombin. Small heparins and fondaparinux show better pharmacological properties (PDB code: 3IRI, 3IRL and 1TB6).

1.1.2. Various delivery methods for heparin

In order to delivery anticoagulants in non-invasive ways, various parental delivery techniques have been studied (**Figure 1.3**). The administration route of LMWHs, including ULMWHs and fondaparinux is the subcutaneous route, however, that of UFH is usually bolus or intravenous infusion. Several research groups have been trying to find alternative and non-invasive routes, such as nasal, transdermal or pulmonary routes for the delivery of heparins [19]. Among them, the delivery of LMWHs via the pulmonary route has shown promising and effective results. Over the past decade, the studies on the pulmonary delivery of heparin showed prolonged effects and increased bioavailability [20]. Recently, PLGA- and PEG-based copolymers, as carriers for pulmonary delivery of LMWH (avg. M.W. 4.5 kDa), showed some potential as effective carriers for the LMWH delivery with a long half-life time (18.6 h) [21]. However, in the case of UFH, the inhaled heparin had no detectable systemic anticoagulant effects for dogs in a recent study [22]. Another research group delivered heparin via the pulmonary route using chitosan and glycol chitosan nanoparticles, but, an unknown LMWH (avg. M.W. 18 kDa) and aPTT (usually not available to LMWH) method was used [23]. A pulmonary delivery of enoxaparin, using chitosan graft glyceryl monooleate (CS–GO), was also studied by aPTT *in vivo* and recently reported [24]. Except for those materials, pegylated liposomes with ardeparin and dendrimeric micelles using polyamidoamine (PAMAM) with enoxaparin, were evaluated in previous research for the pulmonary delivery of anticoagulants [25-27].

The nasal or transdermal route was also studied for the delivery of heparins. The nasal administration of enoxaparin, dalteparin, and tinzaparin with cyclodextrin formulation showed enhanced systemic absorption in rats [28]. However, after that study, there was no significant further research for the last decade. On the other hand, the transdermal delivery of heparin has been improved with different formulations. LMWH needs hydrophobic formulations, like using liposome, because LMWH itself is rarely absorbed onto the skin. It was reported that an LMWH (avg. M.W. 7 kDa), formulated with flexible liposomes, could show a systemic effect via the transdermal route [29]. Moreover, a recent study, about the

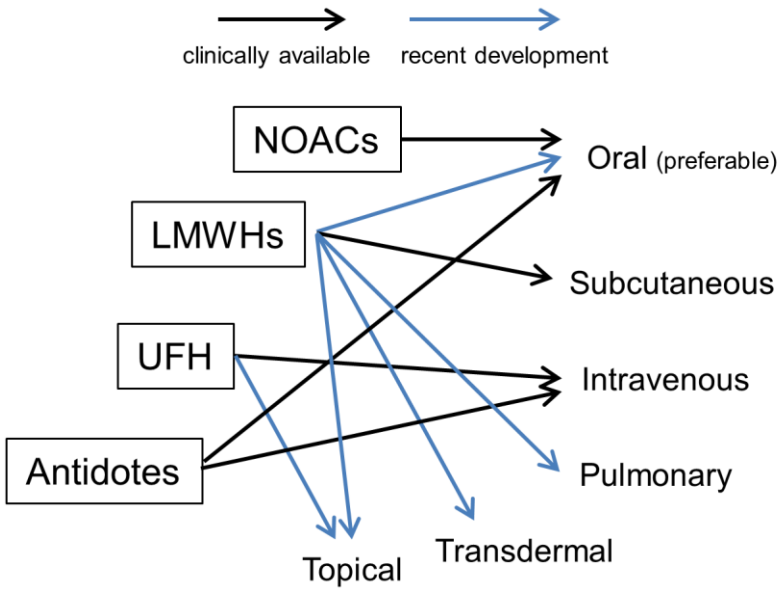

Figure 1.3. Current studied routes for administration of anticoagualnts

influence of chemical and structural features of the LMWH on skin penetration, showed that enoxaparin and bemiparin would be suitable candidates for a transdermal delivery [30]. However, the low bioavailability by the transdermal route still needs to be improved, so the studies on parenteral delivery will be continued.

Anticoagulants mainly inhibit the clotting of blood and the formation of fibrin clots in specific areas beyond its systemic therapeutic effects. The systemic effect of anticoagulants includes INR (international normalized ratio), aPTT, anti-factor Xa activity, PT (prothrombin time), and bleeding time, but locally delivered anticoagulants usually do not change the values all the time. Moreover, their systemic effects could be complicated by interactions with the biological environment. In particular, heparin and LMWH are able to inhibit blood clotting, and they affect wound healing, inflammation, complement activation, and cytokine signals [4].

The transdermal administration of anticoagulants could provide local effects across intact skin. Recently, the formulation of UFH was optimized with enhancers, such as oleic acid and isopropyl myristate as a heparin patch [31]. In the case of enoxaparin, the topical delivery of it with lipid carriers prevents the occurrence of thrombosis at local sites [32]. The transdermal delivery of nadroparin was also enhanced with laser-engineered dissolving microneedle (DMN) arrays and copolymers (PMVE/MA). Moreover, various LMWHs had been prepared by mixing polycationic polymer (Eudragit® RS) as a hydrogel for sustained release [33, 34]. In conclusion, several research groups have designed and characterized drug delivery systems for anticoagulants *in vitro*; and henceforth, the systemic or local effects of them will be further studied *in vivo*.

Among anticoagulants, heparin has been uniquely immobilized on vascular grafts or others to prevent thrombus formation. In clinical studies, heparin-treated polytetrafluoroethylene (PTFE) graft (Propaten®) was implanted in patients; however, it seems need to be improved [35, 36]. The recent results suggest that the immobilization with a reoriented unfractionated heparin derivative or heparin multilayer could optimize its biocompatibility of the decellularized aorta [37, 38]. In addition, beyond its use on the synthetic vascular grafts, heparin can be

immobilized on cell surfaces to avoid blood coagulation and immune reactions. The PEG-conjugated UFH layer on transplanted islets showed an inhibition effect in an allograft model [39]. Moreover, the heparin and 3,4-dihydorxy-L-phenylalanine (DOPA) conjugate improved the survival time of the intrahepatic islet in a xenograft model [40]. Considering the biological functions of heparin, the coating technique with heparin is promising and useful for various biomaterials.

The development of an antidote is very important in the study of anticoagulants, compared with those of other drugs. The use of an anticoagulant is potentially associated with the risk of major or minor bleeding in patients. A major bleeding event during anticoagulant treatment is highly fatal, and it is linked to subsequent death. Considering that fact, patients with a high risk of bleeding should be carefully treated for anticoagulant treatment [41]. Over the last decade, among anticoagulants, heparin and LMWH has an effective antidote: protamine sulfate. The US FDA-approved protamine is quickly able to neutralize the action of heparins in the human body. However, recently developed NOACs do not possess any clinically effective reversal agents when life-threatening bleeding happens [42, 43]. Thus, development of effective antidotes should be considered in association with studies about new anticoagulants.

In general, the recent approaches in anticoagulant delivery could be classified into two categories. One is to improve the delivery and action of parenteral drugs; the other is to develop NOACs and their antidotes. These strategies have attempted to overcome current clinical problems related to the use of anticoagulants. Most anticoagulant agents in the market have advantages and disadvantages, and recent advances in anticoagulant delivery have been trying to make them ideal drugs. In particular, the bleeding and antidote problems of NOACs and limited delivery of heparins need to be solved.

A recent advance in anticoagulant research is on development of new antidotes. For decades, protamine sulfate has been effective only against heparins; in addition, vitamin K indirectly neutralizes the slow action of warfarin. In the case of new oral agents, activated charcoal is only available within approximately 1 h–3 h after administration of NOACs; it cannot reverse the action of anticoagulants.

Recently, three new reversal agents have been developed for NOACs (**Figure 1.4**). First, PER977 (ciraparantag; aripazine; di-arginine piperazine) is a small cationic synthetic molecule that is known to counteract the action of heparins, fondaparinux and all NOACs [44-47]. Second, andexanet alfa is a recombinant protein that is similar to the human coagulation factor Xa, and it could potentially reverse the anti-factor Xa activity in the human body [48]. Third, there is a specific antibody (idarucizumab; aDabi-Fab) to dabigatran in clinical development in order to reverse the anticoagulant effects of dabigatran [49, 50].

Study on anticoagulants will be with the development of antidotes. In the event of bleeding in patients, physicians should determine an appropriate antidote to be administered. In the case of NOACs, in a recent clinical study (n=90), an injected high dose of idarucizumab reversed the anticoagulant effect of dabigatran within minutes [51]. The PER977 has recently proved its safety in animals and dosage has been set for human study, and its effect with edoxaban was reported [46, 52]. A phase III trial about andexanet alfa is in process, and recently, a clinical study against apixaban and rivaroxaban is ongoing [53, 54]. However, all of new antidotes need extremely high doses (0.08–4 g/day) for their effects, and the safety of all of them need to be further studied in humans [42, 54]. Furthermore, the unclear targets and unelucidated mechanism of PER977 also need to be studied.

A recent focus about anticoagulants is on how antidotes can control the action of anticoagualnts including heparins. new oral anticoagualnts have been designed for oral delivery, and their efficacy has been valuated as a long-term treatment option. However, the essential antidotes against them are still in development; therefore, it is important to note that there is no clinically available antidote for patients who are treated by them. Peptides, such as idarucizumab and andexanet alfa, could be effective, but there needs to be studies about the reversibility and real efficacy in humans. In the case of PER977, except for the effect of it in high dosage, its safety and mechanism are still unclear.

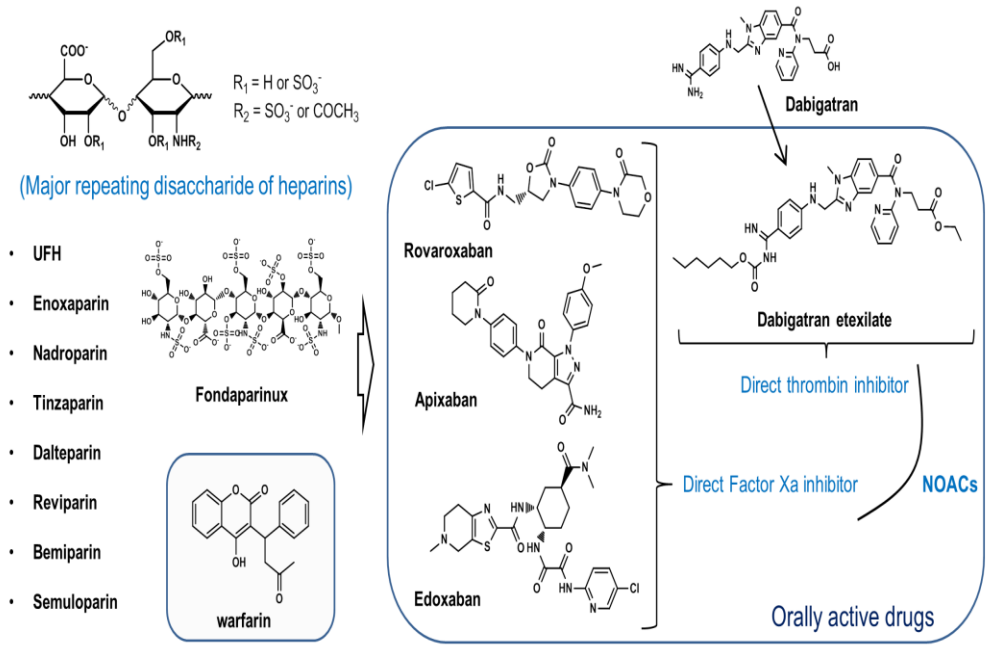

Figure 1.4. There are the molecular structures of anticoagulants and major repeating disaccharide of heparins. Newly developed anticoagulants are orally available.

1.1.3. Oral delivery of heparin

The oral delivery of anticoagulants is the most practical way for continuous daily dosing to patients to prevent unwanted venous thrombosis. Although LMWH, ULMWH, and fondaparinux have shown several advantages over all the other anticoagulants, they have been restricted to be used only in hospitals because of their parenteral injection. Considering the importance of oral delivery, all NOACs were designed to be orally available (**Figure 1.5**). However, considering the safety of heparin and the existence of an antidote, heparins cannot be used interchangeably with other anticoagulants. Oral delivery of heparin is necessary, but the extremely low bioavailability of heparin indicates that it could not be delivered effectively into the bloodstream in an oral form even if they were ULMWHs or fondaparinux. Hydrophilic macromolecules, like heparin, are usually hard to be absorbed in the gastrointestinal (GI) tract without active transport or receptors [55]. In order to increase the oral bioavailability of heparin, various oral delivery methods for heparin have been investigated in different ways.

Heparin with a penetration enhancer was developed for the oral delivery of UFH with clinical trials. About 17 years ago, a clinical trial phase III using sodium N-[8-(2-hydroxybenzoyl) amino] caprylate (SNAC) showed a promising result about orally available heparin [56]. The formulation with SNAC increased the oral uptake of heparin, and prevented thrombosis in experimental models [57, 58]. In a following international phase III trial (n= 2264), DVT or PE occurrence (13.8%) and the incidence of major/minor bleeding (0.7%/2.0%) from oral heparin (30 days, P.O.) were not much different from those (12.7% and 0.4%/1.5 %, respectively) of enoxaparin (10 days, S.C.) [59, 60]. However, it failed to show superior efficacy and was not approved by the US FDA; the reasons could have been an inappropriate enhancer, poor liquid formulation (according to the announcement of the company), and short-term indication (for a month following hip replacement surgery) for oral administration. Since then, a drug delivery system with formulation has been improved, and there currently are long-term indications that need safe oral heparin treatment, such as atrial fibrillation and cancer-associated thrombosis. Several penetration enhancers and chemical conjugation technique have been developed for

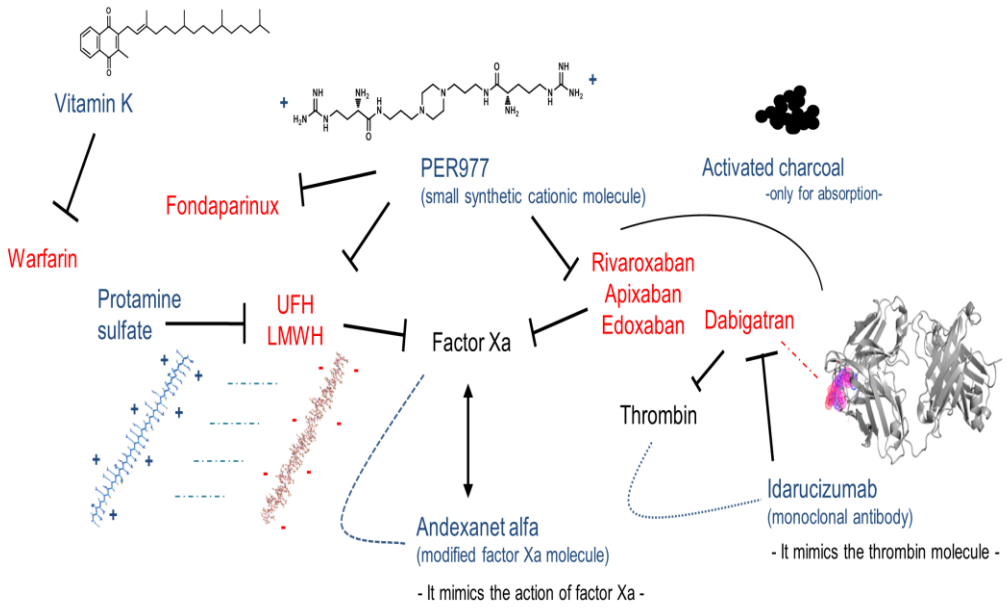

Figure 1.5. Recent advance in the development of antidotes. Cationic molecules such as protamine sulfate and PER 977 and recombinant proteins that are similar to the human coagulation factor Xa or thrombin molecule could be used (PDB code: 4JN2 and 2AWR).

the oral delivery of heparin and LMWHs during the last decade (**Table 1.1**). A polymeric or nanoparticle delivery system could be designed to facilitate the oral uptake of anionic heparins in the GI tract. It is known that a high amount of negative charges of heparins constitute a problem for the diffusion into the intestinal epithelium [81]. To pass the intestinal epithelium via the paracellular or transcellular pathways, it is necessary to use a positive chitosan or lipophilic complex to neutralize the charge and enhance its absorption [82, 83]. Chitosan, soluble chitosan, and polymers with lysine or arginine could make polyelectrolyte complexes with various heparins. Chitosan derivatives, including mono-*N*-carboxymethyl chitosan (MCC) and SNOCC, could increase the intestinal absorption of LMWHs in animal studies [84, 85]. However, drug delivery, using positively charged chitosan and polymers, is usually limited to transport with a tight junction between intestinal epithelial cells [86]. Various proteins, peptides, and drugs are orally delivered using chitosan derivatives and penetration enhancers for decades; however, their delivery efficacy and tissue damage needed to be improved in order to apply them to patients [87].

In the development of a new delivery system, it is important to have a solid absorption mechanism for drug delivery by the oral route. Bile acids, which are released into the small intestine and recycled in the ileum by the enterohepatic circulation, have been the subject of interest as oral absorption enhancers [88]. They can be actively reabsorbed in the ileum by the apical sodium-dependent bile acid transporter (ASBT) [89, 90]. Because the role of bile acids in the human body is on enhancing oral absorption of food, using bile acids by micelle formation or chemical conjugation could be an interacting approach for oral delivery [91, 92]. In order to deliver LMWH by the oral route, LMWH and deoxycholic acid (DOCA) conjugate (LMWH-DOCA) was synthesized. In several animal experiments, the LMWH-DOCA conjugate showed enhanced absorption beyond its hydrophobic property [93, 94]. Recently, the result of a preliminary safety evaluation of LMWH-DOCA conjugate was published. There were no unexpected toxicities after oral administration of the LMWH-DOCA conjugate to animals in a preclinical study [95].

Table 1.1. Recent advances in oral delivery of anticoagulant drugs.

Year	Type of anticoagulant	Method	Materials	Features in oral delivery technique	Ref.
2014	Nadroparin	Chemical conjugation	Oligomeric bile acid conjugate	Bile acid transporter-targeted high-affinity oligomeric bile acid substrates	[61, 62]
2014	Fondaparinux	Enhancer complex	Cationic squalenyl derivative	Spherical multilamellar nanoparticles using trimethyl ammonium chloride salt	[63]
2014	Enoxaparin	Enhancer complex	Chitosan and HPMCP[a]	pH-sensitive polymer HPMCP and chitosan by ionic cross-linking method	[64]
2014	LMWH(5.3 kDa)	Enhancer complex	Chitosan oligomers	Chitosan dimer, tetramer and hexamer	[65]
2013	Enoxaparin	Enhancer complex	Chitosan-based nanocomplex	Polyelectrolyte complexes (evaluated only by APTT[b])	[66]
2013	LMWHs[c]	Enhancer complex	Coacervate	Polyaminomethacrylate coacervates using polyethylene glycol derivates	[67]
2013	Enoxaparin	Enhancer complex	Alginate and chitosan	Alginate coated chitosan core shell nanoparticles	[68]
2012	LMWH(4.3 kDa)[d]	Enhancer complex	Chitosan nanoconstruct	Using N-trimethyl chitosan (low bioavailability; BA = 0.39 %)	[69]
2011	Fondaparinux	Enhancer complex	Lipid nanocapsule	Cationic surfactants; hexadecyltrimethyl ammonium bromide and stearylamine	[70]
2011	LMWH(4.3 kDa)[d]	Chemical conjugation	Lipid nanoparticle	Encapsulation in phosphatidylcholine stabilized biomimetic solid lipid nanoparticles (SLNs)	[71]
2011	Nadroparin	Chemical conjugation	Deocycholic acid + DMSO	Chemical conjugation with deoxycholic acid and physical complex with DMSO	[72]
2010	Nadroparin	Chemical	Deocycholi	Solid tablet form of heparin	[73,

		conjugation	c acid	with other pharmaceutical excipients	74]
2009	Enoxaparin and bemiparin	Enhancer complex	Granules	Ethylcellulose (Aquacoat® ECD) and polycationic Eudragit®RS30D (ERS)	[75]
2009	LMWH(3kDa) [d]	Enhancer complex	Papain	Papain and bovine serum albumin matrix for formulations by spray-dried	[76]
2007	Reviparin	Enhancer complex	SNOCC[e]	Polyelectrolyte complexes with anionic macromolecules using soluble chitosan	[77]
2007	Ardeparin	Enhancer complex	DCEA[f]	A cationic bile acid derivative was used to be complexed with LMWH.	[78]
2006	Tinzaparin	Enhancer complex	Polymethacrylate	A polyester and a polycationic polymethacrylate by double emulsion method	[79]
2006	Ardeparin	Enhancer complex	Dendron	Two polycationic lipophilic-core carbohydrate-based dendron containing arginine and lysine	[80]

[a] Hydroxypropyl methylcellulose phthalate

[b] Activated partial thromboplastin time (APTT)

[c] Enoxaparin, nadroparin, certoparin, and fondaparinux

[d] Unidentified LMWH

[e] N-sulfonato-N,O-carboxymethylchitosan (SNOCC)

[f] Deoxycholylethylamine (DCEA)

The oral delivery of LMWH using bile acids could be improved by a novel oligomeric bile acid system. A deoxycholic acid (M.W. 392 Da) is a relatively small molecule compared with a LMWH (Avg. M.W. 4000–6000 Da). For successful delivery of LMWH via the oral route, LMWH should be saturated with DOCA physically or by chemical conjugation [96]. However, the anticoagulant (Anti-FXa) activity of LMWH was significantly decreased when LMWH was saturated by DOCA because the antithrombin binding sequence in the heparin structure might have interfered with DOCA [97, 98]. Considering that, recently, oligomeric bile acid conjugates was designed to overcome the activity problems. TetraDOCA, the one of the oligomeric bile acid conjugates with four DOCA molecules, showed a high-affinity to ASBT without decreasing the anticoagulant activity [61]. The LMWH-tetraDOCA conjugate showed therapeutic effects in DVT and CAT animal models, and its absorption mechanism was also recently reported [99]. The bile acid transporter mediated transcellular uptake of LMWH explained how a macromolecule, such as LMWH, can be absorbed in the GI tract [62]. In a further study, the tetraDOCA mediated cellular uptake was increased by a physical complex or enhancer formulation [100].

1.1.4. Oral delivery of heparin based nanocomplex

With biological drug development, the clinical importance of orally available nanoparticle has been increased. In clinical therapy, oral delivery is very important for the continuous administration of drugs. The ultimate goal in therapy is the improvement of the quality of life in patients. Continuous oral dosing is related to the oral delivery of drug for patients. Several research groups have designed orally available macromolecules with promising results. Studies on oral delivery of macromolecule need to be continued. The advanced techniques include oligomeric bile acids, liposomal formulation, modified enhancer, and chitosan formulation could link to the oral delivery of nanoparticles [94, 101]. Most genes and proteins are vulnerable in the GI tract and other biological environments. Development of orally available nanoparticles and carriers could show potentials to solve a lot of current problems related to macromolecule delivery and new drug development [87,

102]. Therapeutic gene and macromolecules are needed to be protected by safe and effective carriers like heparin or protamine. Studies on oral heparin lead to the development of new orally available heparin based nanocarrier. Furthermore, considering the importance of bile acid transporter for enhancing oral absorption, the bile acid moiety also will be needed to be further research for oral delivery.

Oral delivery of macromolecules, nanoparticles and nanocomplexes has been improved with development of drug delivery system. Several nanoparticles were studied for oral delivery with other routes including pulmonary and topical delivery. Based on the importance of oral delivery, more safe and effective delivery systems should be studied and developed. Heparin is a safe FDA-approved polysaccharide and its saccharide chains in its molecular structure could protect against proteolytic degradation by enzymes in the GI tract [103]. The negative charge of heparin is similar to that of genes like DNA or RNA. Its successful delivery may lead the development of orally available gene therapy. To measure its potential, the oral delivery of heparin based nanocarriers need to be studied in this research.

1.2. Heparin and angiogenesis inhibitor

1.2.1. Various heparins

There are several commercially available heparin derivatives which are more effective than UFH on the market. The following are classified as LMWHs (avg. M.W. 4–6 kDa): Enoxaparin (by alkaline depolymerization), dalteparin, nadroparin (by nitrous acid depolymerization), and tinzaparin (by heparinase digestion). Whereas he following are classified as ULMWHs (avg. M.W. 2–4 kDa): semuloparin (by depolymerization with phosphazene base), and bemiparin (by alkaline depolymerization) [104-106]. Recently, synthetic homogeneous LMWH and ULMWH were also prepared by chemoenzymatic methods [107, 108]. In addition, the antithrombin-specific pentasaccharide of heparin has been chemically synthesized as fondaparinux (M.W. 1726 Da) [109]. Small heparins target the anti-

factor Xa activity, rather than anti-factor Ⅱ activity, with better bioavailability, dose-independent clearance, predictable effects, and an improved therapeutic index [110]. They exhibit better pharmacodynamic behavior than UFH, thus, the differences in their pharmacologic profile have led to its clinical acceptance [111, 112]. This improvement consequently makes LMWH the drug of choice for the prophylaxis of venous thromboembolism (VTE) and the best-selling anticoagulant on the market, even though its use is limited to subcutaneous injection in a hospital for the short-term [113, 114].

The advanced targeted delivery of heparins has provided convenience to patients with predictable effects. UFH is usually given two or three times daily to a patient, whereas the LMWHs and ULMWHs are given once a day. LMWHs show a longer biological half-life (2–5 h) with improved target selectivity [115]. Moreover, the half-life of semuloparin can be prolonged to 16–20 h, which is similar to that (17–21 h) of fondaparinux [116, 117]. In the case of the excretion and elimination process, UFH is cleared primarily through cellular metabolism in the liver and renal clearance; however, most LMWHs are primarily cleared via renal clearance. Less metabolized and unchanged derivatives from small heparins in the body provide more predictable effects to patients.

In patients with venous thromboembolism and renal insufficiency, the delivery of anticoagulants should be different. Recently, NOACs showed clinical problems related to renal clearance. NOACs are orally available and exhibit a better pharmacodynamic profile than UFH, however, their eliminations totally depend upon renal clearance. This disadvantage results in unexpected results and accumulation problems in patients with renal failure. In that case, UFH or LMWHs should be preferred over NOACs because it is not completely eliminated by the kidney. Current guidelines suggest that if an LMWH is chosen, anti-Xa monitoring should be considered to check that there is no accumulation [118]. Considering the different levels of renal function, LMWH should be used carefully in patients with renal problems (creatinine clearance levels < 30 mL/min) [119]. Among LMWHs and ULMWHs, tinzaparin and dalteparin are likely to be safe in patients with renal dysfunction and thrombotic complications, with their having less risk of plasma

accumulation.

1.2.2. Heparin and anticancer therapy

Heparins have tried to expand their indications including cancer-associated thrombosis (CAT). Based on the efficacy of LMWHs and ULMWHs in the treatment of thrombosis, some clinical studies have indicated that their optimized therapeutic effect could extend to patients with cancer [120]. Current clinical guidelines recommend prophylaxis, using anticoagulants such as heparin and LMWHs, after cancer surgery at least for a week [121-123]. Moreover, it is important to note that patients receiving chemotherapy with cancer are at a high risk for developing venous thromboembolism [124, 125]. Recently, in clinical studies the LMWH confers a potential therapeutic effect in cancer populations without an increase in severe bleeding events [126-128].

Among LMWHs, tinzaparin has showed a promising result in the prevention of recurrent VTE in cancer patients (n= 200); Enoxaparin also recently showed its high efficacy in patients with pancreatic cancer (VTE, 9.9% -> 1.2%) [129]. Moreover, in the case of ULMWHs, semuloparin decreased the occurrence percentage of VTE in patients with cancer from 3.4% (n=1604) to 1.2% (n=1608) [130]. In addition, the successful delivery of heparins in cancer patient is challenging because a variety of malignant tumors complicate the effect of heparin by secreting heparin binding cytokines, vascular growth factors, and even heparinase [115, 131]. Heparins for thromboprophylaxis in cancer patients need to be further studied in future clinical research.

1.2.3. Antiangiogenic effects of heparins

The antiangiogenic effect of heparin is important in anti-cancer therapy and new drug development. Angiogenesis is a fundamental process with formation of new blood vessels from preexisted blood vessels [132, 133]. There are a lot of growth factors related to antiangiogenic process, moreover, most of them have heparin binding domain (HBD) [134-136]. Chemically modified heparin conjugates have advantages in inhibiting growth factors and diminishing the risk of bleeding

[137].

Low molecular weight heparin (LMWH) and its conjugates have been reported to possess antiangiogenic effect via electrostatic interaction with various angiogenic growth factors such as $VEGF_{165}$ [98, 138] (**Figure 1.6**). However, clinical applications of LMWH for anticancer therapy have been restricted due to its anticoagulant effect and insufficient therapeutic efficacy. To overcome these limitations and enhance the antiangiogenic efficacy, LMWH was conjugated with several biomaterials to increase the binding affinity to the HBD of proteins [138]. The conjugation of biomaterials and heparin has enhanced the antiangiogenic effect of LMWH by increasing the binding affinity to growth factors, while decreasing its anticoagulant activity [139-141]. The chemical conjugate of LMWH showed a substantial inhibitory effect on growth factor-mediated cell proliferation, migration, and tube formation of endothelial cells in many studies [98, 139].

1.3. Rationale of the research

Bioconjugate technique is important in drug development and biopharmaceutics. It has made possible the development of several new biomaterials and drugs. Over the last a few dacades, there has been great improvement in understanding of the biological process. However, there are a lot of disease which could not be controlled clinically by drugs and natural materials. Beyond this understanding, it is necessary to develop technological breakthrough to overcome current clinical problems. Bioconjugation usually means the attachment of two biofunctional molecules, and the biofunctional molecules involve polysaccharides, peptide, protein, polymer, gene, flurosence, drug, functional group, nanoparticle and nanocomplex. The conjugation itself with these biomaterials could increase the novelty of them. In addition, the conjugate technique is able to overcome the major drawback of biomaterials related to the use of heparins.

Based on the understanding of unmet clinical needs for ideal delivery route for heparin and its other therapeutic effects, various attempts were made to develop new techniques with heparin. In particular, because the administration of heparin via

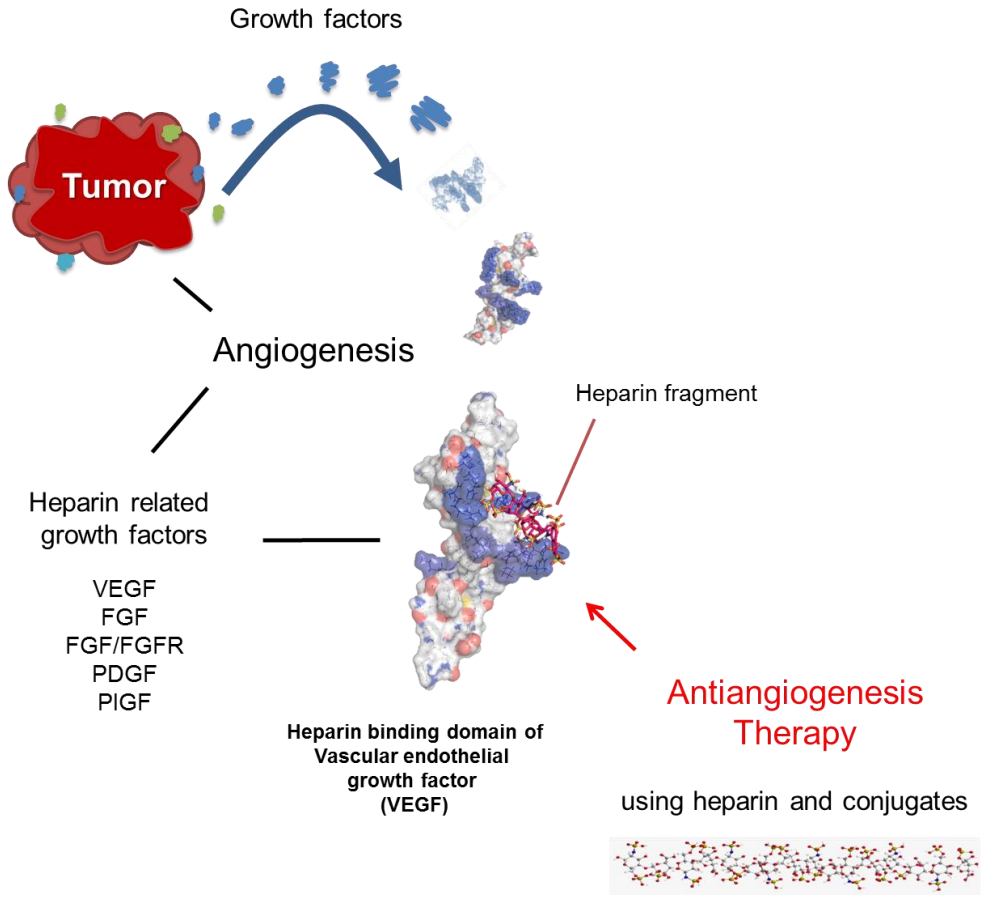

Figure 1.6. Tumor related angiogenesis process and growth factors. Growth factors including VEGF usually have heparin binding domain in their molecular structure. (PDB code: 2VGH)

the oral route is convenient, oral delivery technology with heparin has been developed for long-term treatment. Although there are advances in anticoagulants development, the study on development and delivery of heparin is still important for drug delivery system. Advanced enhancers and chemical conjugation technique have been developed for the delivery of LMWHs. Pulmonary and transdermal delivery of LMWH with formulation have also shown an expeditious action with low toxicity. Of course, heparin and low molecular weight heparins have shown remarkable therapeutic effect and safety clinically for decades. However, the parenteral administration of heparin limits the wide clinical use of them. Oral delivery is the most well-acceptable route for patient and in drug delivery system. So, oral delivery of heparin is clinically necessary, but, the extremely low bioavailability of heparin indicates that it could not be delivered effectively into the bloodstream. First oral heparin was developed a decade ago, but, it was failed by several reasons in clinical trials. However, in this study, we designed and developed an oral end-specific heparin conjugate which is a clear drug candidate.

Current bioconjugate technology has improved the methods for oral delivery of macromolecule. New oral delivery for heparin was tried with tetraDOCA and oral formulation in previous study. Several heparin conjugates have been designed for oral delivery using bile acids, however, without end-specific conjugation, the conjugatation site in heparin could not be confirmed. TetraDOCA, the one of oligomeric bile acid conjugates, was used to for oral absorption. In this study we will introduce end-specific conjugation using heparin and how tetraDOCA conjugate interact with bile acid transporters in the ileum. Using this mechanism we also designed orally available heparin based nanocomplex. Because heparin based nanocarrier are useful in drug delivery system, heparin based oral nanocomplex has potential to be an effective drug, peptide or gene carrier. Oral nanocomplex based heparin and protamine could be a novel oral nanocomplex based delivery system.

In other way, developed bioconjugate technique has improved the therapeutic anticancer effect of heparin by chemical conjugation. Deoxycholic acid conjugation into heparin has several advantages including oral delivery and enhanced tumor inhibition effect, however, the introduction of the hydrophobic bile

acid could cause disruption of the hydrogen bonding interaction and potential toxicities. Depending on the method and material of conjugation, the therapeutic potential of heparin conjugates can be optimized. In this study, there will be discussion of chemical modification with heparin and their pharmaceutical features and its therapeutic effect. Studies on oral and target delivery of macromolecule lead to develop an advanced drug delivery system for nanocomplexes. We also developed heparin and protamine based complexes for EPR effect for anticancer therapy.

Bioconjugate technology can be extended to approach to optimize the physical and chemical properties of biomaterials, and make them useful materials as therapeutic agents. Among polysaccharides, in the case of heparin, there are advantages and disadvantages as an anticoagulant or anti-cancer agent. LMWHs are unique, and their safety and efficacy are distinguished from others. Several studies have shown the anti-angiogenic effect of heparin and its conjugates in relation to growth factor inhibition. For drug development and inhibition of growth factors using heparin conjugates, the function of heparin may be crucial considering the heparin binding site of growth factors. Targeting the heparin binding site in growth factors will provide a promising strategy for drug development and delivery. For this reason we developed several heparin conjugates for oral or parenteral antiangiogenic therapy. Deoxychoic acid or suramine fragment conjugation could be effective methods to develop heparin conjugates as anticancer agents. We also used PEG-protamine as drug carriers for passive tumor targeting effect. Protamine conjugate was also able to formulate with polysaccharides and generate stable nanocomplexes.

Finally, this study consisted of two different parts related to the function of heparin (**Figure 1.7**). First, there is a discussion about oral delivery of heparin using end-specific conjugation and heparin-based oral nanocomplex. Second, antiangiogenic effects of several heparin conjugates and nanocomplex were evaluated. Therefore, the therapeutic evaluation of heparin based bioconjugate and nanocomplex for oral delivery and antiangiogenic therapy would be discussed.

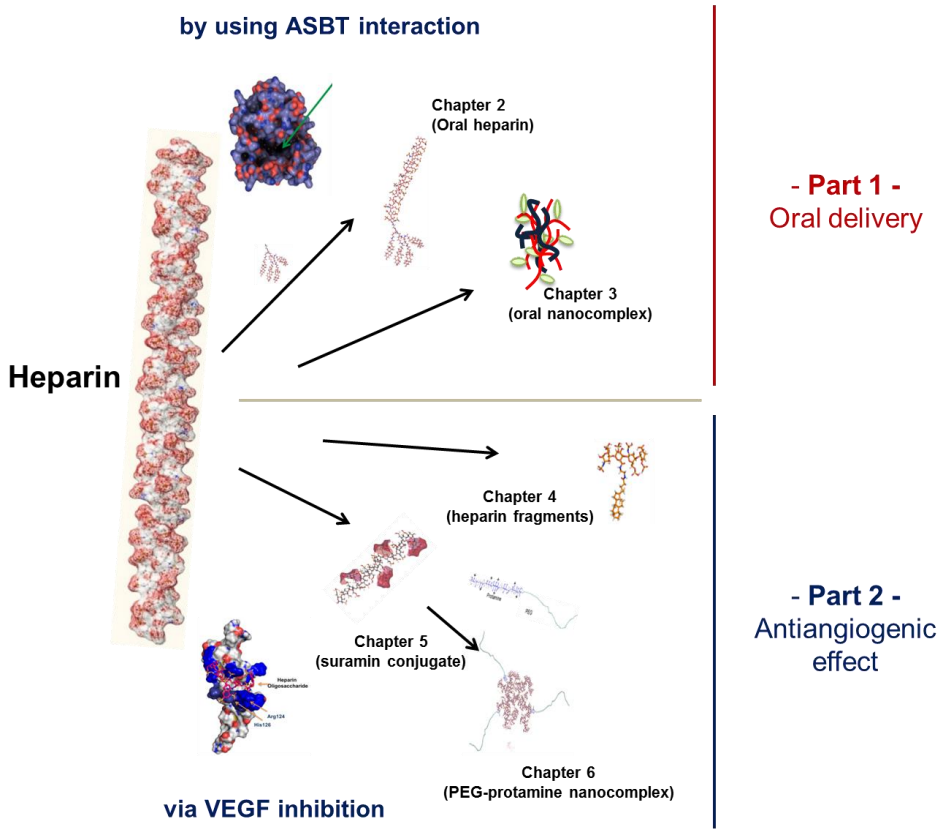

Figure 1.7. Scheme of the study on design and therapeutic evaluation of heparin based bioconjugate and nanocomplex for oral delivery and antiangiogenic therapy

This study was conducted with advanced bioconjugate technology to solve the current problems in heparin based drug development and drug delivery.

References

[1] Research committee of the British Thoracic Society, Optimum duration of anticoagulation for deep-vein thrombosis and pulmonary embolism, Lancet. 1992;340:873-6.

[2] Sandercock PA, Counsell C, Kane EJ. Anticoagulants for acute ischaemic stroke. Cochrane Database Syst Rev. 2015;3:CD000024.

[3] Hirsh J. Current anticoagulant therapy--unmet clinical needs. Thrombosis research. 2003;109 Suppl 1:S1-8.

[4] Rabenstein DL. Heparin and heparan sulfate: structure and function. Nat Prod Rep. 2002;19:312-31.

[5] Capila I, Linhardt RJ. Heparin-protein interactions. Angewandte Chemie. 2002;41:391-412.

[6] Desai UR, Petitou M, Bjork I, Olson ST. Mechanism of heparin activation of antithrombin. Role of individual residues of the pentasaccharide activating sequence in the recognition of native and activated states of antithrombin. The Journal of biological chemistry. 1998;273:7478-87.

[7] Choay J, Petitou M, Lormeau JC, Sinay P, Casu B, Gatti G. Structure-activity relationship in heparin: a synthetic pentasaccharide with high affinity for antithrombin III and eliciting high anti-factor Xa activity. Biochemical and biophysical research communications. 1983;116:492-9.

[8] Hirsh J. Oral anticoagulant drugs. The New England journal of medicine. 1991;324:1865-75.

[9] Hermodson MA, Suttie JW, Link KP. Warfarin metabolism and vitamin K requirement in the warfarin-resistant rat. Am J Physiol. 1969;217:1316-9.

[10] Holford NH. Clinical pharmacokinetics and pharmacodynamics of warfarin.

Understanding the dose-effect relationship. Clin Pharmacokinet. 1986;11:483-504.
[11] Juurlink DN. Drug interactions with warfarin: what clinicians need to know. Can Med Assoc J. 2007;177:369-71.
[12] Horlocker TT, Heit JA. Low molecular weight heparin: biochemistry, pharmacology, perioperative prophylaxis regimens, and guidelines for regional anesthetic management. Anesth Analg. 1997;85:874-85.
[13] Imberty A, Lortat-Jacob H, Perez S. Structural view of glycosaminoglycan-protein interactions. Carbohydrate research. 2007;342:430-9.
[14] Koch MO, Jr JS. Low molecular weight heparin and radical prostatectomy: a prospective analysis of safety and side effects. Prostate Cancer Prostatic Dis. 1997;1:101-4.
[15] Ciccone MM, Cortese F, Corbo F, Corrales NE, Al-Momen AK, Silva A, et al. Bemiparin, an effective and safe low molecular weight heparin: A review. Vasc Pharmacol. 2014;62:32-7.
[16] Furie B, Furie BC. Molecular and cellular biology of blood coagulation. The New England journal of medicine. 1992;326:800-6.
[17] Tran H, Joseph J, Young L, McRae S, Curnow J, Nandurkar H, et al. New oral anticoagulants: a practical guide on prescription, laboratory testing and peri-procedural/bleeding management. Australasian Society of Thrombosis and Haemostasis. Intern Med J. 2014;44:525-36.
[18] Camm AJ, Lip GY, De Caterina R, Savelieva I, Atar D, Hohnloser SH, et al. 2012 focused update of the ESC Guidelines for the management of atrial fibrillation: an update of the 2010 ESC Guidelines for the management of atrial fibrillation. Developed with the special contribution of the European Heart Rhythm Association. Eur Heart J. 2012;33:2719-47.
[19] Ibrahim SS, Osman R, Awad GA, Mortada ND, Geneidy AS. Low molecular weight heparins for current and future uses: approaches for micro- and nano-particulate delivery. Drug Deliv. 2015:1-7.
[20] Qi Y, Zhao G, Liu D, Shriver Z, Sundaram M, Sengupta S, et al. Delivery of therapeutic levels of heparin and low-molecular-weight heparin through a pulmonary route. Proceedings of the National Academy of Sciences of the United

States of America. 2004;101:9867-72.
[21] Patel B, Gupta V, Ahsan F. PEG-PLGA based large porous particles for pulmonary delivery of a highly soluble drug, low molecular weight heparin. Journal of controlled release : official journal of the Controlled Release Society. 2012;162:310-20.
[22] Manion JS, Thomason JM, Langston VC, Claude AK, Brooks MB, Mackin AJ, et al. Anticoagulant effects of inhaled unfractionated heparin in the dog as determined by partial thromboplastin time and factor Xa activity. Journal of Veterinary Emergency and Critical Care. 2015.
[23] Trapani A, Di Gioia S, Ditaranto N, Cioffi N, Goycoolea FM, Carbone A, et al. Systemic heparin delivery by the pulmonary route using chitosan and glycol chitosan nanoparticles. Int J Pharmaceut. 2013;447:115-23.
[24] Wang L, Li L, Sun Y, Ding J, Li J, Duan X, et al. In vitro and in vivo evaluation of chitosan graft glyceryl monooleate as peroral delivery carrier of enoxaparin. Int J Pharm. 2014;471:391-9.
[25] Bai SH, Thomas C, Ahsan F. Dendrimers as a carrier for pulmonary delivery of enoxaparin, a low-molecular weight heparin. J Pharm Sci-Us. 2007;96:2090-106.
[26] Bai SH, Ahsan F. Synthesis and Evaluation of Pegylated Dendrimeric Nanocarrier for Pulmonary Delivery of Low Molecular Weight Heparin. Pharmaceutical research. 2009;26:539-48.
[27] Bai S, Ahsan F. Inhalable liposomes of low molecular weight heparin for the treatment of venous thromboembolism. J Pharm Sci. 2010;99:4554-64.
[28] Yang T, Hussain A, Paulson J, Abbruscato TJ, Ahsan F. Cyclodextrins in nasal delivery of low-molecular-weight heparins: in vivo and in vitro studies. Pharmaceutical research. 2004;21:1127-36.
[29] Song YK, Hyun SY, Kim HT, Kim CK, Oh JM. Transdermal delivery of low molecular weight heparin loaded in flexible liposomes with bioavailability enhancement: comparison with ethosomes. J Microencapsul. 2011;28:151-8.
[30] Franze S, Gennari CG, Minghetti P, Cilurzo F. Influence of chemical and structural features of low molecular weight heparins (LMWHs) on skin penetration. Int J Pharm. 2015;481:79-83.

[31] Patel RP, Gaiakwad DR, Patel NA. Formulation, optimization, and evaluation of a transdermal patch of heparin sodium. Drug Discov Ther. 2014;8:185-93.
[32] Jain A, Mehra NK, Nahar M, Jain NK. Topical delivery of enoxaparin using nanostructured lipid carrier. J Microencapsul. 2013;30:709-15.
[33] Haroun AA, El Nahrawy AM, Maincent P. Enoxaparin-immobilized poly(epsilon-caprolactone)-based nanogels for sustained drug delivery systems. Pure Appl Chem. 2014;86:691-700.
[34] Loira-Pastoriza C, Sapin-Minet A, Diab R, Grossiord JL, Maincent P. Low molecular weight heparin gels, based on nanoparticles, for topical delivery. Int J Pharm. 2012;426:256-62.
[35] Shemesh D, Goldin I, Hijazi J, Zaghal I, Berelowitz D, Verstandig A, et al. A prospective randomized study of heparin-bonded graft (Propaten) versus standard graft in prosthetic arteriovenous access. J Vasc Surg. 2015;62:115-22.
[36] Dorigo W, Pulli R, Castelli P, Dorrucci V, Ferilli F, De Blasis G, et al. A multicenter comparison between autologous saphenous vein and heparin-bonded expanded polytetrafluoroethylene (ePTFE) graft in the treatment of critical limb ischemia in diabetics. J Vasc Surg. 2011;54:1332-8.
[37] Dimitrievska S, Cai C, Weyers A, Balestrini JL, Lin T, Sundaram S, et al. Click-coated, heparinized, decellularized vascular grafts. Acta Biomater. 2015;13:177-87.
[38] Zhou J, Ye X, Wang Z, Liu J, Zhang B, Qiu J, et al. Development of decellularized aortic valvular conduit coated by heparin-SDF-1alpha multilayer. Ann Thorac Surg. 2015;99:612-8.
[39] Im BH, Jeong JH, Haque MR, Lee DY, Ahn CH, Kim JE, et al. The effects of 8-arm-PEG-catechol/heparin shielding system and immunosuppressive drug, FK506 on the survival of intraportally allotransplanted islets. Biomaterials. 2013;34:2098-106.
[40] Jung YS, Jeong JH, Yook S, Im BH, Seo J, Hong SW, et al. Surface modification of pancreatic islets using heparin-DOPA conjugate and anti-CD154 mAb for the prolonged survival of intrahepatic transplanted islets in a xenograft model. Biomaterials. 2012;33:295-303.

[41] Fitzmaurice DA, Blann AD, Lip GY. Bleeding risks of antithrombotic therapy. BMJ. 2002;325:828-31.

[42] Treschan TA, Beiderlinden M. Antidotes for anticoagulants: a long way to go. Lancet. 2015.

[43] Sarich TC, Seltzer JH, Berkowitz SD, Costin J, Curnutte JT, Gibson CM, et al. Novel oral anticoagulants and reversal agents: Considerations for clinical development. Am Heart J. 2015;169:751-7.

[44] Cully M. Reversing anticoagulants. Nature Reviews Drug Discovery. 2015;14:16-.

[45] Crowther M, Crowther MA. Antidotes for Novel Oral Anticoagulants: Current Status and Future Potential. Arteriosclerosis, thrombosis, and vascular biology. 2015;35:1736-45.

[46] Ansell JE, Bakhru SH, Laulicht BE, Steiner SS, Grosso M, Brown K, et al. Use of PER977 to reverse the anticoagulant effect of edoxaban. The New England journal of medicine. 2014;371:2141-2.

[47] Laulicht B, Bakhru S, Jiang X, Chen L, Pan D, Grosso M, et al. Antidote for new oral anticoagulants: mechanism of action and binding specificity of PER977. Journal of Thrombosis and Haemostasis. 2013;11:75-.

[48] Lu GM, DeGuzman FR, Hollenbach SJ, Karbarz MJ, Abe K, Lee G, et al. A specific antidote for reversal of anticoagulation by direct and indirect inhibitors of coagulation factor Xa. Nature Medicine. 2013;19:446-+.

[49] Schiele F, van Ryn J, Canada K, Newsome C, Sepulveda E, Park J, et al. A specific antidote for dabigatran: functional and structural characterization. Blood. 2013;121:3554-62.

[50] Grottke O, van Ryn J, Spronk HM, Rossaint R. Prothrombin complex concentrates and a specific antidote to dabigatran are effective ex-vivo in reversing the effects of dabigatran in an anticoagulation/liver trauma experimental model. Crit Care. 2014;18:R27.

[51] Pollack CV, Jr., Reilly PA, Eikelboom J, Glund S, Verhamme P, Bernstein RA, et al. Idarucizumab for Dabigatran Reversal. The New England journal of medicine. 2015;373:511-20.

[52] Sullivan DW, Jr., Gad SC, Laulicht B, Bakhru S, Steiner S. Nonclinical Safety Assessment of PER977: A Small Molecule Reversal Agent for New Oral Anticoagulants and Heparins. Int J Toxicol. 2015;34:308-17.
[53] Jones D. Anticoagulant antidotes start yielding Phase III promise. Nat Rev Drug Discov. 2015;14:5-6.
[54] Crowther M, Gold A, Lu G, Leeds JM, Wiens BL, Mathur V, et al. ANNEXA (TM)-A PART 2: A phase 3 randomized, double-blind, placebo-controlled trial demonstrating sustained reversal of apixaban-induced anticoagulation in older subjects by andexanet ALFA (PRT064445), a universal antidote for factor XA (FXA) inhibitors. Journal of Thrombosis and Haemostasis. 2015;13:84-5.
[55] Hwang SR, Byun Y. Advances in oral macromolecular drug delivery. Expert Opin Drug Deliv. 2014;11:1955-67.
[56] Baughman RA, Kapoor SC, Agarwal RK, Kisicki J, Catella-Lawson F, FitzGerald GA. Oral delivery of anticoagulant doses of heparin. A randomized, double-blind, controlled study in humans. Circulation. 1998;98:1610-5.
[57] Salartash K, Gonze MD, Leone-Bay A, Baughman R, Sternbergh WC, 3rd, Money SR. Oral low-molecular weight heparin and delivery agent prevents jugular venous thrombosis in the rat. J Vasc Surg. 1999;30:526-31.
[58] Salartash K, Lepore M, Gonze MD, Leone-Bay A, Baughman R, Sternbergh WC, 3rd, et al. Treatment of experimentally induced caval thrombosis with oral low molecular weight heparin and delivery agent in a porcine model of deep venous thrombosis. Ann Surg. 2000;231:789-94.
[59] Hull RD, Kakkar AK, Marder VJ, Pineo GF, Goldberg MM, Raskob GE, et al. Oral SNAC-heparin vs. enoxaparin for preventing venous thromboembolism following total hip replacement. Blood. 2002;100:148a-9a.
[60] Arbit E, Goldberg M, Gomez-Orellana I, Majuru S. Oral heparin: status review. Thromb J. 2006;4:6.
[61] Al-Hilal TA, Park J, Alam F, Chung SW, Park JW, Kim K, et al. Oligomeric bile acid-mediated oral delivery of low molecular weight heparin. Journal of controlled release : official journal of the Controlled Release Society. 2014;175:17-24.

[62] Al-Hilal TA, Chung SW, Alam F, Park J, Lee KE, Jeon H, et al. Functional transformations of bile acid transporters induced by high-affinity macromolecules. Sci Rep. 2014;4:4163.
[63] Ralay-Ranaivo B, Desmaele D, Bianchini EP, Lepeltier E, Bourgaux C, Borgel D, et al. Novel self assembling nanoparticles for the oral administration of fondaparinux: synthesis, characterization and in vivo evaluation. Journal of controlled release : official journal of the Controlled Release Society. 2014;194:323-31.
[64] Fan B, Xing Y, Zheng Y, Sun C, Liang G. pH-responsive thiolated chitosan nanoparticles for oral low-molecular weight heparin delivery: in vitro and in vivo evaluation. Drug Deliv. 2014:1-10.
[65] Zhang HL, Mi J, Huo YY, Huang XY, Xing JF, Yamamoto A, et al. Absorption enhancing effects of chitosan oligomers on the intestinal absorption of low molecular weight heparin in rats. Int J Pharmaceut. 2014;466:156-62.
[66] Wang L, Li L, Sun Y, Tian Y, Li Y, Li C, et al. Exploration of hydrophobic modification degree of chitosan-based nanocomplexes on the oral delivery of enoxaparin. Eur J Pharm Sci. 2013;50:263-71.
[67] Viehof A, Lamprecht A. Oral delivery of low molecular weight heparin by polyaminomethacrylate coacervates. Pharmaceutical research. 2013;30:1990-8.
[68] Bagre AP, Jain K, Jain NK. Alginate coated chitosan core shell nanoparticles for oral delivery of enoxaparin: in vitro and in vivo assessment. Int J Pharm. 2013;456:31-40.
[69] Paliwal R, Paliwal SR, Agrawal GP, Vyas SP. Chitosan nanoconstructs for improved oral delivery of low molecular weight heparin: In vitro and in vivo evaluation. Int J Pharm. 2012;422:179-84.
[70] Ramadan A, Lagarce F, Tessier-Marteau A, Thomas O, Legras P, Macchi L, et al. Oral fondaparinux: use of lipid nanocapsules as nanocarriers and in vivo pharmacokinetic study. Int J Nanomed. 2011;6:2941-51.
[71] Paliwal R, Paliwal SR, Agrawal GP, Vyas SP. Biomimetic solid lipid nanoparticles for oral bioavailability enhancement of low molecular weight heparin and its lipid conjugates: in vitro and in vivo evaluation. Molecular pharmaceutics.

2011;8:1314-21.
[72] Kim SK, Huh J, Kim SY, Byun Y, Lee DY, Moon HT. Physicochemical conjugation with deoxycholic acid and dimethylsulfoxide for heparin oral delivery. Bioconjugate chemistry. 2011;22:1451-8.
[73] Park JW, Jeon OC, Kim SK, Al-Hilal TA, Lim KM, Moon HT, et al. Pharmacokinetic evaluation of an oral tablet form of low-molecular-weight heparin and deoxycholic acid conjugate as a novel oral anticoagulant. Thrombosis and haemostasis. 2011;105:1060-71.
[74] Park JW, Jeon OC, Kim SK, Al-Hilal TA, Moon HT, Kim CY, et al. Anticoagulant efficacy of solid oral formulations containing a new heparin derivative. Molecular pharmaceutics. 2010;7:836-43.
[75] Scala-Bertola J, Rabiskova M, Lecompte T, Bonneaux F, Maincent P. Granules in the improvement of oral heparin bioavailability. Int J Pharm. 2009;374:12-6.
[76] Lanke SSS, Gayakwad SG, Strom JG, D'souza MJ. Oral delivery of low molecular weight heparin microspheres prepared using biodegradable polymer matrix system. J Microencapsul. 2009;26:493-500.
[77] Thanou M, Henderson S, Kydonieus A, Elson C. N-sulfonato-N,O-carboxymethylchitosan: a novel polymeric absorption enhancer for the oral delivery of macromolecules. Journal of controlled release : official journal of the Controlled Release Society. 2007;117:171-8.
[78] Lee DY, Lee J, Lee S, Kim SK, Byun Y. Liphophilic complexation of heparin based on bile acid for oral delivery. Journal of controlled release : official journal of the Controlled Release Society. 2007;123:39-45.
[79] Hoffart V, Lamprecht A, Maincent P, Lecompte T, Vigneron C, Ubrich N. Oral bioavailability of a low molecular weight heparin using a polymeric delivery system. Journal of Controlled Release. 2006;113:38-42.
[80] Hayes PY, Ross BP, Thomas BG, Toth I. Polycationic lipophilic-core dendrons as penetration enhancers for the oral administration of low molecular weight heparin. Bioorgan Med Chem. 2006;14:143-52.
[81] Schluter A, Lamprecht A. Current Developments for the Oral Delivery of Heparin. Curr Pharm Biotechno. 2014;15:640-9.

[82] Salama NN, Eddington ND, Fasano A. Tight junction modulation and its relationship to drug delivery. Adv Drug Deliv Rev. 2006;58:15-28.
[83] Chen MC, Sonaje K, Chen KJ, Sung HW. A review of the prospects for polymeric nanoparticle platforms in oral insulin delivery. Biomaterials. 2011;32:9826-38.
[84] Thanou M, Nihot M, Jansen M, Verhoef JC, Junginger H. Mono-N-carboxymethyl chitosan (MCC), a polyampholytic chitosan derivative, enhances the intestinal absorption of low molecular weight heparin across intestinal epithelia in vitro and in vivo. Journal of pharmaceutical sciences. 2001;90:38-46.
[85] Thanou M, Henderson S, Kydonieus A, Elson C. carboxymethylchitosan: A novel polymeric absorption enhancer for the oral delivery of macromolecules. Journal of controlled release. 2007;117:171-8.
[86] Scott Swenson E, Curatolo WJ. (C) Means to enhance penetration:(2) Intestinal permeability enhancement for proteins, peptides and other polar drugs: mechanisms and potential toxicity. Advanced drug delivery reviews. 1992;8:39-92.
[87] Al-Hilal TA, Alam F, Byun Y. Oral drug delivery systems using chemical conjugates or physical complexes. Adv Drug Deliver Rev. 2013;65:845-64.
[88] Hofmann AF. The enterohepatic circulation of bile acids in mammals: form and functions. Frontiers in bioscience. 2009;14:2584-98.
[89] Roberts MS, Magnusson BM, Burczynski FJ, Weiss M. Enterohepatic circulation - Physiological, pharmacokinetic and clinical implications. Clinical Pharmacokinetics. 2002;41:751-90.
[90] Balakrishnan A, Polli JE. Apical sodium dependent bile acid transporter (ASBT, SLC10A2): a potential prodrug target. Molecular pharmaceutics. 2006;3:223-30.
[91] O'Reilly JR, Corrigan OI, O'Driscoll CM. The effect of mixed micellar systems, bile salt/fatty acids, on the solubility and intestinal absorption of clofazimine (B663) in the anaesthetised rat. Int J Pharmaceut. 1994;109:147-54.
[92] Schaap FG, Trauner M, Jansen PL. Bile acid receptors as targets for drug development. Nature reviews Gastroenterology & hepatology. 2014;11:55-67.
[93] Lee YK, Moon HT, Byun Y. Preparation of slightly hydrophobic heparin

derivatives which can be used for solvent casting in polymeric formulation. Thrombosis research. 1998;92:149-56.
[94] Lee Y, Kim SH, Byun Y. Oral delivery of new heparin derivatives in rats. Pharmaceutical research. 2000;17:1259-64.
[95] Kim JY, Jeon OC, Moon HT, Hwang SR, Byun Y. Preclinical safety evaluation of low molecular weight heparin-deoxycholate conjugates as an oral anticoagulant. Journal of applied toxicology : JAT. 2015.
[96] Lee YK, Kim SK, Lee DY, Lee S, Kim CY, Shin HC, et al. Efficacy of orally active chemical conjugate of low molecular weight heparin and deoxycholic acid in rats, mice and monkeys. Journal of controlled release : official journal of the Controlled Release Society. 2006;111:290-8.
[97] Park JW, Jeon OC, Kim SK, Al-Hilal TA, Jin SJ, Moon HT, et al. High antiangiogenic and low anticoagulant efficacy of orally active low molecular weight heparin derivatives. Journal of controlled release : official journal of the Controlled Release Society. 2010;148:317-26.
[98] Park J, Jeong JH, Al-Hilal TA, Kim JY, Byun Y. Size Controlled Heparin Fragment-Deoxycholic Acid Conjugate Showed Anticancer Property by Inhibiting VEGF165. Bioconjugate chemistry. 2015;26:932-40.
[99] Al-Hilal TA, Alam F, Park JW, Kim K, Kwon IC, Ryu GH, et al. Prevention effect of orally active heparin conjugate on cancer-associated thrombosis. Journal of controlled release : official journal of the Controlled Release Society. 2014.
[100] Alam F, Al-Hilal TA, Chung SW, Seo D, Mahmud F, Kim HS, et al. Oral delivery of a potent anti-angiogenic heparin conjugate by chemical conjugation and physical complexation using deoxycholic acid. Biomaterials. 2014;35:6543-52.
[101] Renukuntla J, Vadlapudi AD, Patel A, Boddu SH, Mitra AK. Approaches for enhancing oral bioavailability of peptides and proteins. Int J Pharmaceut. 2013;447:75-93.
[102] Ensign LM, Cone R, Hanes J. Oral drug delivery with polymeric nanoparticles: the gastrointestinal mucus barriers. Adv Drug Deliv Rev. 2012;64:557-70.
[103] Macadam A. The Effect of Gastrointestinal Mucus on Drug Absorption. Adv

Drug Deliver Rev. 1993;11:201-20.
[104] Viskov C, Just M, Laux V, Mourier P, Lorenz M. Description of the chemical and pharmacological characteristics of a new hemisynthetic ultra-low-molecular-weight heparin, AVE5026. Journal of thrombosis and haemostasis : JTH. 2009;7:1143-51.
[105] Cosmi B, Palareti G. Old and new heparins. Thrombosis research. 2012;129:388-91.
[106] Planes A. Review of bemiparin sodium--a new second-generation low molecular weight heparin and its applications in venous thromboembolism. Expert opinion on pharmacotherapy. 2003;4:1551-61.
[107] Xu Y, Masuko S, Takieddin M, Xu H, Liu R, Jing J, et al. Chemoenzymatic synthesis of homogeneous ultralow molecular weight heparins. Science. 2011;334:498-501.
[108] Xu Y, Cai C, Chandarajoti K, Hsieh PH, Li L, Pham TQ, et al. Homogeneous low-molecular-weight heparins with reversible anticoagulant activity. Nat Chem Biol. 2014;10:248-50.
[109] Bauer KA. Fondaparinux sodium: A selective inhibitor of factor Xa. Am J Health-Syst Ph. 2001;58:S14-S7.
[110] Gerotziafas GT, Petropoulou AD, Verdy E, Samama MM, Elalamy I. Effect of the anti-factor Xa and anti-factor IIa activities of low-molecular-weight heparins upon the phases of thrombin generation. Journal of Thrombosis and Haemostasis. 2007;5:955-62.
[111] Jeske WP, Hoppensteadt D, Gray A, Walenga JM, Cunanan J, Myers L, et al. A common standard is inappropriate for determining the potency of ultra low molecular weight heparins such as semuloparin and bemiparin. Thrombosis research. 2011;128:361-7.
[112] Hirsh J, Raschke R. Heparin and low-molecular-weight heparin: the Seventh ACCP Conference on Antithrombotic and Thrombolytic Therapy. Chest. 2004;126:188S-203S.
[113] Melnikova I. The anticoagulants market. Nat Rev Drug Discov. 2009;8:353-4.
[114] Chaudhari K, Hamad B, Syed BA. Antithrombotic drugs market. Nat Rev

Drug Discov. 2014;13:571-2.
[115] Walenga JM, Lyman GH. Evolution of heparin anticoagulants to ultra-low-molecular-weight heparins: a review of pharmacologic and clinical differences and applications in patients with cancer. Critical reviews in oncology/hematology. 2013;88:1-18.
[116] Dubruc C, Karimi-Anderesi N, Lunven C, Zhang M, Grossmann M, Potgieter H. Pharmacokinetics of a New, Ultra-Low Molecular Weight Heparin, Semuloparin (AVE5026), in Healthy Subjects. Results From the First Phase I Studies. Blood. 2009;114:443-.
[117] Donat F, Duret JP, Santoni A, Cariou R, Necciari J, Magnani H, et al. The pharmacokinetics of fondaparinux sodium in healthy volunteers. Clin Pharmacokinet. 2002;41 Suppl 2:1-9.
[118] Garcia DA. Parenteral Anticoagulants: Antithrombotic Therapy and Prevention of Thrombosis, 9th ed: American College of Chest Physicians Evidence-Based Clinical Practice Guidelines (vol 141, pg e24S, 2012). Chest. 2013;144:721-.
[119] Trujillo-Santos J, Schellong S, Falga C, Zorrilla V, Gallego P, Barron M, et al. Low-molecular-weight or unfractionated heparin in venous thromboembolism: the influence of renal function. The American journal of medicine. 2013;126:425-34 e1.
[120] Verso M, Agnelli G. New strategies of VTE prevention in cancer patients. Thrombosis research. 2014;133 Suppl 2:S128-32.
[121] Agnelli G, Verso M. Management of venous thromboembolism in patients with cancer. Journal of thrombosis and haemostasis : JTH. 2011;9 Suppl 1:316-24.
[122] Chew HK, Davies AM, Wun T, Harvey D, Zhou H, White RH. The incidence of venous thromboembolism among patients with primary lung cancer. Journal of Thrombosis and Haemostasis. 2008;6:601-8.
[123] Sandhu R, Pan CX, Wun T, Harvey D, Zhou H, White RH, et al. The Incidence of Venous Thromboembolism and Its Effect on Survival Among Patients With Primary Bladder Cancer. Cancer-Am Cancer Soc. 2010;116:2596-603.
[124] Khorana AA, Francis CW, Culakova E, Kuderer NM, Lyman GH. Frequency, risk factors, and trends for venous thromboembolism among hospitalized cancer patients. Cancer-Am Cancer Soc. 2007;110:2339-46.

[125] Blom JW, Vanderschoot JPM, Oostindier MJ, Osanto S, van der Meer FJM, Rosendaal FR. Incidence of venous thrombosis in a large cohort of 66 329 cancer patients: results of a record linkage study. Journal of Thrombosis and Haemostasis. 2006;4:529-35.
[126] Kuderer NM, Ortel TL, Francis CW. Impact of venous thromboembolism and anticoagulation on cancer and cancer survival. Journal of clinical oncology : official journal of the American Society of Clinical Oncology. 2009;27:4902-11.
[127] Haas SK, Freund M, Heigener D, Heilmann L, Kemkes-Matthes B, von Tempelhoff GF, et al. Low-molecular-weight heparin versus placebo for the prevention of venous thromboembolism in metastatic breast cancer or stage III/IV lung cancer. Clin Appl Thromb Hemost. 2012;18:159-65.
[128] Tardy B, Chalayer E, Chapelle C, Mismetti P. The effect of low molecular weight heparin on survival in cancer patients: an updated systematic review and meta-analysis of randomized trials: comment. Journal of thrombosis and haemostasis : JTH. 2014;12:1572-3.
[129] Lee AYY, Kamphuisen PW, Meyer G, Bauersachs R, Janas MS, Jarner MF, et al. A Randomized Trial of Long-Term Tinzaparin, a Low Molecular Weight Heparin (LMWH), Versus Warfarin for Treatment of Acute Venous Thromboembolism (VTE) in Cancer Patients - the CATCH Study. Blood. 2014;124.
[130] Agnelli G, George DJ, Kakkar AK, Fisher W, Lassen MR, Mismetti P, et al. Semuloparin for thromboprophylaxis in patients receiving chemotherapy for cancer. The New England journal of medicine. 2012;366:601-9.
[131] Nasser NJ, Na'amad M, Weinberg I, Gabizon AA. Pharmacokinetics of low molecular weight heparin in patients with malignant tumors. Anticancer Drugs. 2015;26:106-11.
[132] Brem S, Brem H, Folkman J, Finkelstein D, Patz A. Prolonged tumor dormancy by prevention of neovascularization in the vitreous. Cancer research. 1976;36:2807-12.
[133] Parangi S, Dietrich W, Christofori G, Lander ES, Hanahan D. Tumor suppressor loci on mouse chromosomes 9 and 16 are lost at distinct stages of tumorigenesis in a transgenic model of islet cell carcinoma. Cancer research.

1995;55:6071-6.
[134] Folkman J, Langer R, Linhardt RJ, Haudenschild C, Taylor S. Angiogenesis inhibition and tumor regression caused by heparin or a heparin fragment in the presence of cortisone. Science. 1983;221:719-25.
[135] Smorenburg SM, Van Noorden CJ. The complex effects of heparins on cancer progression and metastasis in experimental studies. Pharmacological reviews. 2001;53:93-105.
[136] Munoz EM, Linhardt RJ. Heparin-binding domains in vascular biology. Arteriosclerosis, thrombosis, and vascular biology. 2004;24:1549-57.
[137] Yin W, Zhang J, Jiang Y, Juan S. Combination therapy with low molecular weight heparin and Adriamycin results in decreased breast cancer cell metastasis in CH mice. Experimental and therapeutic medicine. 2014;8:1213-8.
[138] Park J, Kim JY, Hwang SR, Mahmud F, Byun Y. Chemical Conjugate of Low Molecular Weight Heparin and Suramin Fragment Inhibits Tumor Growth Possibly by Blocking VEGF165. Molecular pharmaceutics. 2015;12:3935-42.
[139] Chung SW, Lee M, Bae SM, Park J, Jeon OC, Lee HS, et al. Potentiation of anti-angiogenic activity of heparin by blocking the ATIII-interacting pentasaccharide unit and increasing net anionic charge. Biomaterials. 2012;33:9070-9.
[140] Kim JY, Shim G, Choi HW, Park J, Chung SW, Kim S, et al. Tumor vasculature targeting following co-delivery of heparin-taurocholate conjugate and suberoylanilide hydroxamic acid using cationic nanolipoplex. Biomaterials. 2012;33:4424-30.
[141] Lee E, Kim YS, Bae SM, Kim SK, Jin S, Chung SW, et al. Polyproline-type helical-structured low-molecular weight heparin (LMWH)-taurocholate conjugate as a new angiogenesis inhibitor. International journal of cancer Journal international du cancer. 2009;124:2755-65.

Part A: Study of oral delivery of macromolecule via apical sodium dependant bile acid transporter

Chapter: 2

Oral delivery of heparin by using site-specific end conjugation with tetraDOCA

2.1. Introduction

Anticoagulant therapy with heparin and low molecular weight heparin (LMWH) is widely used in healthcare therapeutics [1, 2]. Thromboembolic disorders such as deep vein thrombosis, pulmonary embolism and stroke are potential lethal diseases, thus patients at high risk of them need to be treated by heparin and anticoagulants [3]. Heparin has been the drug of choice for the treatment or the prevention of thromboembolic disease and is also a safe carbohydrate drug extracted from animal sources that exist in nature [4-6]. Among heparins, LMWHs are more effective and have predictable effect than unfractionated heparin (UFH) in preventing blood coagulation because of lower bleeding risk, higher bioavailability and predictable effect [7-9].

There are several kinds of clinically approved LMWHs which were introduced in the past decades [10]. The average molecular weight of LMWHs is usually 4000-5000 Da, which is lower than that of UFH (12000-15000 Da). LMWHs are generally prepared by controlled chemical or enzymatic depolymerization from UFH [11, 12]. Nadroparin, dalteparin and reviparin can be prepared by deaminative cleavage with nitrous acid, while tinzaparin can be obtained using heparinase [13].

Enoxaparin (Lovenox®, Sanofi–Aventis) is the best-selling heparin on the market [14]. Among LMWHs, enoxaparin has been uniquely prepared by alkaline depolymerization with benzethonium salt. This suitable method using controlled depolymerization of natural heparin from porcine intestinal mucosa has gained maximum market of LMWHs [15]. One of properties of enoxaparin is that its end component consists of the reducing end. Reducing end means that the end monosaccharide residue of polysaccharide is in acetal form which is related to

glycosylation reaction. On the other hand, about 20 % of the end components of enoxaparin contain the reducing end named 1,6 anhydro derivative.

Glycosylation is an important reaction in the field of glycochemistry to synthesize natural glycoproteins and glycans. Chemical glycosylation could also serve as a general strategy for modulating the end of monosaccharide [16]. Glycosylation with oligosaccharides is one of the most challenging chemical technique in organic synthesis, however, in case of polysaccharide or macromolecules, the glycosyl donors of polysaccharide usually used in glycosylation are too stable and rare to be modified by chemical reaction due to their enormous size and dynamics [17-19]. Nevertheless, the end conjugation of oligosaccharides using chemical glycosylation has showed the possibility for polysaccharide end-specific conjugation [20, 21].

Clinical use of enoxaparin could be extended using the chemical glycosylation and glycation reaction. End-specific conjugation provides several advantages such as monitoring in vivo tissue distribution by dye conjugation maintaining its biological action [22]. Furthermore, biological functional groups such as oral enhancers might be introduced into the end site of enoxaparin. The oral delivery of enoxaparin by conjugation would increase its therapeutic use because the application of heparin has always been limited by its requirement for injection [23].

In our previous studies, we introduced several kinds of nadroparin and bile acid conjugates [24-27]. Nadroparin is the one of famous LMWHs, and DOCA conjugation has been found to promote the intestinal absorption of nadroparin [28, 29]. Moreover, we had designed nadroparin and tetraDOCA conjugate to facilitate the oral administration of nadroparin [30, 31]. However, the conjugation was not end-specific because the end-aldehyde group of nadroparin was completely eliminated after commercial processes [1, 32]. The tail end of polysaccharide of nadroparin was not chemically active. Beside, side-conjugation of nadroparin was not preferred due to heparin's heterogeneity and complexity. Since the recognition of heparin by antithrombin depends on specific heparin sequence, the precise end-specific conjugation is preferred for the rational drug design of polysaccharide

conjugate [6].

Here, we designed enoxaparin and tetraDOCA conjugate (enoxaTD) using chemical glycosylation reaction for end-specific reaction and oral delivery. At first, end reactivity of heparin was confirmed using different kinds of LMWHs and Benedict's reagent. We also optimized the synthesis processes to synthesize new tetraDOCA (TD). After then, TD was conjugated to the tail end of enoxaparin by glycation. The conjugate was confirmed by several methods of characterization. Moreover, for anticoagulant therapy, we evaluated the oral absorption of enoxaTD and therapeutic anticoagulant effect of enoxaTD in animal models.

2.2. Materials and methods

2.2.1. Materials

Enoxparin was obtained from Hebei changshan biochemical pharmaceutical Co. (Shijiazhuang, China). L-lysine, deoxycholic acid, ethylenediamine, 2,2-dimethoxypropan, N,N'-Dicyclohexylcarbodiimide (DCC), ethylcarbodiimide hydrochloride, sodium cyanoborohydride and N-Hydroxysuccinimide (NHS) were purchased from Sigma chemical Co. (St. Louis, MO, USA). Tinzaparin was obtained from the Nanjing King-Friend Biochemical Pharmaceutical Company Ltd. (Nanjing, China). Tetrahydrofuran and N,N-dimethylformide were purchased from Merck (Darmstadt, Germany) and Coatest anti-Factor Xa assay kit was purchased from Chromogenix (Milano, Italy). DMEM high glucose medium, fetal bovine serum, penicillin–streptomycin and trypsin-EDTA were obtained from GIBCO (Grand Island, NY, USA).

2.2.2. Synthesis of enoxaTD

EnoxaTD was prepared by Enoxaparin and tetraDOCA conjugation. TetraDOCA was synthesized using optimized method compared to previous method [31, 33]. Briefly, L-lysine was dissolved in methanol, and then 2,2-dimethoxypropan and HCl was added to the solution. After 3 h reaction, lysine methyl ester was concentrated under reduced pressure. In the other batch, L-lysine

was dissolved in water (160 mL) and THF. It was stirred with sodium carbonate and di-tert-butyl-dicarbonate, then di-boc-lysine was extracted using ethyl acetate. The lysine methyl ester and di-boc-lysine were reacted by N,N'-Dicyclohexylcarbodiimide (DCC) and N-Hydroxysuccinimide (NHS) in ethyl acetate. After deprotection with acetyl chloride, NHS-activated deoxycholic acid (DOCA) was mixed at 4 ℃ overnight. It was purified by column chromatography, and then the conjugate was stirred with ethylenediamine (EDA) at room temperature for 3 days to get TD.

To synthesize EnoxaTD using glycosylation, enoxaparin was dissolved in distilled water (1 mL). Synthesized tetraDOCA in DMF was added to the solution, and then stirred at 60 ℃. Sodium cyanoborohydride was added to the solution, then the reaction continued. The product was precipitated in cold ethanol 3 times for purification. After the reaction and purification, EnoxaTD was dissolved in distilled water, and then lyophillzed for 3 days to get white powder. The purity of product was checked by TLC using methanol.

2.2.3. Characterization of enoxaTD

Benedict's reagent was used to confirm the possibility of chemical glycosylation and aldehyde group in enoxaparin. It was prepared using 10 g of anhydrous sodium carbonate (10 g), sodium citrate (17.3 g) and copper (II) sulphate pentahydrate (1.73 g) in distilled water (100 mL) [34]. Glucose, enoxaparin and tinzaparin (100 mg) were dissolved in benedict's solution (1 mL), and then the solution was heated at 75 ℃.

The synthesized materials were characterized using proton nuclear magnetic resonance (NMR) and mass spectrometer. ^{1}H NMR spectra were recorded at 500 MHz using D_2O and DMSO-d_6 as co-solvent (DMSO-d_6, 75%). The calculation process using NMR analysis and sulfuric acid assay were introduced in the previous studies [35, 36]. In both cases, the mixtures with various molecular ratios of enoxaparin and TetraD were prepared. In NMR analysis, the conjugation ratio was calculated by analyzing the NMR peaks at 0.8-1.5 and 5.0-6.5 ppm. In sulfuric acid

assay, they were dissolved in water and mixed with sulfuric acid solution at 70 °C. After heating, the absorbance (420 nm) of solution was measured by using UV/Vis spectrometer. The molecular structures of materials were visualized by ChemBioDraw Ultra 12.0 (Cambridge Soft Corporation) and PyMOL 1.7.0.1 (DeLano Scientific). The factor Xa complex was simulated by AutoDock Vina 1.0.3 and MGLTools-1.4.6 (The Scripps Research Institute, USA) using the crystal Structure of the antithrombin-thrombin-heparin ternary complex (protein data bank [PDB] code, 1TB6) [37].

2.2.4. Anti-FXa assay

The therapeutic effect of enoxaparin is correlated to the inhibitory effect of factor Xa. Anti-factor Xa activity was measured by following the manufacter's protocol. Briefly, enoxaparin and enoxaTD (100 μL) was mixed with 100 μL of antithrombin III (ATIII) solution, and then the solution was incubated at 37 °C for 3 min. After the reaction with 100 μL of factor Xa (FXa), the substrate (200 μL) was added and incubated at 37 °C for 3 min. Anti-FXa activity of enoxaTD was calculated using the absorbance values at 405 nm by UV/Vis spectrometer (n=3).

2.2.5. Characterization of enoxaTD by nitrous acid degradation

Enoxaparin and enoxaTD were degraded by nitrous acid depolymerization. They were dissolved in distilled water (100 mg/mL). Sodium nitrite solution (20mg/0.2mL) and HCl solution (1 N, 0.8 mL) were added to each heparin solution (1 mL). After 4 h reaction without light, the solution and precipitate (in enoxaTD) were separated by centrifuge. They were lysophilized using freeze-dryer, and then analyzed by NMR and Matrix-Assisted Laser Desorption Ionization Mass Spectrometer (MALDI-TOF MS). Their dried weights were used for calculation of the conjugation ratio (fragment analysis) (n=3).

2.2.6. Cell viability test

The cytotoxicity of enoxaTD was evaluated using MDCK (Madin-darby canine kidney) cell in different concentrations. MDCK was cultured in DMEM high

glucose medium supplemented with 10 % (v/v) FBS, penicillin–streptomycin, NEAA (non-essential amino acids), sodium bicarbonate and HEPES (4-(2-hydroxyethyl)-1-piperazineethanesulfonic acid). When 96-well plate was confluent with MDCK cells, the media were replaced with DMEM containing enoxaTD with different concentrations. After incubation at 37 °C for 24 h, the media were removed. DMEM (100 μL) with 10 μL of CCK-8 solution was added to each well, and then the plate was additionally incubated for 1 h. Cell viability was calculated from the absorbance value (OD 450 - 600 nm) compared with that of untreated group (n=3).

2.2.7. Evaluation of cellular uptake of EnoxaTD

Bile acid transporter overexpressed MDCK cell was developed in the previous work [31]. Briefly, The MDCK cells were transfected in Opti-MEM® I (GIBCO, Invitrogen,CA, USA) medium using SLC10A2 (sodium/bile acid co-transporter family) and Lipofectamine 2000® following the manufacturer's instruction. Apical sodium-dependent bile acid transporter (ASBT) overexpressed MDCK cell was then cultured in DMEM high glucose media.

To visualize the enoxaTD, a reactive dye named cyanine 5 (cy5) amine was coupled with it using EDAC/NHS reaction. EnoxaTD (10 mg) was dissolved in distilled water (1 mL), and then EDAC (10 mg) and NHS (5 mg) was mixed and stirred at pH 4 for 20 min. Cy5 in DMF was added into the solution and incubated without light for 6 h. The product was precipitated by excess of cold acetone and ethanol. After lyophilization, enoxaTD-cy5 was further purified by washing methanol, and then the purity of it was checked by TLC.

MDCK, ASBT overexpressed MDCK and caco-2 cell were prepared in Lab-Tek chambered coverglass (Nunc) for confocal microscopy images. For the experiment, cells were incubated in FBS free DMEM medium with enoxaTD-cy5 (200 μg/mL) for 30 min. After washing with Hank’s Balanced Salt Solution (HBSS) solution 3 times, the wells were filled with 4 % cold paraformaldehyde solution. The plates were additionally incubated in a refrigerator (4 °C) for 10 min. They were again washed with normal saline 4 times and DAPI (4, 6-diamidino-2-

phenylindole) staining was conducted. In case of caco-2 cell line, phalloidin-FITC (Sigma) was treated before DAPI staining to visualize filamentous actin in microscopy. The fluorescence images were acquired with a confocal laser scanning microscopy (Carl Zeiss LSM710, Leica DM IRB/E; Leica Co., Germany).

2.2.8. Pharmacokinetic study

All procedures for animal experiment were approved by the Committee on the Use and Care on Animals according to the regulations of the Institutional Animal Ethics Committee of the Seoul National University. The pharmacokinetics of enoxaparin and EnoxaTD were studied on the basis of anti-factor Xa activity levels in the plasma of rats. Sprague–Dawley (SD) rats (Orientbio Inc., Seongnam, Korea) were fasted for 12 h before oral administration. EnoxaTD was dissolved in drinking water with solubilizers including labrasol and poloxamer 188. After oral administration of the materials, blood (450 μL) was collected from a capillary in the vein of rats. Blood samples were immediately mixed with sodium citrate solution (50 μL) and kept in ice bath. The samples were centrifuged at 2500 g at 4 °C for 20 min, and then the resulting plasma samples (200 μL) were frozen and stored below -20°C until analyzed by anti-FXa chromogenic assay.

2.2.9. DVT study

The animal model for DVT was prepared as described in the previous study [26, 38]. Briefly, SD rats (male, 250-280 g) were fasted for 12 h. After administration of enoxaparin (by subcutaneous) or enoxaTD (by oral), the rats were anesthetized with ketamine and xylazine. After a surgical procedure to gain access into the abdominal cavity, the vena cava of rat was loosely tied, and the branched blood vessels were completely tied. 1 mL/kg of warmed human plasma was injected via the tail vein of rats 1 h after administration, followed by the ligation of the vena cava. The wet weight of the thrombus in the vena cava was measured 3 h after administration (n=4).

2.2.10. Animal study to monitor bleeding effects

7 weeks old male C57BL/6 mice (Orientbio Inc., Seongnam, Korea) were anesthetized with ketamine and xylazine by intraperitoneal injection. Before cutting, the tail is immersed in a pre-warmed (37 ºC) 50 mL tube containing normal saline for 5 min. 3-4 mm of the distal tip of the tail was cut using a scalpel blade, and immediately insert into the 50 mL tube containing normal saline. Venous blood flowing in tube was detected, and the primary bleeding time (clotting time) was measured using electrical stop-clocks (n= 4-5). The maximum time of measurement for primary bleeding was 600 seconds.

2.2.11. Statistical analysis

Statistical analysis was performed by comparing the means of groups in in vitro and in vivo experiments using one-way analyses of variance (ANOVA) followed by Bonferroni's post-hoc tests.

2.3. Results

2.3.1. Confirmation of end-specific activity

The end-specific activities of glucose, enoxaparin and tinzaparin were evaluated using Benedict's reagent (blue alkaline solution). LMWHs such as enoxaparin, nadroparin and tinzaparin have same major sequences in the middle of molecular structure, however, the end of each polysaccharide is different from each other due to different chemical processing from unfractionated heparin. Since enoxaparin has reducing sugar moiety at the end of polysaccharide, it reduced Cu^{2+} to Cu^{+} in Benedict's reagent with the formation of a precipitate of Cu_2O (**Figure 2.1**). Glucose, which was used as a control, was rapidly changed by the reaction (**Figure 2.2**). Enoxaparin also slowly changed the color of solution a few minutes later, however, tinzaparin did not show any differences (**Figure 2.3)**.

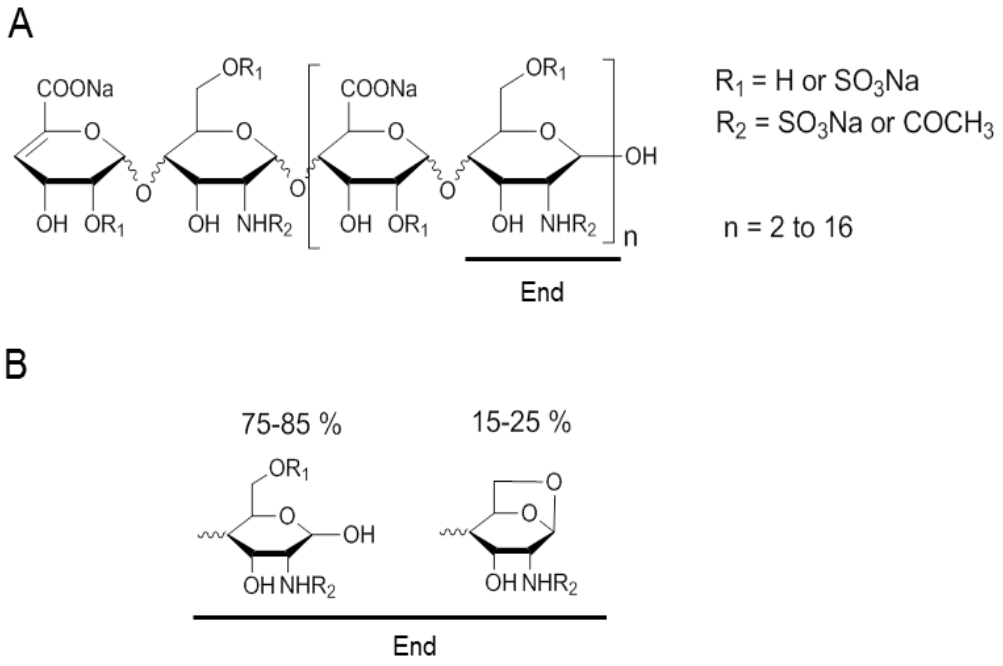

Figure 2.1. (A) Molecular structure of enoxaparin (B) Enoxaparin has the reducing sugar moiety in the end of its structure (75-85 %)

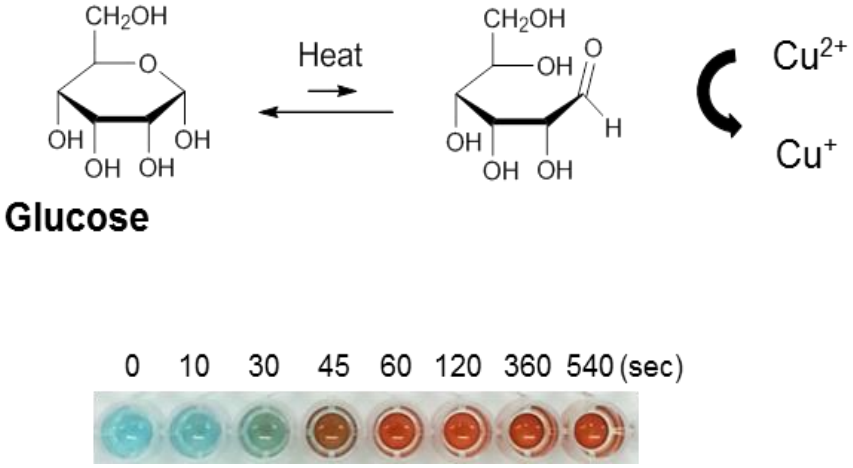

Figure 2.2. Benedict reaction of glucose. Glucose (reducing sugar) reacted with Benedict's reagent, and changed the color of solution.

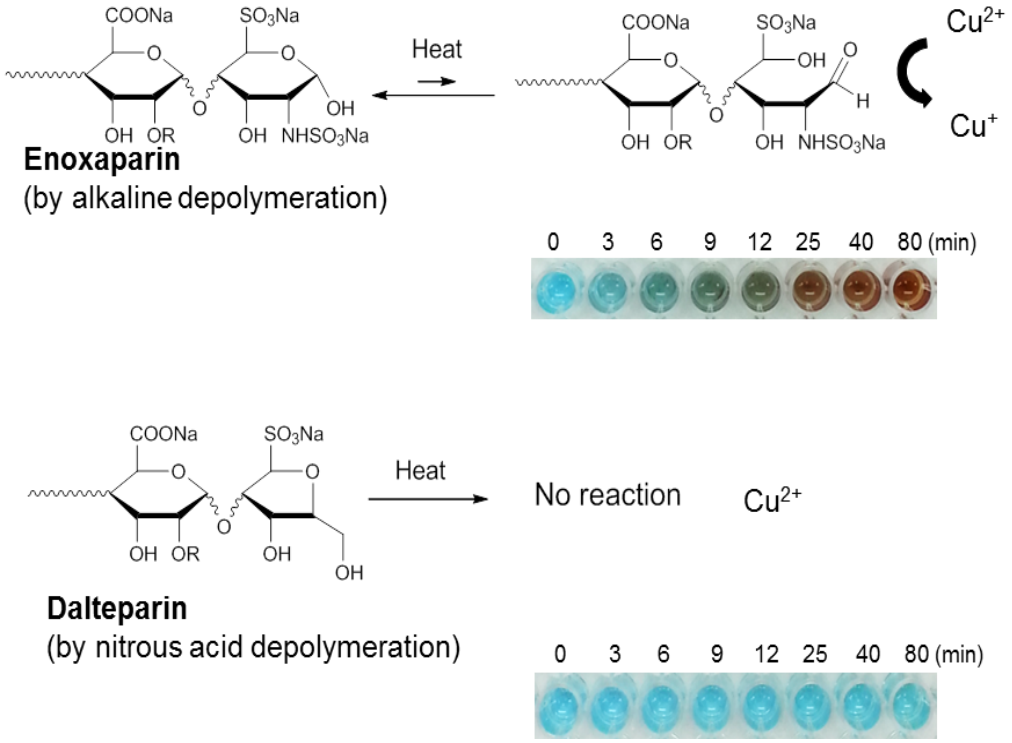

Figure 2.3. Glycation of enoxaparin and the reaction with benedict's reagent. Enoxaparin which has reducing sugar moiety in the end of structure reacted with Benedict's reagent.

2.3.2. Synthesis and characterization

All synthesized compounds were initially evaluated by using TLC, NMR and mass chromatography. TetraDOCA was conjugated to enoxaparin in a step (**Figure 2.4**). The optimized simple synthesis process was used to synthesize EnoxaTD from bile acid, L-lysine and enoxaparin. The molecular structure of EnoxaTD was drawn in **Figure 2.5**. The molecular binding between the antithrombin and EnoxaTD was also virtually simulated to visualize that the end-specific conjugation would not affect the biological activity of enoxaparin (**Figure 2.6**). After the conjugation, the anticoagulant activitiy (94.7 ± 4.6 IU/mL) of EnoxaTD was not significantly different from that (103.3 ± 10.4 IU/mL) of enoxaparin (**Figure 2.7**). The conjugation ratio was calculated by using sulfuric acid assay, NMR peak analysis method and acid depolymerization method. The molecular coupling ratio of EnoxaTD was 0.72 ± 0.13, 0.84 ± 0.17 and 0.83 ± 0.04 by sulfuric acid assay, NMR and fragment analysis, respectively (**Figure 2.5)**. The mixtures with various molecular ratios of enoxaparin and TD were used in NMR analysis and sulfuric assay to calculate the conjugation ratio. On the other hand, fragment analysis depended on the mass of degradation products after nitrous acid depolymerization.

End-specific conjugation of the product was proved by using Benedict's reagent compared with enoxaparin. The color of EnoxaTD solution (40 mg/mL) was slightly changed due to unreacted enoxaparin, however, that of enoxaparin (40 mg/mL) was completely changed (**Figure 2.7**). Moreover, we tested cell viability using the CCK-8 assay to confirm whether it is cytotoxic or not before we started cell-related experiments. The product was not cytotoxic because it did not decrease the viability of MDCK cell even when it was treated in high concentration (100-2000 μg/mL) for 24 h.

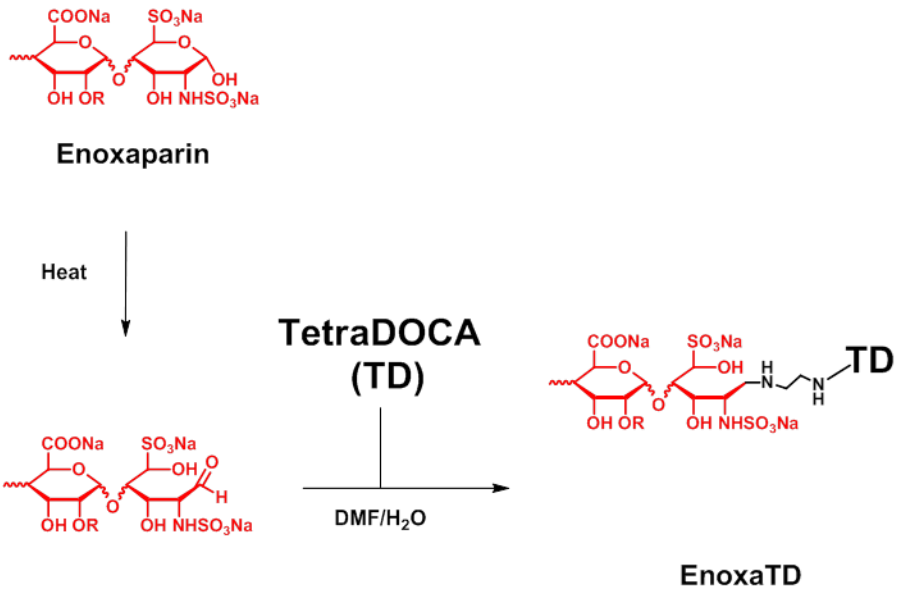

Figure 2.4. Scheme of chemical synthesis of EnoxaTD by glycation reaction using enoxaparin and tetraDOCA.

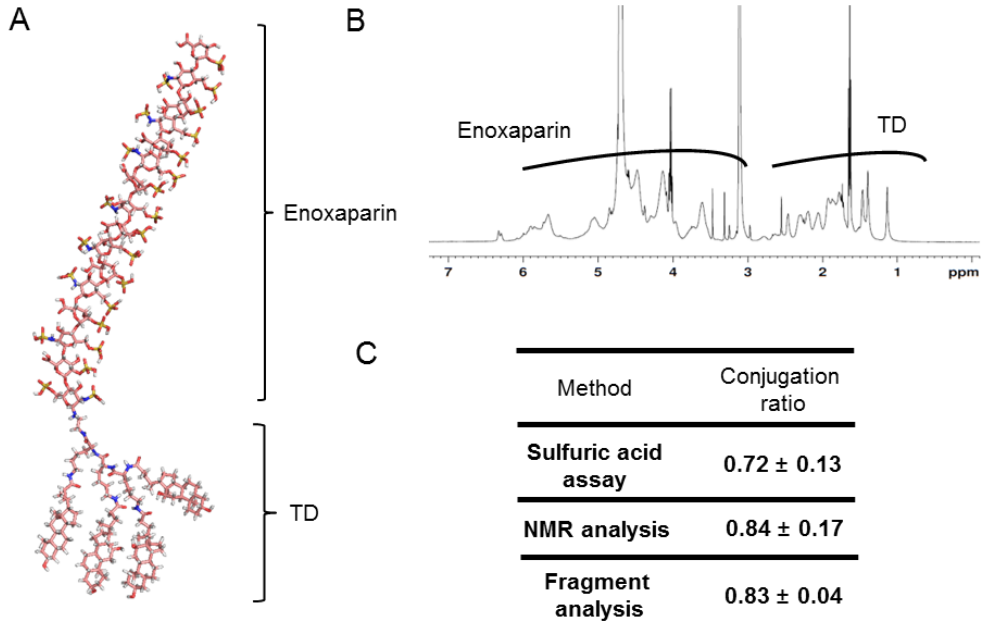

C

Method	Conjugation ratio
Sulfuric acid assay	**0.72 ± 0.13**
NMR analysis	**0.84 ± 0.17**
Fragment analysis	**0.83 ± 0.04**

Figure 2.5. (A) Molecular structure of enoxaTD (B) ^{1}H-NMR data of enoxaTD (C) Conjugation ratio was determined in different methods.

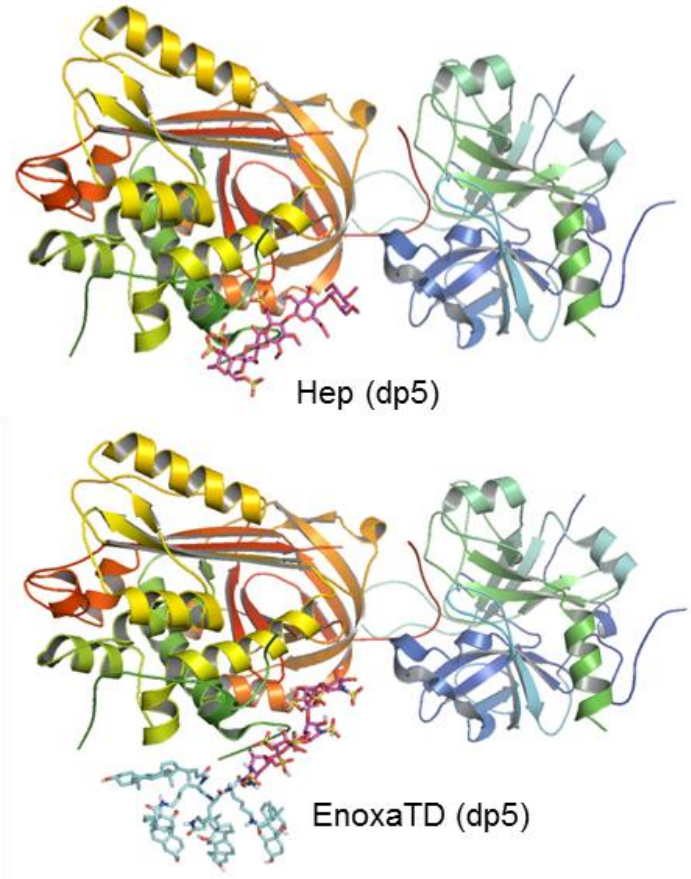

Figure 2.6. Virtual computer simulation of antithrombin and enoxaTD (dp5) to visualize the end-specific conjugation effect from antithrombin-heparin complex (PDB: 1TB6)

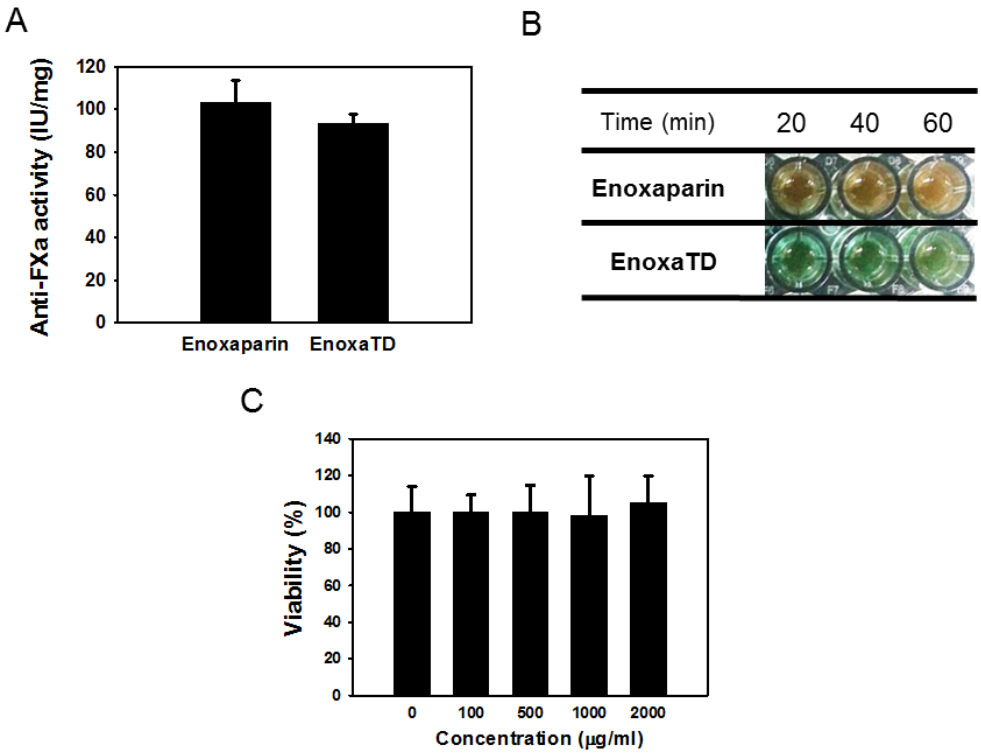

Figure 2.7. (A) Anti FXa activity (B) The reaction of enoxaparin and enoxaTD with Benedict's reagent (40 mg/mL) (C) Cell viability with MDCK cell in high dose (100-2000 µg/mL)

2.3.3. Characterization with depolymerization

EnoxaTD was degraded and analyzed to calculate its molecular ratio and degradation products. After depolymerization with nitrous acid, water-insoluble materials were precipitated from water (**Figure 2.8**). Water-insoluble materials could be dissolved in methanol and ethanol. This property was similar to that of TD. Degradation products of EnoxaTD in water were analyzed by using MALDI-TOF. Degradation products from enoxaparin and EnoxaTD in water were similar to each other. On the other hand, the NMR peaks of water-insoluble material from EnoxaTD matched those found at the NMR peaks of TD as shown in **Figure 2.8.**

2.3.4. Cellular uptake of EnoxaTD

The cellular uptake of EnoxaTD was determined by apical sodium dependent bile acid transporter (ASBT) overexpressed MDCK cells and Caco-2 cell by cy5 conjugation. At first, carboxylic group of EnoxaTD was conjugated to cy5 amine for fluorescence signal. EnoxaTD treated ASBT overexpressed MDCK and MDCK cells showed different results related to the cellular binding and uptake (**Figure 2.9**). To confirm the cellular uptake and absorption route in Caco-2 cell, FITC-labeled phalloidin and cy5-labeled EnoxaTD were treated. As a result, the cellular uptake was detected, and transcellular interaction which avoided tight junctions was also observed in Caco-2 cell (**Figure 2.10**).

2.3.5. PK study

The main motive for chemical glycosylation of enoxaparin is to increase the bioavailability of the non-absorbable enoxaparin in oral delivery. Oral absorption of bile acid conjugates and their absorption mechanism were confirmed in previous studies [30, 31]. Because enoxaparin cannot be measured directly in the plasma, the anti-FXa profile was used to study pharmacokinetic profiles. Intravenously injected EnoxaTD in rats showed similar effects to that of enoxapain in vivo (**Figure 2.11**). However, orally administrated enoxaparin showed lower absorption, it compared to that of EnoxaTD. The maximum concentration of EnoxaTD was 0.60 ± 0.08 IU/mL, whereas that of enoxaparin was 0.17 ± 0.05 IU/mL. The detailed pharmacokinetic

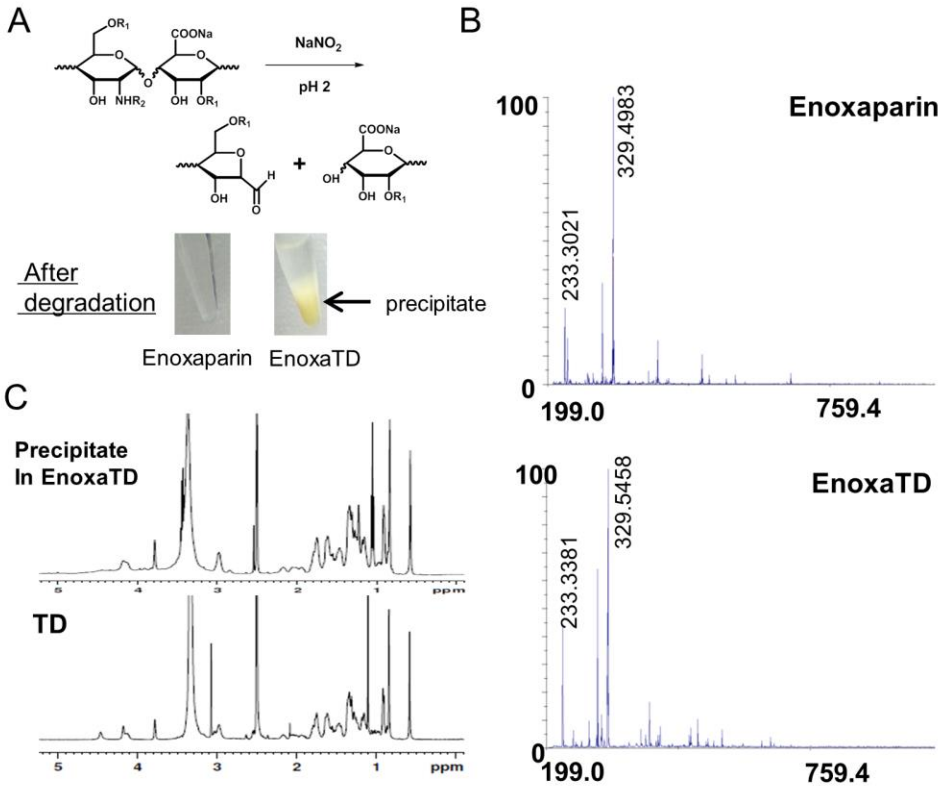

Figure 2.8. (A) Scheme of molecular reaction by nitrous acid depolymerzation and the picture of results (B) Similar MALDI-TOF results from water-soluble degradation products (C) ^{1}H-NMR data of water-insoluble degradation products from enoxaTD compared to that of TD

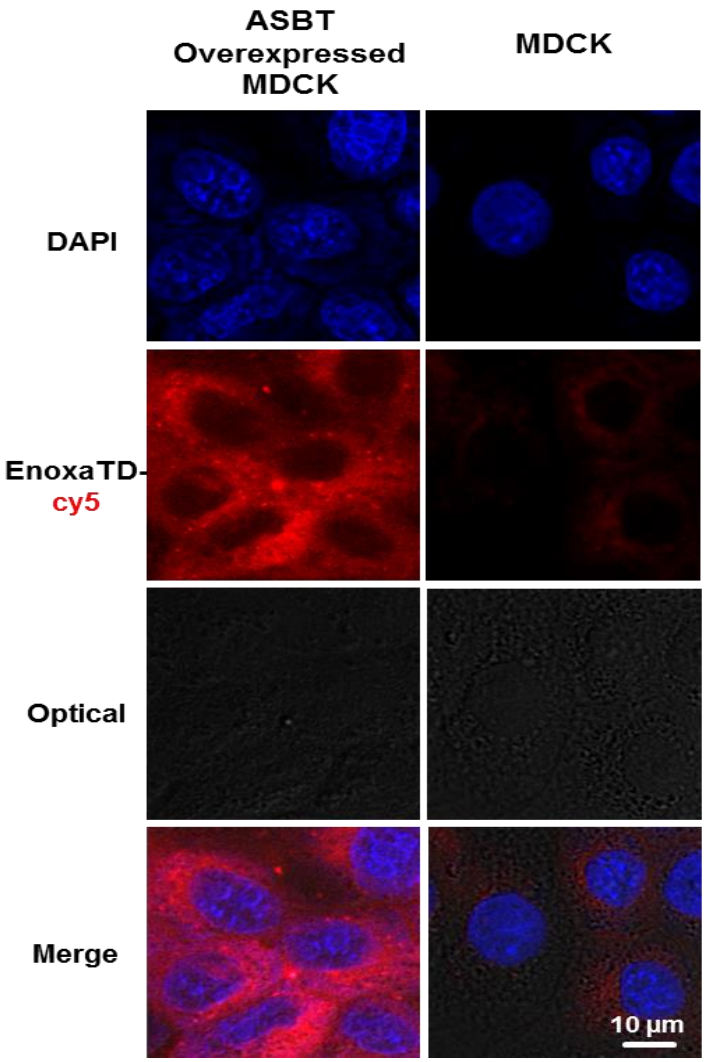

Figure 2.9. The cellular uptake of enoxaTD in MDCK and ASBT overexpressed MDCK cell

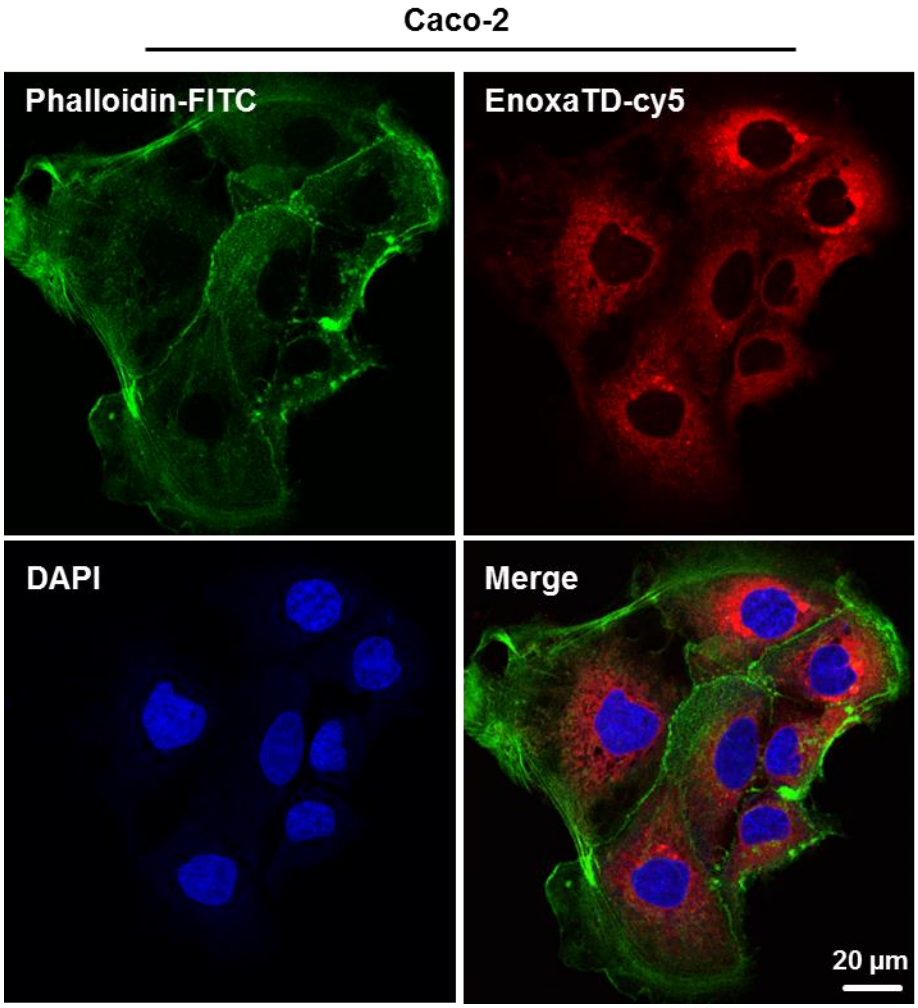

Figure 2.10. There is the signal from enoxaTD inside the caco-2 cell. F-actin was stained by using phalloidin-FITC to visualize tight junction

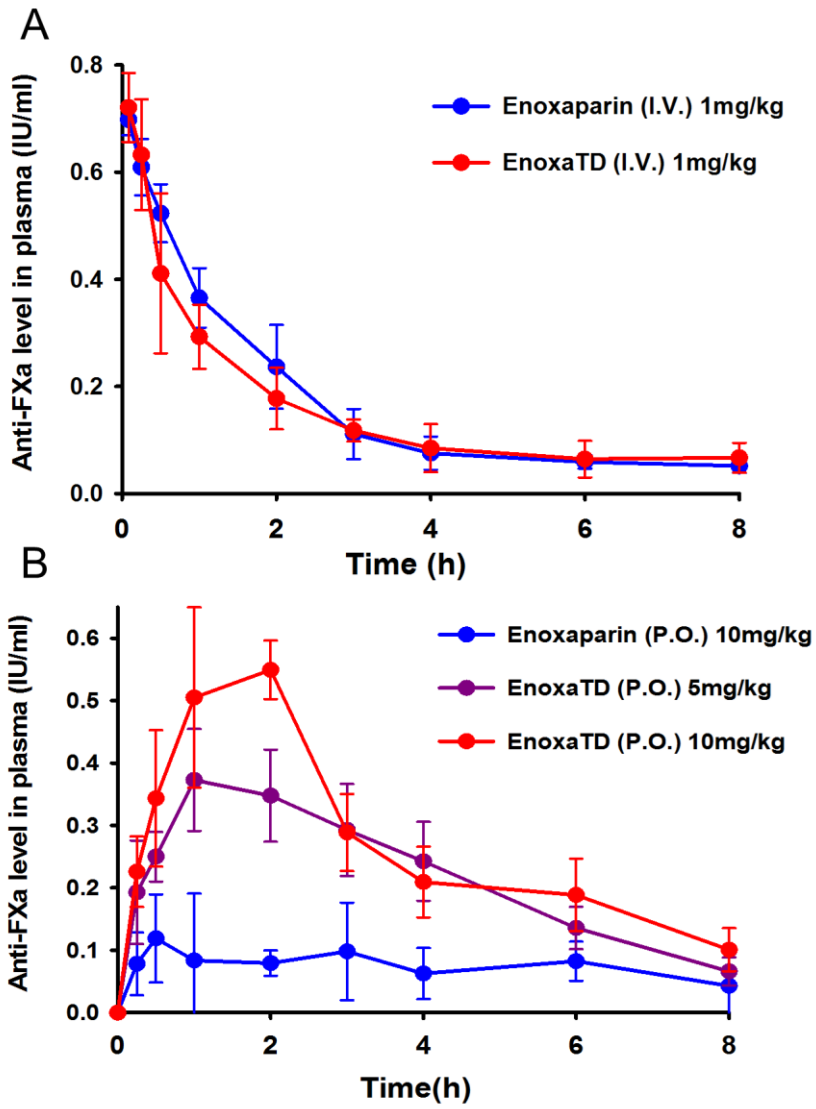

Figure 2.11. (A) Anti-FXa activities of intravenously injected enoxaparin and enoxaTD in rats (B) Anti-FXa activities of orally administered enoxaparin and enoxaTD

profile of enoxaparin and EnoxaTD is written in **Table 2.1**.

2.3.6. DVT and bleeding experiment

The therapeutic effect of EnoxaTD was evaluated by using a venous thrombosis animal model with SD rats. Normal saline was treated orally as a control. The wet weight of the thrombus in the vena cava was 49.3 ± 10.8 mg in the control group. The weights of mice treated by 10 mg/kg of enoxaparin (subcutaneous), 5 mg/kg of EnoxaTD (oral) and 10 mg/kg of EnoxaTD (oral) were 11.4 ± 2.7, 12.5 ± 2.0 and 6.05 ± 2.1, respectively (**Figure 2.12**). Orally administered EnoxaTD group showed reduced thrombus formation due to the oral absorption of EnoxaTD.

The primary bleeding time in rats was calculated by considering the side effect of anticoagulants. The primary bleeding which does not exceed 600 seconds was only measured after cutting. The rat's tail was cut using a scalpel blade after administration of enoxaparin and EnoxaTD. The primary clotting (bleeding) time in the control group was 225.2 ± 57.0 seconds. Those of EnoxaTD (oral, 1 h) and enoxaparin (subcutaneous, 1 h) treated group were 332.0 ± 74.7 seconds and 380.0 ± 51.6 seconds, respectively (**Figure 2.13**). The primary bleeding times were different from that of the control group. The detailed profile of bleeding time of enoxaparin and EnoxaTD is shown in **Figure 2.14**.

Table 2.1. Pharmacokinetic parameters of enoxaparin and EnoxaTD in rats

Materials	Dose (mg/ kg)	C_{max} [a] (IU/mL)	$AUC_{0\text{-}8\ h}$ [c] (IU•h/mL)	$t_{1/2}$ [d] (h)	MRT [e] (h)	F [f] (%)
Enoxaparin (I.V.)	1	-	1.53 ± 0.19	2.59 ± 1.15	-	-
EnoxaTD (I.V.)	1	-	1.46 ± 0.34	2.18 ± 0.12	-	-
Enoxaparin (P.O.)	10	0.17 ± 0.05	0.64 ± 0.18	-	3.73 ± 0.84	4.2
EnoxaTD (P.O.)	5	0.42 ± 0.02	2.01 ± 0.13	-	3.13 ± 0.11	26.3
EnoxaTD (P.O.)	10	0.60 ± 0.08	3.04 ± 0.75	-	3.07 ± 0.16	19.9

Results are the mean ± standard deviation.

[a] Maximum concentration

[b] Area under the curve

[d] Half-life of drug

[e] Mean residence time

[f] Bioavailability

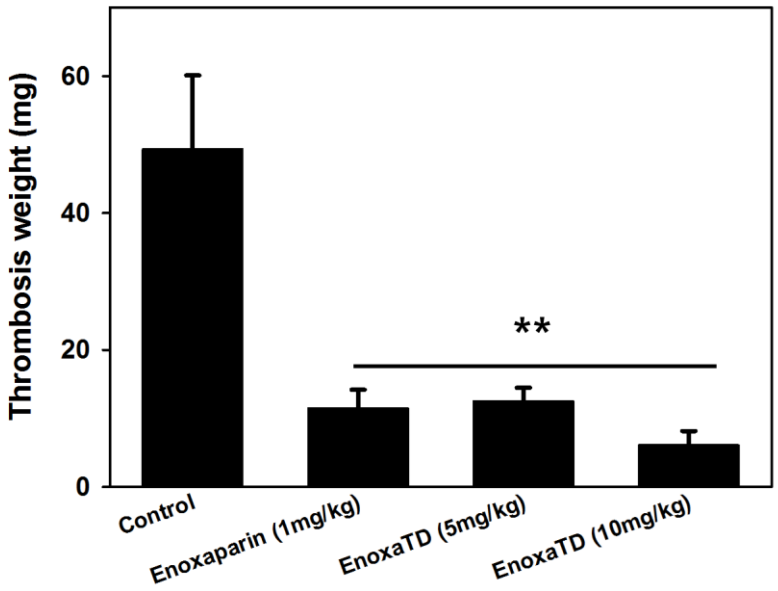

Figure 2.12. Inhibition effect of thrombus formation by enoxaparin and EnoxaTD in rats

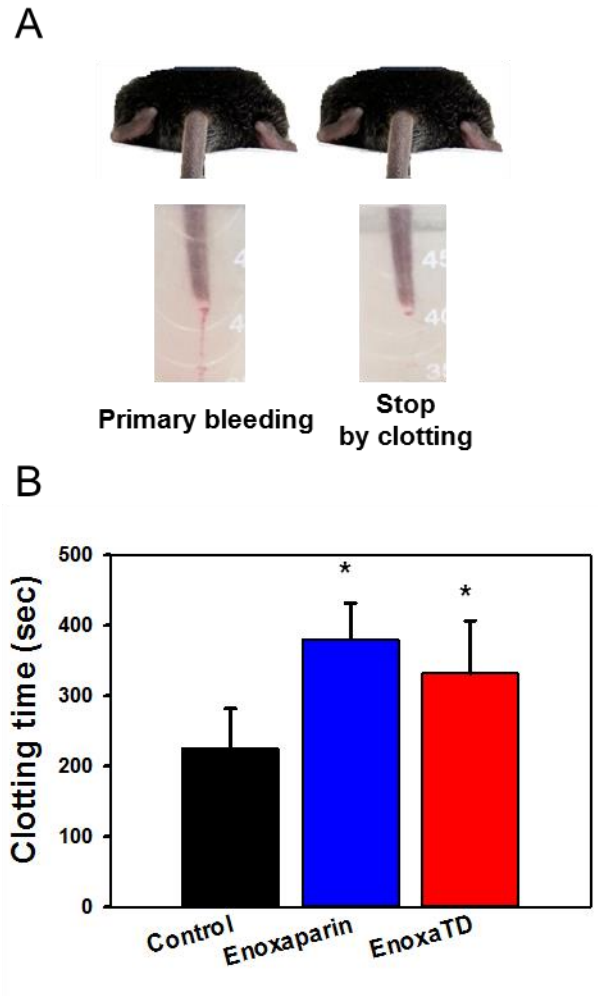

Figure 2.13. (A) Scheme of primary bleeding experiment using mice (B) The clotting time was calculated after cutting the tail

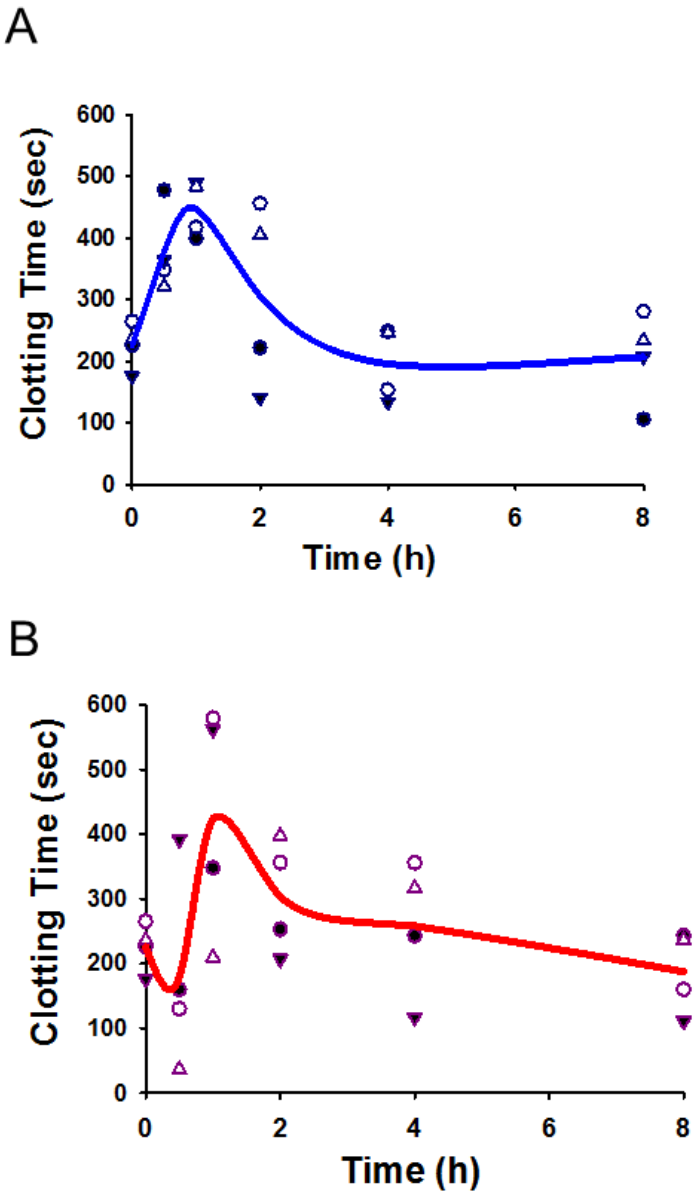

Figure 2.14. (A) Clotting time in enoxaparin treated group (S.C.) (B) Clotting time in enoxaTD treated group (P.O.) with time.

2.4. Discussion

There are several anticoagulants such as UFH, LMWH, VLWMH, vitamin K antagonist and new FXa inhibitors in the field of clinical thromboembolism. Newly developed direct Factor Xa inhibitors including rivaroxaban, apixaban and edoxaban have tried to be treated to patient with venous thromboembolic (VTE) disorders because they are orally available. The oral delivery of anticoagulants is clinically important because it is commonly used for prevention. Although heparin is safe, effective and animal-derived agent, it has not been absorbed in the gastrointestinal (GI) tract.

About a hundred years ago, an American chemist who is named Stanley Rossiter Benedict developed Benedict's Solution which can detect reducing sugars with free aldehyde or ketone groups. It was clinically used as the reagent of choice for measuring sugar content for more than 50 years with other methods [34]. It is also known that polysaccharides such as starches and dextrins do not react with Benedict's reagent considering that the reaction rarely happens at the ends of long carbohydrate chains.

Due to the end-specific conjugation, EnoxaTD has not shown any different properties compared to enoxaparin except the oral uptake in the GI-tract. End-specific conjugation is important for polysaccharide-based drug development because the conjugation itself could not change the therapeutic properties of polysaccharide. EnoxaTD is water-soluble and its anti-FXa activity was almost maintained after the conjugation. In addition, the TD moiety in the molecular structure of EnoxaTD did not affect the molecular binding between the heparin saccharide (dp5) and heparin binding site in antithrombin because van der Waals force of TD is different from electrostatic interaction between heparin and proteins. Hydrophobic effect-literally means water fearing effect of TD revealed only with solubilizer or organic solvent such as DMF or DMSO. Moreover, this property could be used for the analysis of EnoxaTD. After depolymerization of EnoxaTD with nitrous acid, the hydrophobic part of it was precipitated from the water

solution. The mass and NMR spectra of water-insoluble materials were similar to those of TD, which means that the TD in EnoxaTD should be expelled after depolymerization.

The focus of this study was on the oral delivery of enoxaparin. It has been reported that some macromolecules like chitosan or positively charged biomaterials could be absorbed via paracellular route in the GI tract. However, in case of EnoxaTD, the cellular uptake of it was occurred in non-junctional (the transcellular route) location in the caco-2 experiment. The oral delivery was confirmed by using FXa assay because enoxaparin cannot be measured directly in the plasma. Compared to enoxaparin, EnoxaTD showed higher bioavailiability, Cmax and AUC values in PK experiment.

Based on the oral delivery of EnoxaTD, we further investigated the therapeutic effects of it in disease model of DVT and bleeding. DVT, the formation of a blood clot within a deep vein predominantly in the legs, should be prevented. DVT leads to pulmonary embolism, a potentially life-threatening complication. Heparin has been a drug of choice to effectively prevent DVT for decades. Beyond its therapeutic effect, orally active heparin is clinically important for prophylactic treatment considering the paranteral injection of heparin. In this study, we evaluated the anti-thrombogenic effect of EnoxaTD in a rat thrombosis model. The efficacy of enoxaparin and EnoxaTD was enough to prevent DVT in rats. Moreover, the use of Antithrombotic agents is associated with the increased occurrence of bleeding; it has both positive and negative effects. The therapeutic effect of heparin should be linked to the bleeding time, however, uncontrolled bleeding is apparent toxicity. Enoxaparin and EnoxaTD showed controlled bleeding effect with a similar pattern in animal study.

2.5. Conclusion

The present study showed that enoxaparin has an end-specific activity related to glycosylation. Using the chemical glycosylation, enoxaparin was

conjugated to the optimized TD for oral delivery. Orally active EnoxaTD has a promising therapeutic potential for treating DVT without toxicity. Therefore, given the importance of oral delivery, EnoxaTD could be used in long-term maintenance therapy for preventing blood coagulation.

References

[1] Linhardt RJ, Gunay NS. Production and chemical processing of low molecular weight heparins. Seminars in thrombosis and hemostasis.1999;25 Suppl 3:5-16.

[2] Tyrell DJ, Kilfeather S, Page CP. Therapeutic uses of heparin beyond its traditional role as an anticoagulant. Trends in pharmacological sciences. 1995;16:198-204.

[3] White RH. The epidemiology of venous thromboembolism. Circulation. 2003;107:I4-8.

[4] Horlocker TT, Heit JA. Low molecular weight heparin: biochemistry, pharmacology, perioperative prophylaxis regimens, and guidelines for regional anesthetic management. Anesth Analg. 1997;85:874-85.

[5] Birkmeyer NJO, Finks JF, Carlin AM, Chengelis DL, Krause KR, Hawasli AA, et al. Comparative Effectiveness of Unfractionated and Low-Molecular-Weight Heparin for Prevention of Venous Thromboembolism Following Bariatric Surgery. Arch Surg-Chicago.2012;147:994-8.

[6] Imberty A, Lortat-Jacob H, Perez S. Structural view of glycosaminoglycan-protein interactions. Carbohydrate research. 2007;342:430-9.

[7] Geerts WH, Jay RM, Code KI, Chen E, Szalai JP, Saibil EA, et al. A comparison of low-dose heparin with low-molecular-weight heparin as prophylaxis against venous thromboembolism after major trauma. The New England journal of medicine. 1996;335:701-7.

[8] Planes A. Review of bemiparin sodium--a new second-generation low molecular weight heparin and its applications in venous thromboembolism. Expert opinion on

pharmacotherapy. 2003;4:1551-61.
[9] Chapman TM, Goa KL. Bemiparin: a review of its use in the prevention of venous thromboembolism and treatment of deep vein thrombosis. Drugs. 2003;63:2357-77.
[10] Agnelli G, George DJ, Kakkar AK, Fisher W, Lassen MR, Mismetti P, et al. Semuloparin for thromboprophylaxis in patients receiving chemotherapy for cancer. The New England journal of medicine. 2012;366:601-9.
[11] Coyne E. From heparin to heparin fractions and derivatives. Seminars in thrombosis and hemostasis. 1985;11:10-2.
[12] Linhardt RJ, Loganathan D, al-Hakim A, Wang HM, Walenga JM, Hoppensteadt D, et al. Oligosaccharide mapping of low molecular weight heparins: structure and activity differences. Journal of medicinal chemistry. 1990;33:1639-45.
[13] Cosmi B, Palareti G. Old and new heparins. Thrombosis research. 2012;129:388-91.
[14] Melnikova I. The anticoagulants market. Nat Rev Drug Discov. 2009;8:353-4.
[15] Ingle RG, Agarwal AS. A world of low molecular weight heparins (LMWHs) enoxaparin as a promising moiety--a review. Carbohydr Polym. 2014;106:148-53.
[16] Sola RJ, Griebenow K. Chemical glycosylation: new insights on the interrelation between protein structural mobility, thermodynamic stability, and catalysis. FBS Lett. 2006;580:1685-90.
[17] Galonic DP, Gin DY. Chemical glycosylation in the synthesis of glycoconjugate antitumour vaccines. Nature. 2007;446:1000-7.
[18] Bohe L, Crich D. A propos of glycosyl cations and the mechanism of chemical glycosylation; the current state of the art. Carbohydrate research.2015;403:48-59.
[19] Crich D. Mechanism of a chemical glycosylation reaction. Acc Chem Res. 2010;43:1144-53.
[20] Durand G, Seta N. Protein glycosylation and diseases: Blood and urinary oligosaccharides as markers for diagnosis and therapeutic monitoring. Clin Chem. 2000;46:795-805.
[21] Nigudkar SS, Demchenko AV. Stereocontrolled 1,2-cis glycosylation as the driving force of progress in synthetic carbohydrate chemistry. Chem Sci.

2015;6:2687-704.
[22] Hansen SU, Miller GJ, Cole C, Rushton G, Avizienyte E, Jayson GC, et al. Tetrasaccharide iteration synthesis of a heparin-like dodecasaccharide and radiolabelling for in vivo tissue distribution studies. Nat Commun. 2013;4:2016.
[23] Goldberg M, Gomez-Orellana I. Challenges for the oral delivery of macromolecules. Nat Rev Drug Discov. 2003;2:289-95.
[24] Park K, Kim YS, Lee GY, Nam JO, Lee SK, Park RW, et al. Antiangiogenic effect of bile acid acylated heparin derivative. Pharmaceutical research. 2007;24:176-85.
[25] Kim SK, Lee DY, Lee E, Lee YK, Kim CY, Moon HT, et al. Absorption study of deoxycholic acid-heparin conjugate as a new form of oral anti-coagulant. Journal of controlled release : official journal of the Controlled Release Society. 2007;120:4-10.
[26] Kim SK, Lee DY, Kim CY, Nam JH, Moon HT, Byun Y. A newly developed oral heparin derivative for deep vein thrombosis: non-human primate study. Journal of controlled release : official journal of the Controlled Release Society. 2007;123:155-63.
[27] Hwang SR, Seo DH, Al-Hilal TA, Jeon OC, Kang JH, Kim SH, et al. Orally active desulfated low molecular weight heparin and deoxycholic acid conjugate, 6ODS-LHbD, suppresses neovascularization and bone destruction in arthritis. Journal of controlled release : official journal of the Controlled Release Society. 2012;163:374-84.
[28] Kim SK, Vaishali B, Lee E, Lee S, Lee YK, Kumar TS, et al. Oral delivery of chemical conjugates of heparin and deoxycholic acid in aqueous formulation. Thrombosis research. 2006;117:419-27.
[29] Park JW, Jeon OC, Kim SK, Al-Hilal TA, Lim KM, Moon HT, et al. Pharmacokinetic evaluation of an oral tablet form of low-molecular-weight heparin and deoxycholic acid conjugate as a novel oral anticoagulant. Thrombosis and haemostasis. 2011;105:1060-71.
[30] Al-Hilal TA, Chung SW, Alam F, Park J, Lee KE, Jeon H, et al. Functional transformations of bile acid transporters induced by high-affinity macromolecules.

Sci Rep. 2014;4:4163.
[31] Al-Hilal TA, Park J, Alam F, Chung SW, Park JW, Kim K, et al. Oligomeric bile acid-mediated oral delivery of low molecular weight heparin. Journal of controlled release : official journal of the Controlled Release Society. 2014;175:17-24.
[32] Rabenstein DL. Heparin and heparan sulfate: structure and function. Nat Prod Rep. 2002;19:312-31.
[33] Park JW, Jeon OC, Kim SK, Al-Hilal TA, Jin SJ, Moon HT, et al. High antiangiogenic and low anticoagulant efficacy of orally active low molecular weight heparin derivatives. Journal of controlled release : official journal of the Controlled Release Society. 2010;148:317-26.
[34] Benedict SR. A reagent for the detection of reducing sugars. 1908. The Journal of biological chemistry. 2002;277:e5.
[35] Nichifor M, Carpov A. Bile acids covalently bound to polysaccharides 1. Esters of bile acids with dextran. Eur Polym J. 1999;35:2125-9.
[36] Park J, Jeong JH, Al-Hilal TA, Kim JY, Byun Y. Size Controlled Heparin Fragment-Deoxycholic Acid Conjugate Showed Anticancer Property by Inhibiting $VEGF_{165}$. Bioconjugate chemistry. 2015;26:932-40.
[37] Li W, Johnson DJ, Esmon CT, Huntington JA. Structure of the antithrombin-thrombin-heparin ternary complex reveals the antithrombotic mechanism of heparin. Nat Struct Mol Biol. 2004;11:857-62.
[38] Kim SK, Lee DY, Kim CY, Moon HT, Byun Y. Prevention effect of orally active heparin derivative on deep vein thrombosis. Thrombosis and haemostasis. 2006;96:149-53.

Chapter: 3

Oral delivery of bile acid conjugated nanocomplex using heparin and protamine

3.1. Introduction

Oral delivery is the most clinically acceptable delivery route for patients. However, it is hard to deliver some therapeutic agents including macromolecule, peptide and gene via oral route. For decades, several researchers have tried to develop an oral agent for macromolecule delivery [1, 2]. Especially, nanoparticles and nanocomplex are remarkable carriers for a therapeutic agent, however, they are not usually available as an oral tablet [3, 4].

Despite many advantages, oral delivery of nanoparticle and complex face several problems to overcome in the GI tract [4]. The gastric mucosa maintained acidic pH, and there are a lot of enzyme and bacteria in the intestine. To penetrate various barriers in on the epithelial surface, nanocarriers need an active uptake mechanism using receptors or transporters in the intestine.

In our previous studies, we introduced macromolecule based bile acid conjugates for oral delivery [5-8]. DOCA conjugation has been found to promote the intestinal absorption of macromoles [9, 10]. Moreover, oral delivery technique with bile acid has been improved in recent years [11, 12].

Here, we developed a new nanocomplex using two FDA-approved biomaterials for oral delivery. A negatively charged heparin and positively charged peptide named protamine have shown clinical therapeutic potential [13-15]. Using the polysaccharide, peptide and bile acids, we could design an orally available nanocomplex. It was possible to control the surface charge and the size of nanoparticle by using the formulation of heparin and protamine. Moreover, the bile acids in nanoparticle enhanced the oral delivery of the nanocomplex via the interaction with bile acid transporters. Nanocomplex with caco-2 and MDCK cell

was studied. Cy5-conjugated nanocomplex was treated to rats and mice, and the signal was measured. This study would provide therapeutic potential for advanced drug delivery system.

3.2. Materials and methods

3.2.1. Materials

LMWH (Nadroparin) was obtained from the Nanjing King-Friend Biochemical Pharmaceutical Company Ltd. (Nanjing, China). Deoxycholic acid (DOCA), N-hydroxylsuccinimide (NHS), protamine sulfate and 1-ethyl-3-(3-dimethylaminopropyl)carbodiimide (EDAC) were purchased from Sigma chemical Co. (St. Louis, MO, USA).

3.2.2. Synthesis and preparation of oral nanocomplex

Protamine sulfate or LMWH with Et-DOCA (N-deoxycholylethylenediamine) were reacted using EDAC and NHS in water/DMF at room temperature for 12 h. Then, the products were purified by acetone precipitation, followed by ethanol. The purity of products was checked by TLC. Protamine-DOCA and LMWH-DOCA were lysophilzed after dissolving in DW. Conjugation was checked by 1H NMR and MALDI-TOF MS. After synthesis, nanocomplexes were prepared by mixing protamine-DOCA and LMWH or protamine and LMWH-DOCA in solution.

3.2.3. Cell viability test

Toxicity of materials was evaluated by using caco-2 cell. At first, caco-2 cell was cultured in DMEM high glucose medium supplemented with 10% (v/v) FBS, penicillin–streptomycin, NEAA (non-essential amino acids), sodium bicarbonate and HEPES (4-(2-hydroxyethyl)-1-piperazineethanesulfonic acid). When 96-well plate was confluent with caco-2 cells, the media were replaced with DMEM containing LMWH-DOCA and Protamine DOCA and their nanocomplexes

in different concentrations. After incubation at 37°C for 10 h, the media were removed. DMEM (100 μL) with 10 μL of CCK-8 solution was added to each well, and then the plate was additionally incubated for 1 h. Cell viability was calculated using a microplate fluorescence reader from the absorbance value (OD 450 nm – OD 600 nm) compared with that of untreated group.

3.2.4. Nanocomplex analysis

The size distribution of LMWH- DOCA based nanocomplex were measured using dynamic light scattering instrument at 0.5 mg/mL. The images of the Nanocomplex were captured through scanning electron microscope (SEM) and transmission electron microscopy (TEM). The stability test was conducted in acidic and basic condition. The pH of drinking water was adjusted using 1N HCl and NaOH solution.

3.2.5. Cell binding and uptake study of nanocomplex

MDCK, MDCK-ASBT and caco-2 cells were cultured in DMEM high glucose medium. Transfected MDCK cells by the human ASBT gene (SLC10A2) were prepared in our previous work. ASBT over-expressed MDCK or MDCK cells were incubated with the nanocomplex in FBS-free DMEM with 2 % DMSO. After incubation, the cells were washed with FBS containing DMEM medium several times, and then fixed by using cold 4 % paraformaldehyde. The plates were washed with normal saline, and hoechst 33258 solution was added. In the case of caco-2 cell line, phalloidin-FITC was treated. The fluorescence images were acquired and analyzed by using a confocal laser scanning microscopy (Carl Zeiss LSM710, Germany).

3.2.6. Animal study after oral administration

All procedures for animal experiments were approved by the Committee of the Use and Care on Animals according to the regulations of the Institutional Animal Ethics Committee of the Seoul National University animal care facility. 7-week-old male C57BL/6 and BALB/c nude mice were obtained from Orient Bio

Inc. (Seungnam, South Korea). They were acclimatized for 2 weeks, and then fasted for 12 h. The oral nanocomplex-cy5 solution with 2 % DMSO was administrated to mice. BALB/c nude mice were used for body distribution image, and C57BL/6 mice were sacrificed in each time point. The intestine and other organs were washed more than 4 times with normal saline, and then fixed by using 10% formalin solution.

3.3. Results

3.3.1. Characterization of oral nanocomplex with protamine and heparin-DOCA

Protamine/heparin-DOCA nanocomplex and heparin/protamine-DOCA nanocomplex were made by mixing two different charged materials (**Figure 3.1**). Stable nanocomplexes could be generated by the charge-to-charge interaction. Both positively and negatively charged nanocomplexes were initially prepared. However, positively charged nanocomplex (protamine-DOCA oversaturated) showed cytotoxicity in high concentration. Unlike blood stream, orally administrated materials could exist in high dose in local area of the GI tract. Therefore, orally available nanocomplex should not have any cytotoxicity even in high dose.

Negatively charged nanocomplex (heparin-DOCA oversaturated) showed no significant toxicity (**Figure 3.2**). They were stable in drinking water, and the size of the nanocomplex was approximately 150 nm in DLS analysis (**Figure 3.3**). The nanocomplex remained stable in pH 2, 7 and 9. The morphology of nanocomplex was visualized in detail by using transmission electron microscope and Scanning electron microscope (**Figure 3.4**).

.

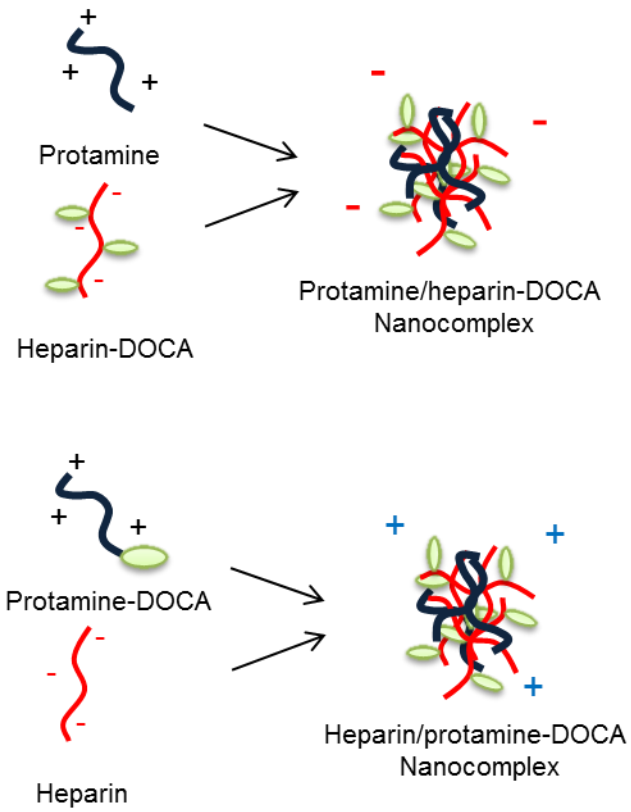

Figure 3.1. Molecular scheme of formulating heparin-DOCA oversaturated nanocomplex and protamine-DOCA oversaturated nanocomplex. The net charge of nanocomplex can be controlled by formulation.

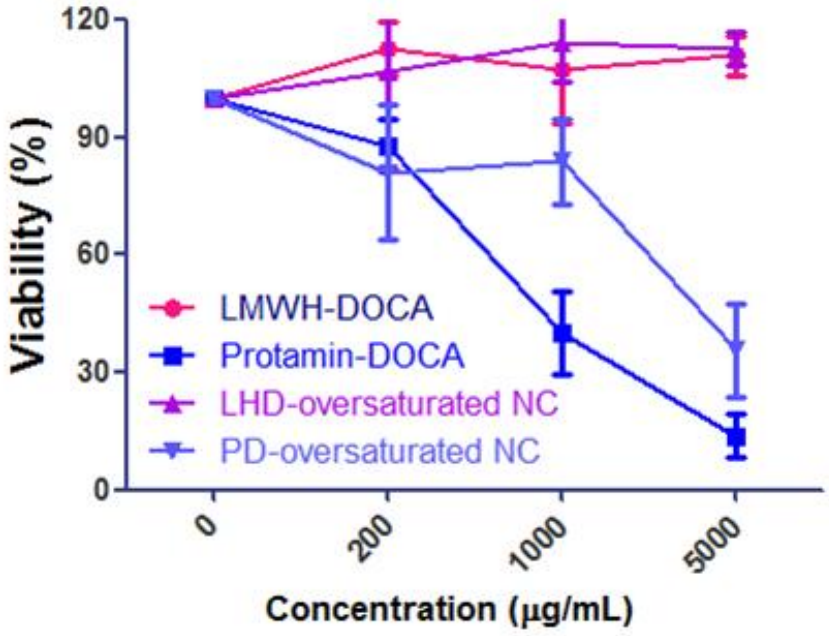

Figure 3.2. Caco-2 cell viability test using high dose of LMWH-DOCA, Protamine-DOCA, heparin-DOCA (LHD) oversaturated nanocomplex and Protamine-DOCA (PD) oversaturated nanocomplex. Positively charged materials showed cytotoxicity.

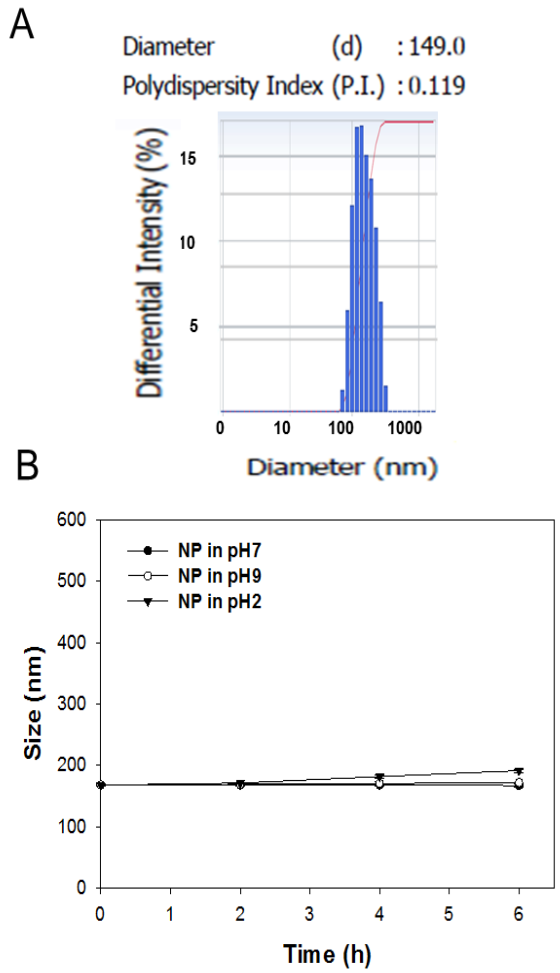

Figure 3.3. (A) Molecular size distribution of negatively charged nanocomplex. The average diameter of nanocomplex was 149.0 (B) Stability of nanocomplex in drinking water (in different pH condition).

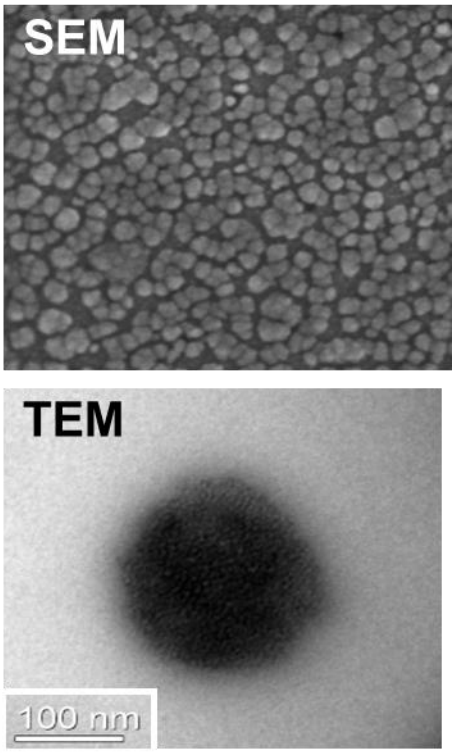

Figure 3.4. SEM and TEM image of negatively charged nanocomplexes (protamine/heparin and protamine/heparin-DOCA based nanocomplexes).

3.3.2. Absorption mechanism study of oral nancomplex

In this experiment, DOCA was conjugated to nanocomplexes to increase the interaction between nanocomplexes and bile acid transporters in the ileum for oral delivery. It needed to confirm that the conjugated DOCA in nanocomplex could bind to apical sodium bile acid transporter (ASBT). Before starting cell related experiments, Cy5 NHS ester (lumiprobe), fluoresceinamine or fluorescein isothiocyanate isomer was conjugated to the molecular structure of protamine or heparin-DOCA.

Caco-2 cells were cultured in DMEM high glucose medium supplemented with 10% (v/v) FBS, penicillin–streptomycin and HEPES. Then, the nanocomplex that consists of protamine-cy5 and LMWH-FITC-DOCA was treated to the caco-2 cells at 37 ℃. The fluorescence images with caco-2 cell at each time point were acquired by using a confocal laser scanning microscopy (Carl Zeiss LSM710, Germany). After treatment, nanocomplexes could bind to the caco-2 cell surface, and remained. About 1 h later, nanocomplexes started to penetrated into the cell, then, there are lots of nanocomplexes detected in the cytoplasm (**Figure 3.5**).

To confirm the binding and uptake of nanocomplex on cell surface, ASBT overexpressed MDCK cell was cultured in high glucose DMEM. Then, the nanocomplex was treated into the plate, and after incubation the cells were fixed. In confocal image, the nanocomplex showed better the cellular binding and uptake in MDCK-ASBT than MDCK cell (**Figure 3.6-7**). The image with ASBT (20nm-gold antibody) and the nanocomplex was also acquired by using TEM.

This nanocomplex could bind to the ASBT on caco-2 and MDCK cell. It means that nanocomplex could be delivered by transcellular route. Since chitosan based nanoparticle developed nanoparticle and complex have been considered to be absorbed via paracellular route (**Figure 3.8**). In the cell experiment, phalloidin fluorescein isothiocyanate (FITC) was treated with nanocomplex to caco-2 cells to detect tight junctions. As a result, nanocomplexes were not in the tight junctions but they were present in the transcellular region. It means that chitosan-based positive nanoparticles and this nanocomplex could be absorbed in different ways.

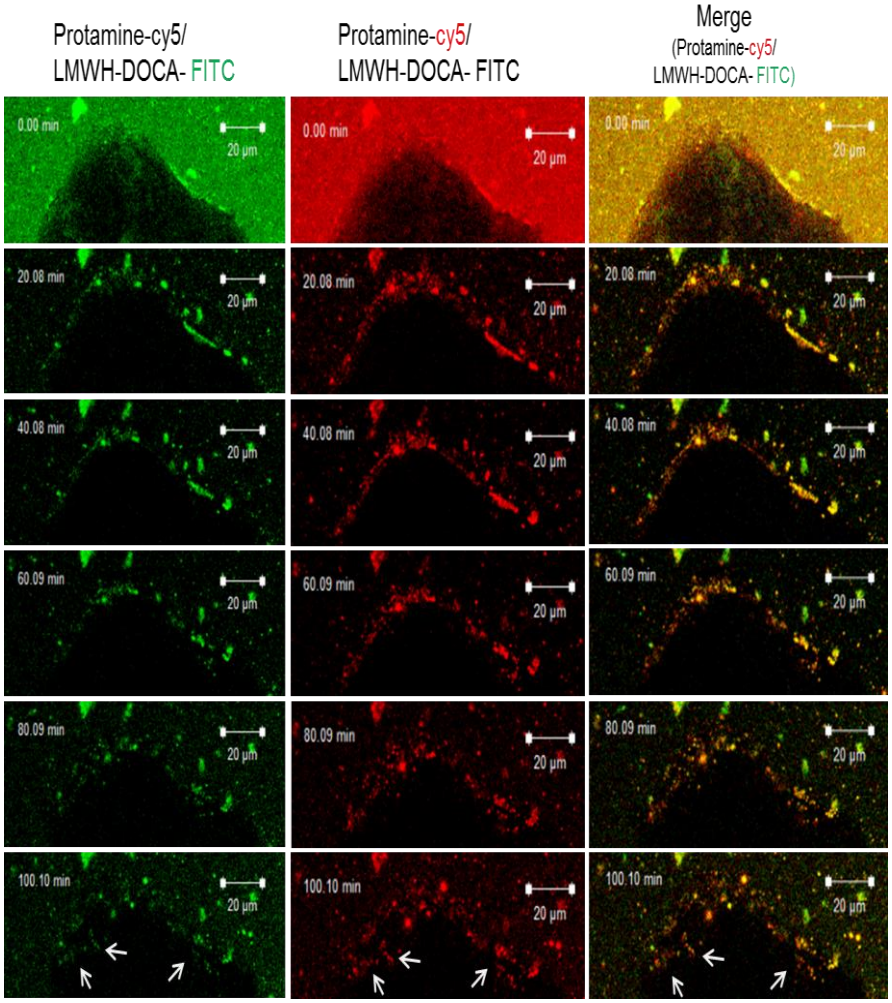

Figure 3.5. The images of nanocomplex treated caco-2 cell. Nanocomplexes could bind and penetrate slowly into the cell after treatment. Protamine was conjugated to FITC (green), and LMWH-DOCA was conjugated to cy5.

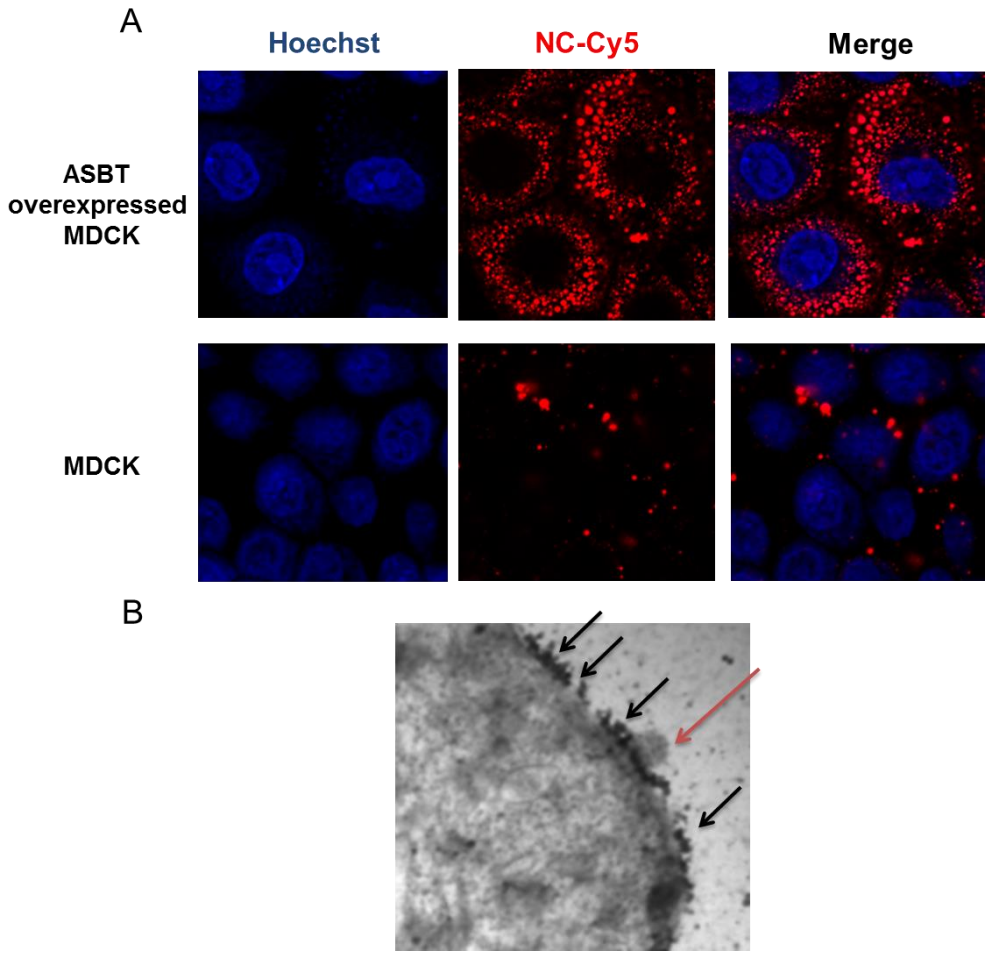

Figure 3.6. (A) The confocal image of nanocomplex (NC) treated ASBT overexpressed MDCK cell. (B) TEM image of ASBT-MDCK after the nanocomplex treatment.

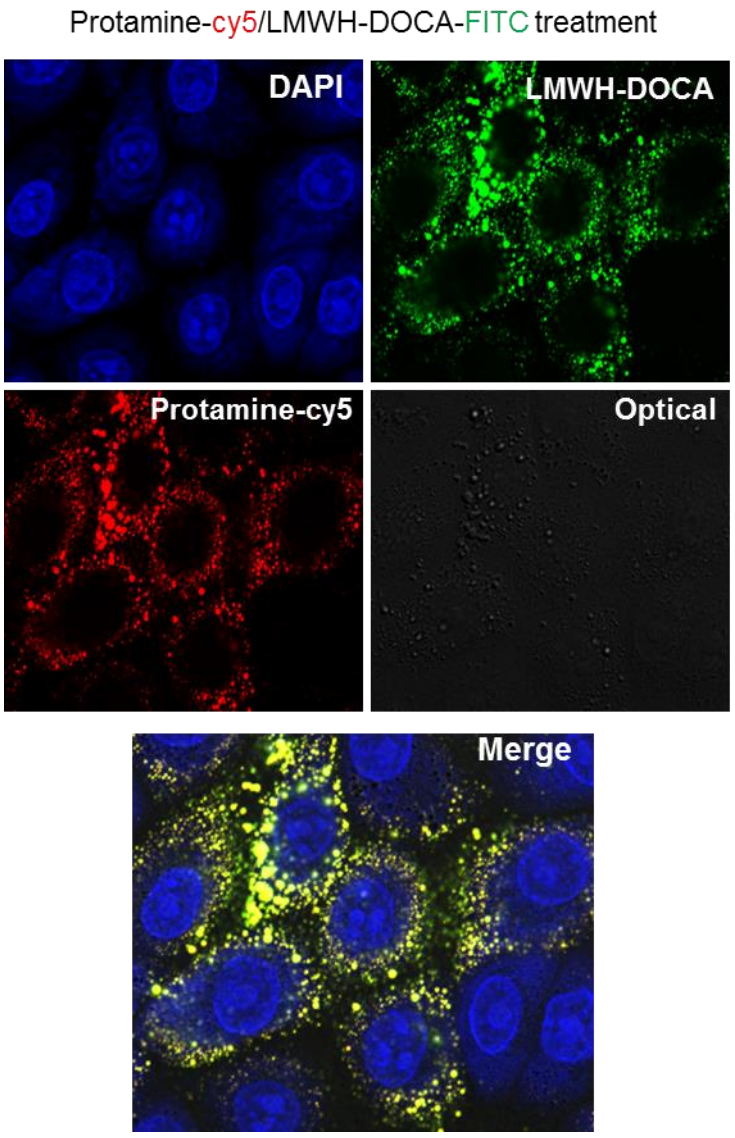

Figure 3.7. The confocal image of nanocomplex(NC) treated ASBT overexpressed MDCK cell. The signal from protamine-cy5.5 (red) and LMWH-DOCA(green) could be overlapped.

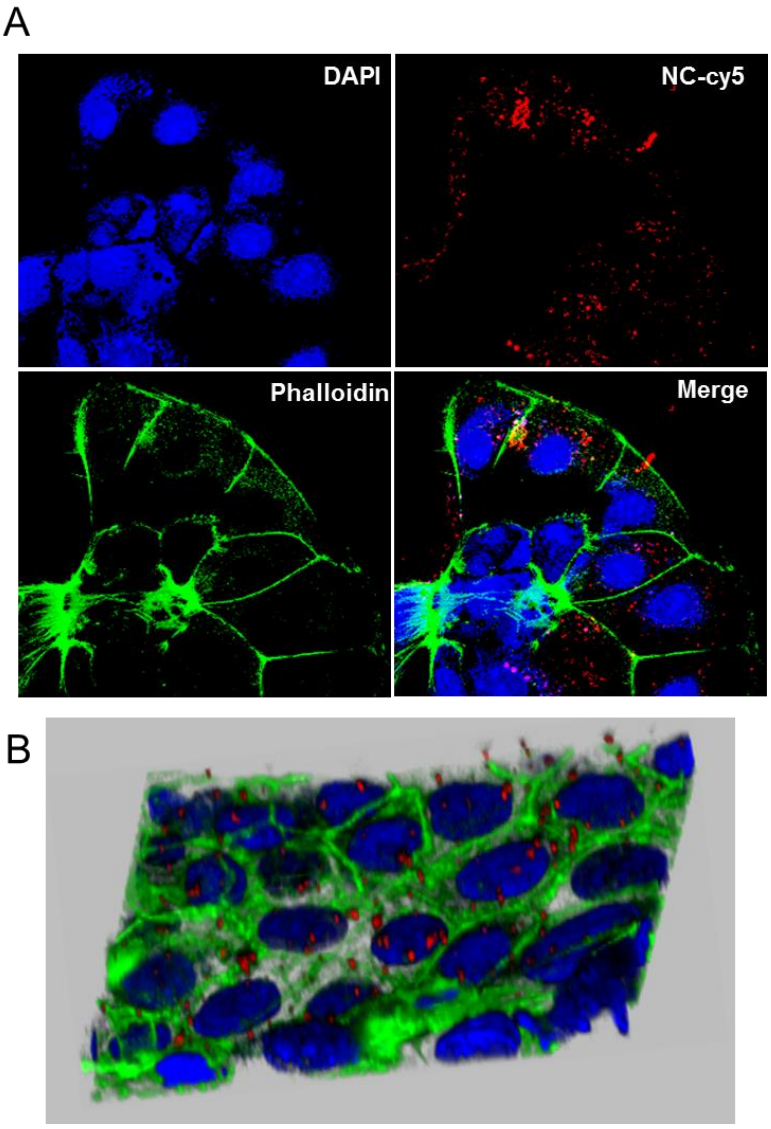

Figure 3.8. Representative confocal images of caco-2 showed the binding and uptake of nanocomplex-cy5 (red). Phalloidin-fluorescein isothiocyanate (FITC) was used to detect tight junctions (green).

3.3.3. Animal study after oral treatment of nanocomplex

The Cy5-conjugated nancomplex was treated to rats and mice via oral route to confirm that the nanocomplex could interact with ASBT in the ileum and then be absorbed. The orally treated nanocomplexs were detected in the intestine in mice after oral administration. However, the results from PK study using rats showed that there is no significant amount of nanocomplex in the blood (**Figure 3.9**). Absorbed nanocomplexes stayed in the small intestine (**Figure 3.10-11**). The retention period of the nanocomplexes was also measured via cy5 signal. As a result, the intensity in the ileum lasts more than 1 – 3 days. The section image of the ileum in mice showed that nanocomplexes in the villi after oral nanocomplex treatment (8 h) (**Figure 3.12-13**). The signal in the ileum was strong than any other part in the intestine.

3.4. Discussion

The oral delivery of drug, peptide or gene is the most practical way for continuous daily dosing to patients for therapy. Although nanoparticles and nanocomplexes have shown great targeting and therapeutic effect, they were restricted to be used only by parenteral injection. Many research groups have tried to develop new nanoparticles and complexes, however, a few researchers tried to use oral nanoparticles. Cosidering biological barrier in the small intestine, the oral delivery of nanoparticle is not easy. Oral delivery of nanopaticle has great therapeutic potentials, but, the low bioavailability of oral nanoparticle indicates that it could not be delivered effectively into the bloodstream in an oral form. Using the enterohepatic circulation, bile acid conjugated nanocomplex was tested after oral administration. In the result, the oral nanocomplexes showed cellular uptake and binding *in vitro* and *in vivo* experiments. The orally treated nanocomplexs were detected in the intestine, then they stayed there for a while. Oral delivery to the epithelial cells in the ileum showed promising potential as a new oral nanocomplex.

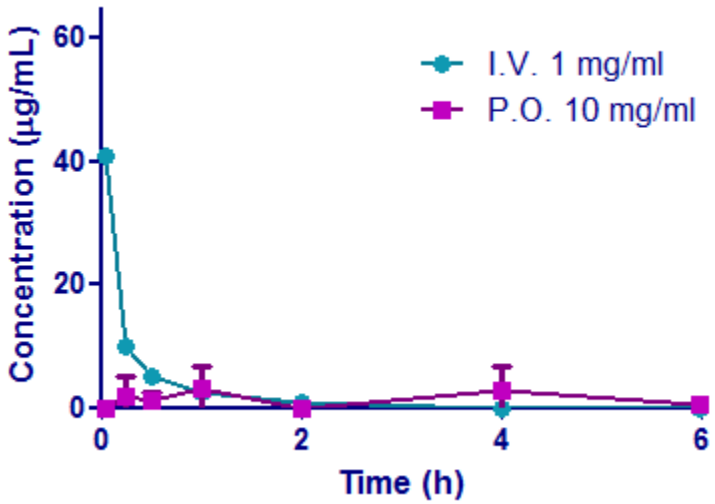

Figure 3.9. PK study of nanocomplex in rats

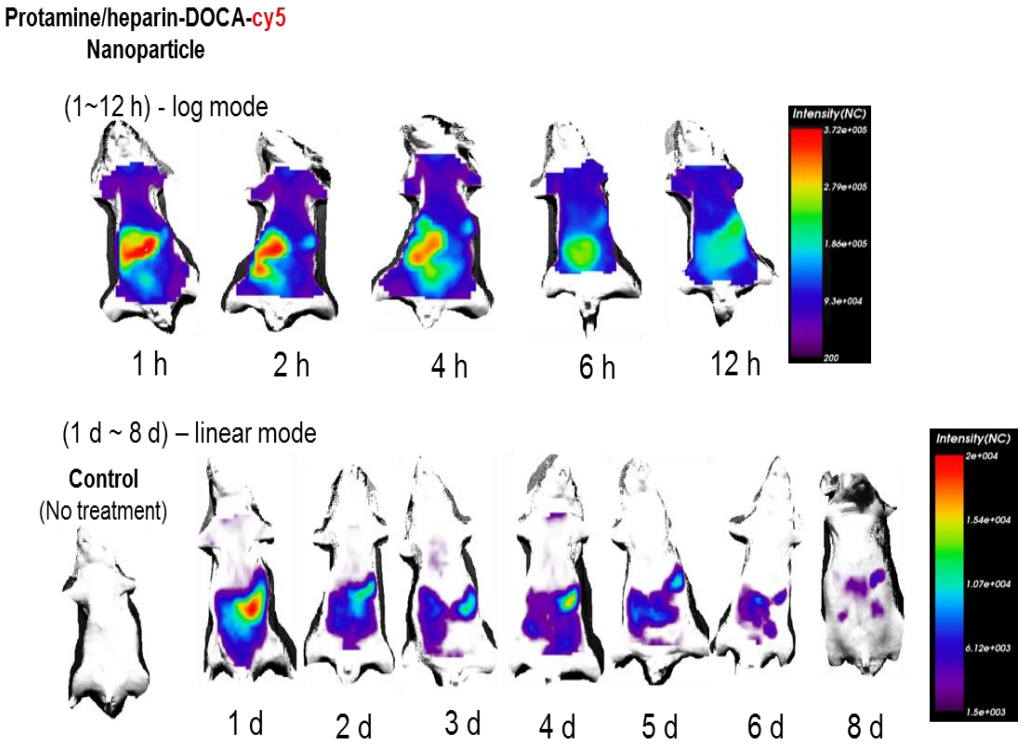

Figure 3.10. Body distribution images of mice after oral administration of nanocomplex. The signal from cy5 group in nanocomplex was measured. The signal in abdominal region lasts for a few days.

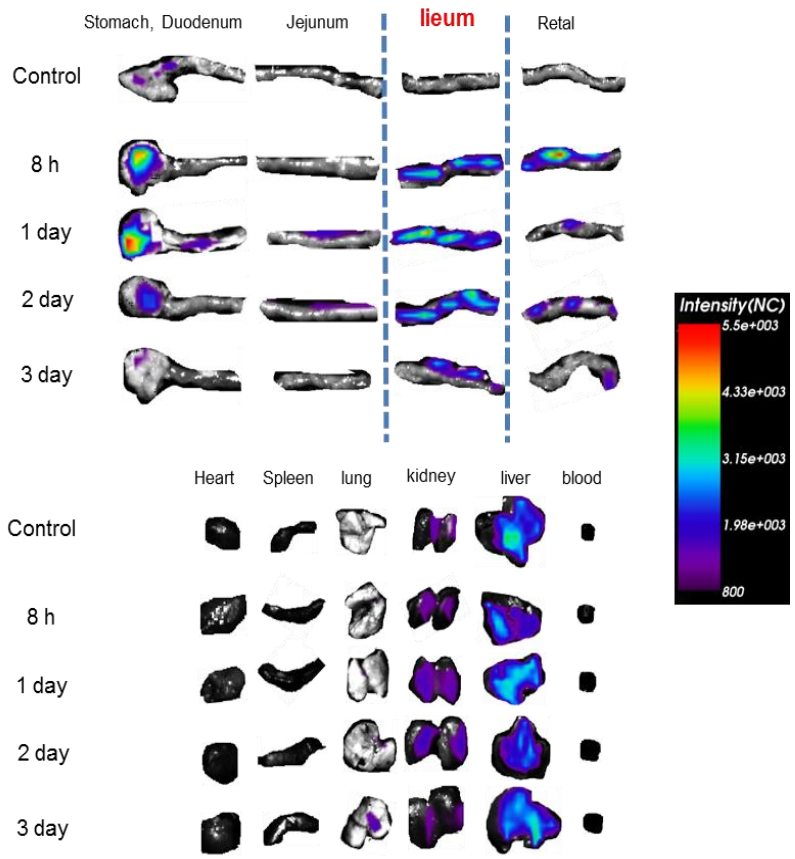

Figure 3.11. Organ distribution images of mice. The ileum showed strong signal than other organs.

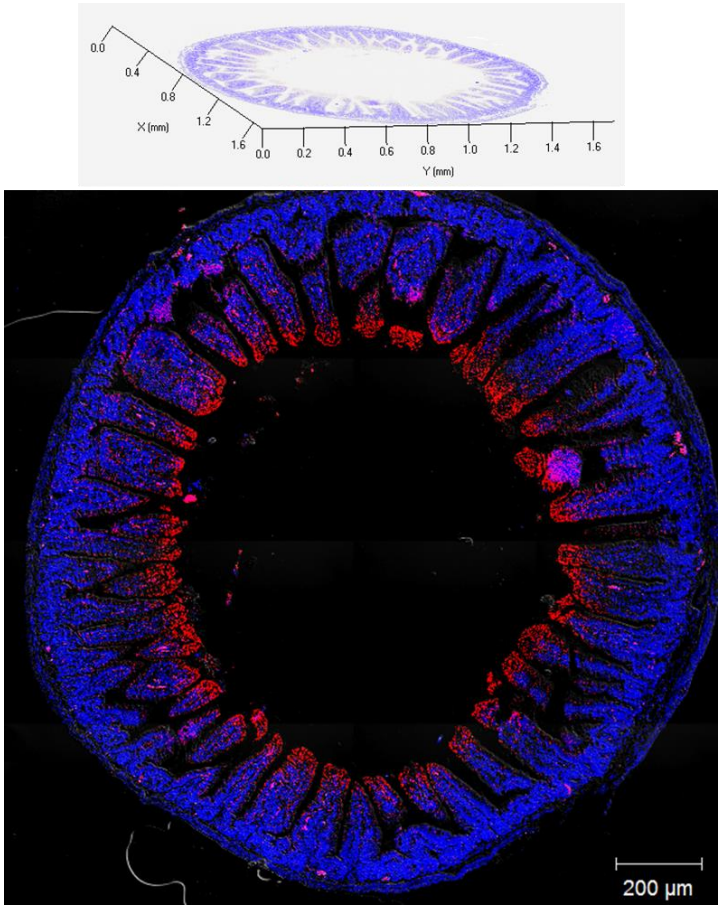

Figure 3.12. The section image of the ileum in mice after oral nanocomplex treatment (8 h). There are cy5 fluorescent signal from nanocomplex in intestinal tissue.

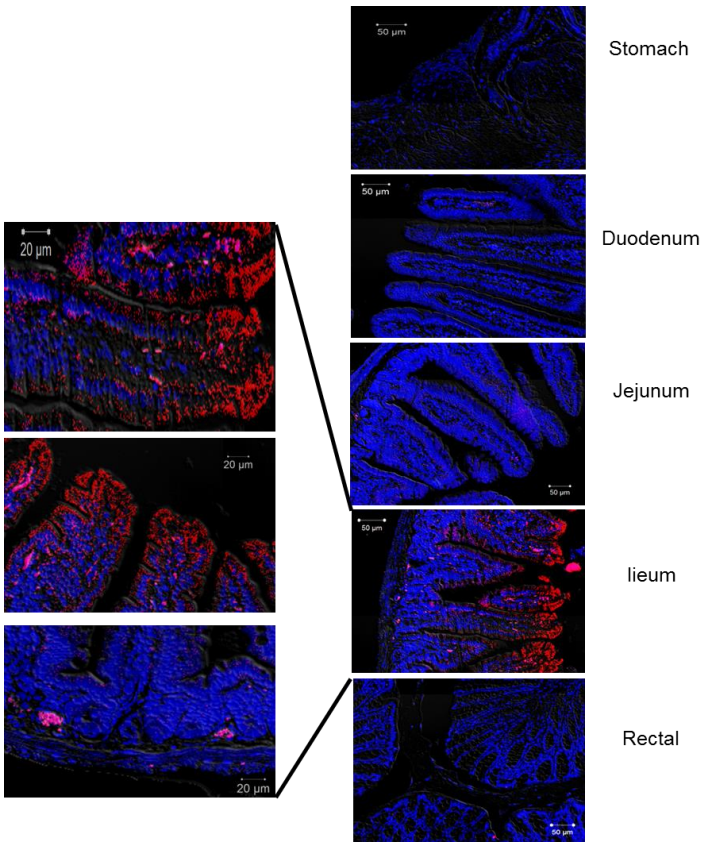

Figure 3.13. The image of the organs including the stomach, ileum and rectal. The ileum showed strong signal than other parts.

3.5. Conclusion

Orally available nanocomplexes would shield gene and drugs from harsh condition in the intestine, and overcome the limitations of current nanoparticle system. Safe heparin, bile acid and protamine based nanocomplex showed potential to deliver biomaterials to the ileum in the small intestine via ASBT without toxicity. ASBT mediated nanocomplex delivery system will be suitable for targeted, sustained delivery of therapeutic macromolecules into the GI tract. The oral delivery of safe and functional nanocomplexes would invoke the benefits of advanced oral delivery system providing a clinical therapeutic potential.

References

[1] Al-Hilal TA, Alam F, Byun Y. Oral drug delivery systems using chemical conjugates or physical complexes. Adv Drug Deliver Rev. 2013;65:845-64.

[2] Hwang SR, Byun Y. Advances in oral macromolecular drug delivery. Expert Opin Drug Deliv.2014;11:1955-67.

[3] Pridgen EM, Alexis F, Kuo TT, Levy-Nissenbaum E, Karnik R, Blumberg RS, et al. Transepithelial transport of Fc-targeted nanoparticles by the neonatal fc receptor for oral delivery. Sci Transl Med.2013;5:213.

[4] Ensign LM, Cone R, Hanes J. Oral drug delivery with polymeric nanoparticles: the gastrointestinal mucus barriers. Adv Drug Deliv Rev. 2012;64:557-70.

[5] Park K, Kim YS, Lee GY, Nam JO, Lee SK, Park RW, et al. Antiangiogenic effect of bile acid acylated heparin derivative. Pharmaceutical research. 2007;24:176-85.

[6] Kim SK, Lee DY, Lee E, Lee YK, Kim CY, Moon HT, et al. Absorption study of deoxycholic acid-heparin conjugate as a new form of oral anti-coagulant. Journal of controlled release : official journal of the Controlled Release Society. 2007;120:4-10.

[7] Kim SK, Lee DY, Kim CY, Nam JH, Moon HT, Byun Y. A newly developed oral heparin derivative for deep vein thrombosis: non-human primate study. Journal of controlled release : official journal of the Controlled Release Society. 2007;123:155-63.

[8] Hwang SR, Seo DH, Al-Hilal TA, Jeon OC, Kang JH, Kim SH, et al. Orally active desulfated low molecular weight heparin and deoxycholic acid conjugate, 6ODS-LHbD, suppresses neovascularization and bone destruction in arthritis. Journal of controlled release : official journal of the Controlled Release Society. 2012;163:374-84.

[9] Kim SK, Vaishali B, Lee E, Lee S, Lee YK, Kumar TS, et al. Oral delivery of chemical conjugates of heparin and deoxycholic acid in aqueous formulation. Thrombosis research. 2006;117:419-27.

[10] Park JW, Jeon OC, Kim SK, Al-Hilal TA, Lim KM, Moon HT, et al. Pharmacokinetic evaluation of an oral tablet form of low-molecular-weight heparin and deoxycholic acid conjugate as a novel oral anticoagulant. Thrombosis and haemostasis. 2011;105:1060-71.

[11] Al-Hilal TA, Chung SW, Alam F, Park J, Lee KE, Jeon H, et al. Functional transformations of bile acid transporters induced by high-affinity macromolecules. Sci Rep. 2014;4:4163.

[12] Al-Hilal TA, Park J, Alam F, Chung SW, Park JW, Kim K, et al. Oligomeric bile acid-mediated oral delivery of low molecular weight heparin. Journal of controlled release : official journal of the Controlled Release Society. 2014;175:17-24.

[13] Thu MS, Bryant LH, Coppola T, Jordan EK, Budde MD, Lewis BK, et al. Self-assembling nanocomplexes by combining ferumoxytol, heparin and protamine for cell tracking by magnetic resonance imaging. Nat Med. 2012;18:463-7.

[14] Hirsh J. Heparin. The New England journal of medicine. 1991;324:1565-74.

[15] Cosmi B, Palareti G. Old and new heparins. Thrombosis research. 2012;129:388-91.

Part B: Development of angiogenesis inhibitors using heparin conjugates

Chapter: 4

Antiangiogenic effect of orally available size-controlled heparin fragment and deoxycholic acid conjugates

4.1. Introduction

Heparin is a highly sulfated, long and linear polysaccharide which is widely used clinically as an anticoagulant [1, 2]. Heparin can also bind to a variety of proteins including growth factors, growth factor receptors and chemokines since heparin has a similar structure to heparan sulfate which is present on endothelial cell surface and in extracellular matrix (ECM) [3, 4]. Among growth factors, the members of VEGF family are key regulators of normal and pathological angiogenesis [5]. In particular $VEGF_{165}$ stands out primarily having a heparin-binding domain consisting of arginine and lysine residues [6].

Unfractionated heparin (UFH) is a polydispersed biomaterial with a molecular weight ranging from 5000~40000 Da and an average molecular weight of 12000 Da [1]. Low molecular weight heparin (LMWH) is generally prepared through the controlled, chemical or enzymatic depolymerization of heparin having an average molecular weight of 4500~6000 Da [1, 7, 8]. Very low molecular weight heparin (VLMWH), ultra-low molecular weight heparin (ULMWH) or heparin fragments are usually described as a mixture having an average molecular weight of less than 4000 Da. Compared to UFH, smaller heparins have several benefits such as a higher bioavailability, longer half-life, wider therapeutic window and lower bleeding risk [9, 10].

In the recent years, clinical application of heparin of lower molecular weights is preferred due to subsequent reduced adverse effects [11, 12]. ULMWHs such as bemiparin and semuloparin, showed similar or better efficacy than LMWHs, but with lower risk of bleeding and heparin-induced thrombocytopenia (HIT) [13, 14]. Smaller heparins also displayed anti-angiogenic effects potentially better than that of LMWH with a safety profile [15, 16]. Therefore, they have been evaluated in

clinical trials as adjuvants in patients with cancer because they are effective and suitable for long-term treatment [12, 17].

Many researches have shown the anti-angiogenesis effect of heparin on the outgrowth of primary tumor [18]. Several studies also conducted on inhibition of tumor angiogenesis via the targeting of relevant angiogenic growth factors and showed therapeutic results using heparin fragment and heparin-based oligosaccharides [4, 19, 20]. Heparin-based materials competitively bind to heparin-binding growth factors, thereby inhibiting their interaction with heparan sulphate [15, 21]. Structural studies about the heparin-binding site of growth factors provided important information for the optimal size requirement in heparin-based antitumor drug design [19]. Because the recognition of glycosaminoglycan by protein depends on molecular binding, the proper molecular size could be essential for the rational design of carbohydrate-derived drug [22]. The molecular size of unfractionated heparin is enormous, compared to the size of heparin binding domain of growth factors.

In the previous studies, we developed orally active heparin conjugates which can enhance heparin absorption in the intestine using deoxycholic acid (DOCA) [23, 24]. In the oral delivery of heparin-like polysaccharides, bile acid conjugation to heparin proved to be effective for enhancing its absorption in the intestine while eliminating the anticoagulant activity of heparin [25, 26]. The DOCA conjugation has been found to promote the intestinal absorption by enhancing the hydrophobic properties of LMWH and increase the membrane interaction of LMWH without any systemic and local toxicity [27, 28]. The heparin conjugates also showed an enhanced antiangiogenic effect and reduced primary tumor volume [29-32]. An orally available safe heparin conjugate is suitable for a long-term anticancer therapy and it has therapeutic potential to target the other heparin binding growth factors.

In the present study, we synthesized size-controlled heparin fragments in order to find out the size-optimized heparin-based conjugates ideal for inhibiting $VEGF_{165}$ induced angiogenic effects. Moreover, heparin fragments were conjugated with DOCA to minimize the anticoagulant effect as well as enhance oral absorption.

We evaluated the antiangiogenic therapeutic effect of DOCA-conjugated heparin fragments (HFD) using HUVECs and the tumor growth inhibition behavior in tumor animal model. We also proved that HFDs exhibit optimized therapeutic effects in relation to size control. This study could be discussed in terms of the controlled size requirements for heparin-based drug development considering the size of the target.

4.2. Materials and methods

4.2.1. Materials

Heparin, Deoxycholic acid (DOCA), N-hydroxylsuccinimide (NHS), 1-ethyl-3-(3-dimethylaminopropyl)carbodiimide (EDAC), ethylene-diamine, sodium nitrite (NaNO2) and formamide were purchased from Sigma chemical Co. (St. Louis, MO, USA). LMWH (Nadroparin) was obtained from the Nanjing King-Friend Biochemical Pharmaceutical Company Ltd. (Nanjing, China). N,N-dimethylformide (DMF) was purchased from Merck (Darmstadt, Germany). Coatest anti-Factor Xa assay kit was purchased from Chromogenix (Milano, Italy). Growth factor reduced Matrigel was purchased from BD Bioscience. Endothelial basal medium (EBM) were obtained from Clonetics Corp. (San Diego, CA, USA) and endothelial growth medium-2 (EGM-2) was from Lonza (Walkersville, ML, USA). Suramin fragment (disodium 8-amino-1,3,6-naphthalenetrisulfonate) was obtained from TCI (Tokyo Chemical Industry co., Japan). Recombinant vascular endothelial growth factor$_{165}$ was obtained from Peprotech (Rocky Hills, NJ, USA).

4.2.2. Synthesis of size-controlled and deoxycholic acid conjugated heparins

Heparin fragments were prepared by controlled nitrous acid depolymerization of LMWH. Briefly, LMWH (1 g) was dissolved in 20 mL of water and its pH was adjusted to 2 with 1N HCl. $NaNO_2$ was added, and the reaction mixture was incubated at 4 ℃, and stirred for 30 min. The molar ratios between LMWH and $NaNO_2$ were 1:1, 1:2.5 and 1:4. The pH of solution was

adjusted to 6 with NaOH, and then the solution was precipitated in ethanol. Both the precipitant and 100 mg of $NaBH_4$ were dissolved in 20 mL of water, followed by incubation for 1 h. Heparin fragments were recovered by precipitation in ethanol. HFDs were synthesized following the previous procedure [39]. Briefly, heparin fragments and Et-DOCA (N-deoxycholylethylenediamine) were reacted using EDAC and NHS in formamide/DMF at room temperature for 12 h. Then the products were purified by methanol precipitation, followed by ethanol. The purity of products was checked by TLC using methanol solvent.

4.2.3. Characterization

The average molecular weight and polydispersion were measured by gel permeation chromatography (GPC) and mass spectrometer. The lyophilized samples were dissolved in 1 mL of distilled water and further analyzed by GPC using TSK-2000 column at a flow rate of 1 mL/min. The eluted materials were monitored by the refractive index (RI) detector and the eluent was 0.05 M Na_2SO_4 buffer. The dextran standard curve was used for the molecular weight calculation. The synthesized materials were characterized using proton nuclear magnetic resonance (^{1}H NMR, JEOL JNM-LA NMR, Japan). ^{1}H NMR spectra were recorded at 500 MHz using D_2O and DMSO-d_6 as solvent. The chemical conjugation ratio of heparin and deoxycholic acid was determined by analyzing the NMR peaks at 1-1.2 and 5.0-5.5 ppm using mixed LMWH and DOCA solution with different weight ratios.

4.2.4. Anticoagulant activity test

Heparin and heparin conjugates (100 μL) was mixed with 100 μL of antithrombin III (ATIII) solution and incubated at 37 °C for 3 min and 100 μL of Factor Xa (FXa) was added to the solution. The substrate (200 μL) was then added and incubated at 37 °C for 3 min. Anti-FXa activity was calculated from the absorbance at 405 nm by UV/Vis spectrometer (n=3).

4.2.5 Cell viability test

The cytotoxic effect of DOCA conjugated heparin was evaluated by using SCC7 and MDA-MB231 cancer cells, respectively. The cells were seeded into 96-well plate ($1 \times 10_4$ cells /well) in 100 μL of supplemented DMEM. When the plate was confluent with cells, LHD and HFDs were added to reach a total medium volume of 200 μL. The samples were incubated at 37 °C for 24 h. To determine the number of live cells, 10 μL of CCK-8 solution was added to each well and incubated for 1 h. Absorbance was quantified at 450 nm using a microplate fluorescence reader. Cell viability was expressed as a ratio of absorbance by the untreated the control group (n=6).

4.2.6. Endothelial tubular formation assay

HUVECs were cultured in EGM-MV2 medium for 6 days. We prepared a 96-well plate in incubator and a growth factor free Matrigel in ice bath. 100 μL of Matrigel was added to the 96-well plate and incubated for 30 min at 37 °C. Then, HUVECs (4×10^4 cells/well) were placed on the Matrigel and cultured in 50 μL of EBM medium containing $VEGF_{165}$ (40 ng/mL, Peprotech). Then, 50 μL of LHD or HFDs (40 μg/mL) was added. After 6 h of incubation in 5% CO_2 at 37°C, the vessel formation was observed through a reverse phase-contrast photomicroscope and branch points were counted (n=4).

4.2.7. Cell proliferation assay

The anti-proliferation effect of LMWH, LHD and HFDs were assayed with HUVECs with VEGF. Cells were seeded at a density of 1×10^4 cells per well in 100 μL of M199 medium (1% FBS). The samples were incubated with VEGF (10 ng/mL) at 37°C for 72 h and the medium was changed every day. To determine the final cell growth, 10 μL of CCK-8 solution was added. Absorbance was quantified at 450 nm using a microplate fluorescence reader after 2 h. Cell growth was expressed as ratios of absorbance by the $VEGF_{165}$ untreated the control group (n=5).

4.2.8. Wound healing assay

After HUVECs were harvested by trypsin-EDTA, the cells were seeded in a 24-well plate in EGM-MV2 medium. After the cells reached confluence, HUVECs were wounded with a pipet chip by creating a wound in the center of well and incubated further in M199 medium (FBS 1 %) for 2 h. LHD and HFDs were added into each well with different concentrations and incubated with $VEGF_{165}$ (10 ng/mL). The migration of the cells was stopped 24 h later by exchanging the M199 medium with 4 % paraformaldehyde solution. After the cells were fixed for 20 min at 4 °C, they were washed with normal saline, and stained with 0.001 % toluidine blue (Sigma-Aldrich Corp.) for 60 min (n=5).

4.2.9. Tumor growth inhibition by HFDs (SCC7)

SCC7 (murine squamous cell carcinoma) was cultured in high glucose DMEM medium containing 10% fetal bovine serum and antibiotics. After SCC7 cells were harvested, 10-week-old male C3H/HeN mice (Orient Bio, Korea) were injected with cells (1×10^6 cells/60 μL) subcutaneously into the flanks of mice. On day 6, mice in each group received 10 mg/kg daily of HFD1, HFD2 or HFD3, with 2 mg/kg of poloxamer and labrasol as solubilizer. Mice were fasted for 4 h before oral administration. The size of tumor and body weight was daily measured. Tumor volumes were calculated as $a^2 \times b \times 0.52$ (a = width, and b = length) (n=7). All procedures for animal experiment were approved by the Committee on the Use and Care on Animals according to the regulations of the Institutional Animal Ethics Committee of the Seoul National University animal care facility.

4.2.10. Human tumor growth inhibition by HFD2

We investigated the therapeutic effect of HFD2 on growth of human breast cancer (MDA-MB231) in 10-week-old male athymic nude mice (n=7). A subcutaneous tumor was established by inoculating MDA-MB231 cells (1×10^7 cell/100 μL) into the back of a mouse. After sacrifice of the mice, tumor tissues were histologically evaluated by staining with anti-CD34 antibodies and proliferating cell nuclear antigen (PCNA). The number of microvessels was measured by counting in four areas at × 200.

4.2.10. Statistical analysis

We analyzed the results by comparing the means of groups in in vitro and in vivo experiments using one-way analyses of variance (ANOVA) followed by Bonferroni's post-hoc tests using sigmaplot 12. P-values less than 0.05 were considered to be statistically significant.

4.3. Results

4.3.1. Synthesis and Characterization

The heparin fragments were synthesized from LMWH by depolymerization using nitrous acid. The molecular structures are shown in **Figure 4.1,** and the characterizations of these molecules are described in detail in **Table 4.1**. They have different average molecular weights according to the reaction ratio of $NaNO_2$. LHD which is a LMWH and DOCA conjugate, was studied in our previous research [30]. DOCA conjugation was expected to enhance the bile acid transport mediated cellular uptake and eliminate the side effect of heparin for the oral anticancer therapy (**Figure 4.2**). The molecular coupling ratios of DOCA to the LMWH, heparin fragment 1, heparin fragment 2 and heparin fragment 3 were 4.0, 3.0, 1.9 and 1.3, respectively. **Figure 4.3** shows the weight and molecular based coupling ratios of LHD and HFDs.

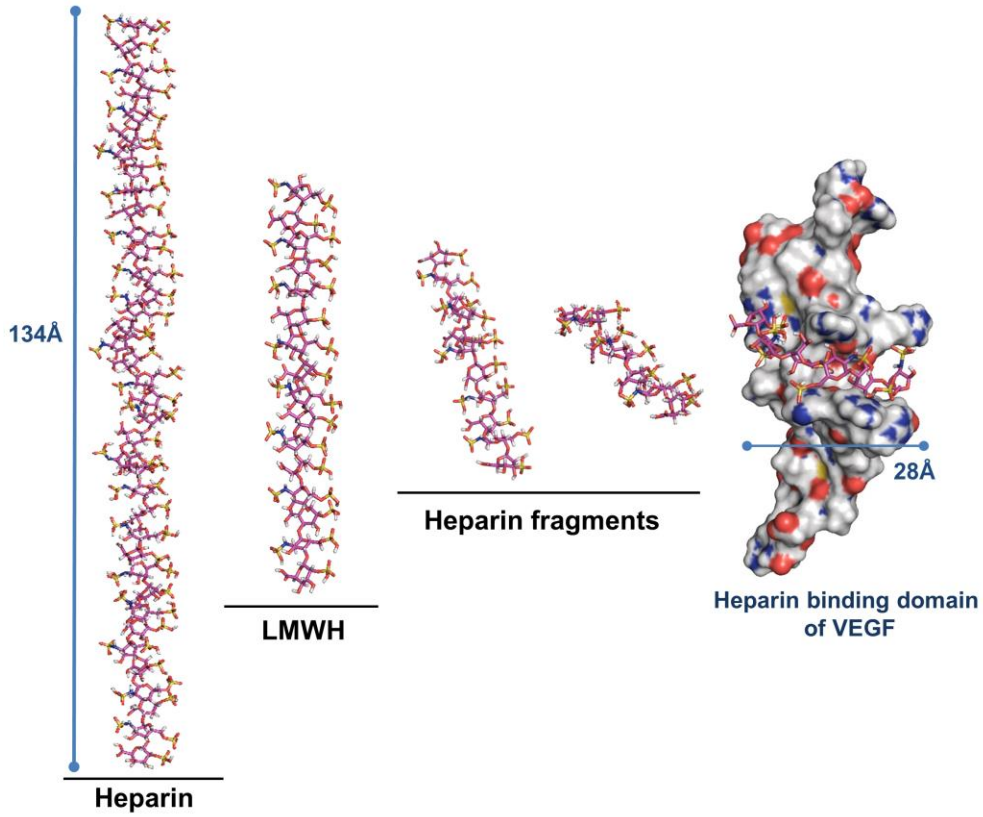

Figure 4.1. Molecular structures of unfractionated heparin (UFH), low molecular weight heparin (LMWH), heparin fragments with the heparin binding domain of vascular endothelial growth factor (VEGF)

Table 4.1. Characterization of low molecular weight heparin (LMWH) and heparin fragments

Materials	Average molecular weight (Da) [a]	Average DP [b]	Polydispersity index [c]	Molecular lengths (Å) [d]	Anti-Xa activity (%) [e]
LMWH	4765	18	1.65	64	100 ± 0.1
Heparin fragment 1	3289	12	1.68	47	92.5 ± 8.2
Heparin fragment 2	1835	7	1.22	25	72.9 ± 2.8
Heparin fragment 3	1443	5	1.04	19	39.6 ± 14.2

[a] Measured and calculated by gel permeation chromatography program

[b] Degree of polymerization (Based on the average molecular weight)

[c] Polydispersity (PD= Mw/Mn, Mw; Weight-average molecular weight, Mn; Number-average molecular weight)

[d] Measured using PyMOL program

[e] Relative activity to LMWH, measured using Coatest anti-FXa chromogenic assay

Results are the mean ± standard deviation

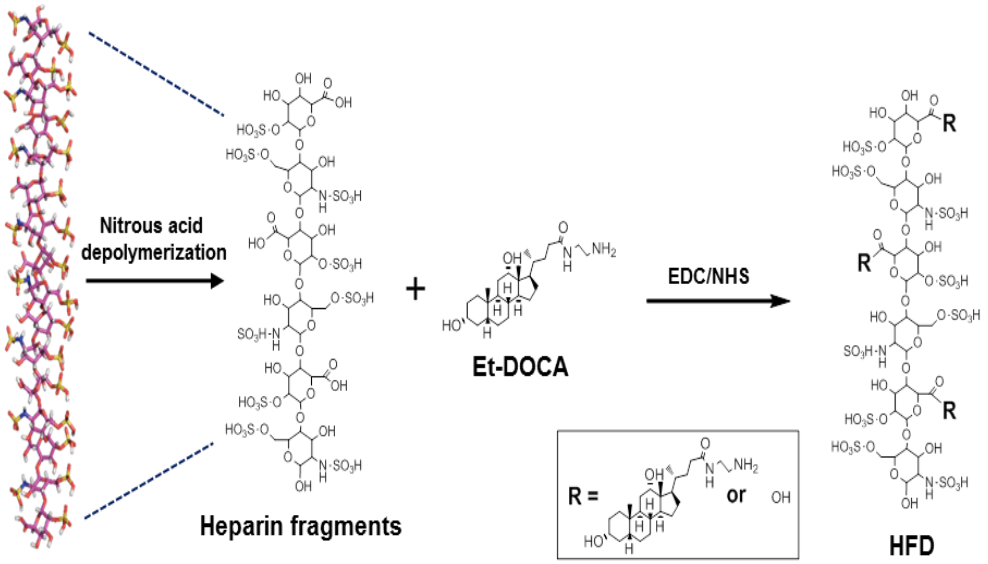

Figure 4.2. Synthetic scheme for the preparation of heparin fragment-deoxycholic acid conjugate (HFD) to eliminate the anticoagulant activity of heparin fragment and enhance the oral uptake. After the size control of heparin using nitrous acid depolymerization, HFD was prepared by deoxycholic acid conjugation.

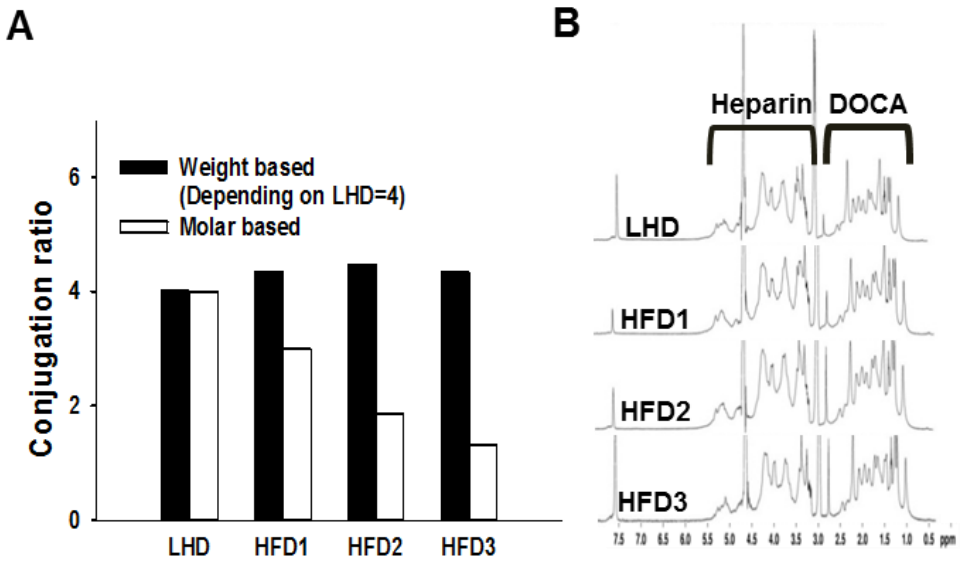

Figure 4.3. (A) Conjugation ratio (B) NMR peak data of LHD and HFDs

4.3.2. Anti-FXa and Cell Viability Assays

The anticoagulant activities of LMWH, heparin fragment, LHD and HFD were evaluated by the anti-FXa chromogenic assay. Even though heparin fragment 1, heparin fragment and heparin fragment 3 have decreased molecular sizes, they still exhibited anticoagulant effects about 92.5%, 72.9% and 40.6%, respectively (**Figure 4.3**). However their anti-FXa activities were significantly decreased after DOCA conjugation as shown in **Figure 4.4**. We then tested cell viability after synthesis of HFDs using the CCK-8 assay with HUVEC, SCC7 and MDA-MB-231 cell lines. In various concentrations, LHD and HFDs did not influence cell viability (**Figure 4.5**).

4.3.3. *In vitro* VEGF inhibition test

The inhibitory effects of LHD and HFDs on VEGF were evaluated using VEGF-accelerating angiogenesis conditions. In case of $VEGF_{165}$ inducing HUVEC tubular formation assay, the tubular formation inhibitory effects of LHD, HFD1, HFD2 and HFD3 showed 71.7%, 53.5%, 46.8% and 63%, respectively. Among them, HFD2 exhibited the maximum inhibition of tubule formation (**Figure 4.6**). However, at the same concentration (20 μg/mL), LHD did not exhibit significant effect. Using HUVEC, the effects of LHD and HFDs on cell proliferation were also evaluated. As shown in **Figure 4.6**, LHD and HFDs both inhibited HUVEC cell proliferation at 100 μg/mL. They also inhibited the proliferation of HUVEC cells at 10 μg/mL. In VEGF-induced wound healing assay (**Figure 4.7**), LHD and HFDs on scratch wound inhibited the migration of HUVECs after creating scratch wound and $VEGF_{165}$ treatment. Among HFDs, HFD2 strongly decreased the wound healing to 42.1% at 10 μg/mL and 25.1% at 100 μg/mL compared with 69.4% of untreated the positive control group.

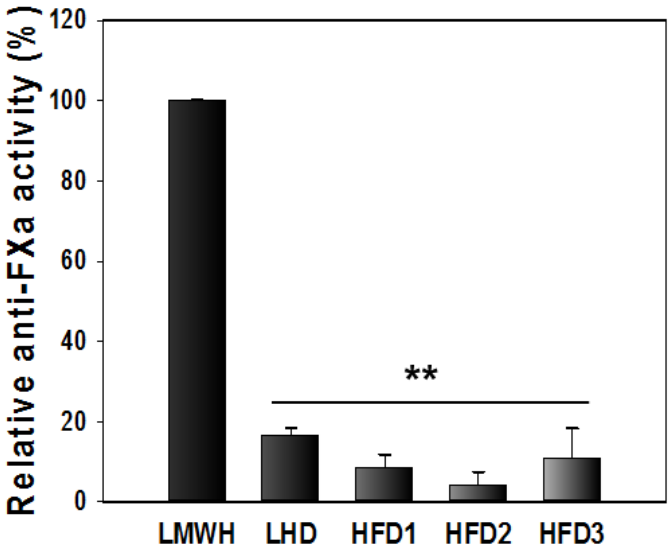

Figure 4.4. Relative anticoagulant activities (Anti-FXa) of LHD and HFDs (n=3). ***p*<0.001 vs. the control group.

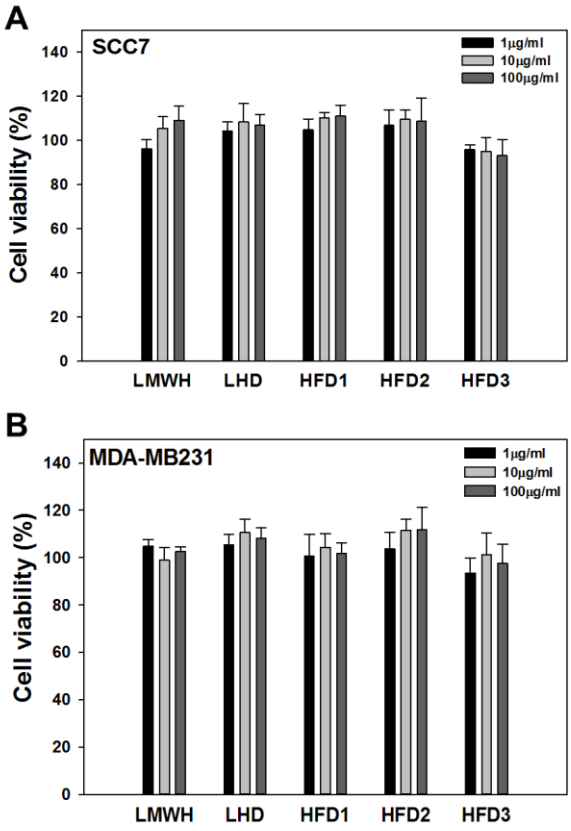

Figure 4.5. *In vitro* cytotoxicity assay of LMWH, LHD and HFDs against (A) SCC7 and (B) MDA-MB231. The percentage of live cells was calculated by dividing the number of live cells by the total number of live and dead cells compared to untreated the control group. The data are plotted as mean ± SD (n=6).

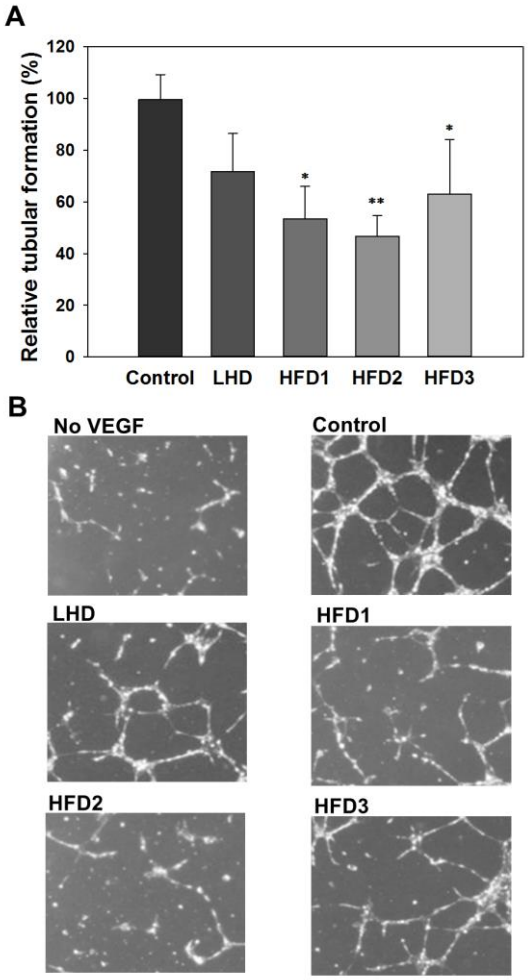

Figure 4.6. The antiangiogenic effect of LHD and HFDs on endothelial tube formation with $VEGF_{165}$ (A) The degree of tube formation was quantified by counting the number of branch points. (B) Representative photomicrographs of HUVECs after treatment of LHD or HFDs. Each bar indicates the mean ± SD (n=4). *p<0.05 vs. the control group, **p<0.001 vs. the control group

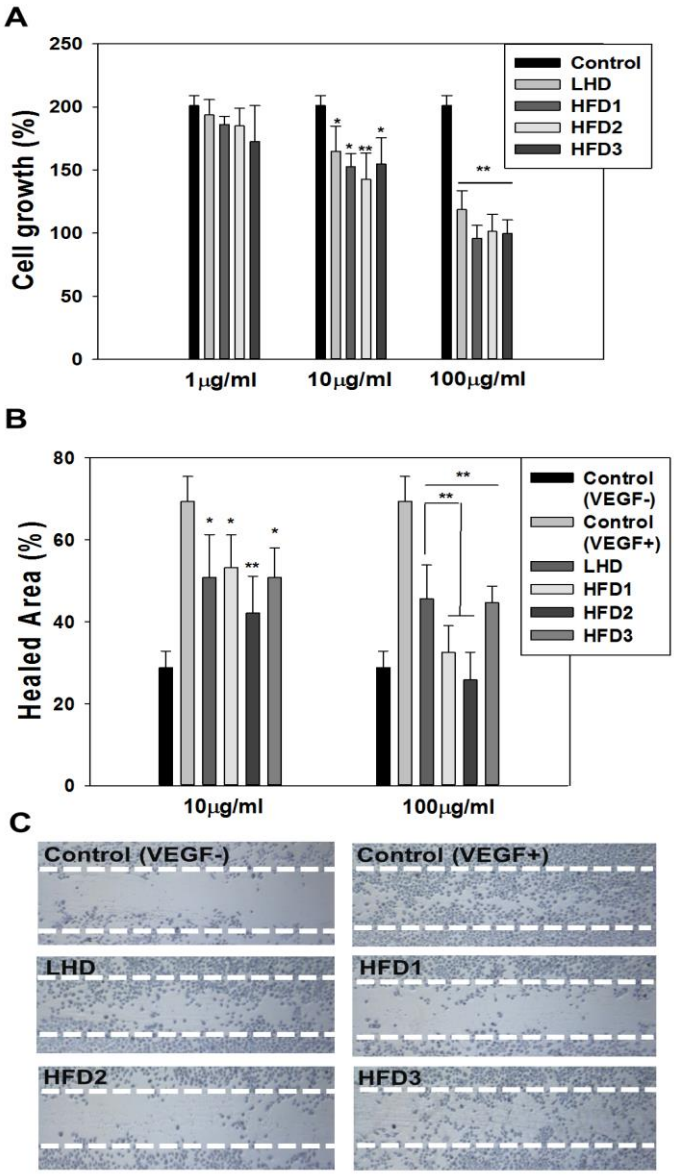

Figure 4.7. The effects of LHD and HFDs on VEGF-induced endothelial cell proliferation and wound healing assay (A) Cell proliferation after 72 h incubation was evaluated using CCK assay (B) Confluent layers of HUVECs were wounded and then, $VEGF_{165}$ (20 ng/mL) was added. The wound area was measured after 24 h. Each bar indicates the mean ± SD (n=5). *p<0.05 vs. the control group **p<0.001 vs. the control group

4.3.4. *In vivo* tumor inhibition effect of orally administered HFDs

Anticancer effects of HFDs were studied in a tumor graft model using SCC7 cells. After the oral administration of 10 mg/kg/day of HFD1, HFD2 and HFD3, all of them exhibited therapeutic potentials in SCC7 animal model. When 10 mg/kg/day of HFD1, HFD2 and HFD3 were treated, tumor growth rates were significantly lowered by 65%, 77% and 58%, respectively, compared with the the control group (**Figure 4.8**). HFDs treatment did not cause any loss of body weight. HFD3 which has the lowest average molecular weight showed less tumor inhibition effect in vivo compared with HFD2. Therefore, based on this experiment, HFD2 was determined to have the proper molecular size to inhibit cancer growth in the mouse model.

After the murine cancer experiment, we confirmed anti-cancer therapeutic effect of HFD2 in a human breast carcinoma model (**Figure 4.9**). When the mice were treated with HFD2 orally, the tumor growth rates in HFD2 treated group were much lower than in the the control group. Orally administered HFD2 at 10 mg/kg/day significantly decreased tumor volumes by 77%. In the examination of vascular structure at tumor tissues, tumor tissue sections were stained with anti-CD34 antibody and then visualized. Especially, treatment with HFD2 of 10 mg/kg/day decreased the number of CD34 positive blood vessels by 82 % and inhibited cell proliferation compared to the the control group in the PCNA-staining result. Therefore, we chose HFD2 as a bile acid conjugated and polysaccharide-based drug candidate with an optimized molecular size for tumor growth inhibitory effect.

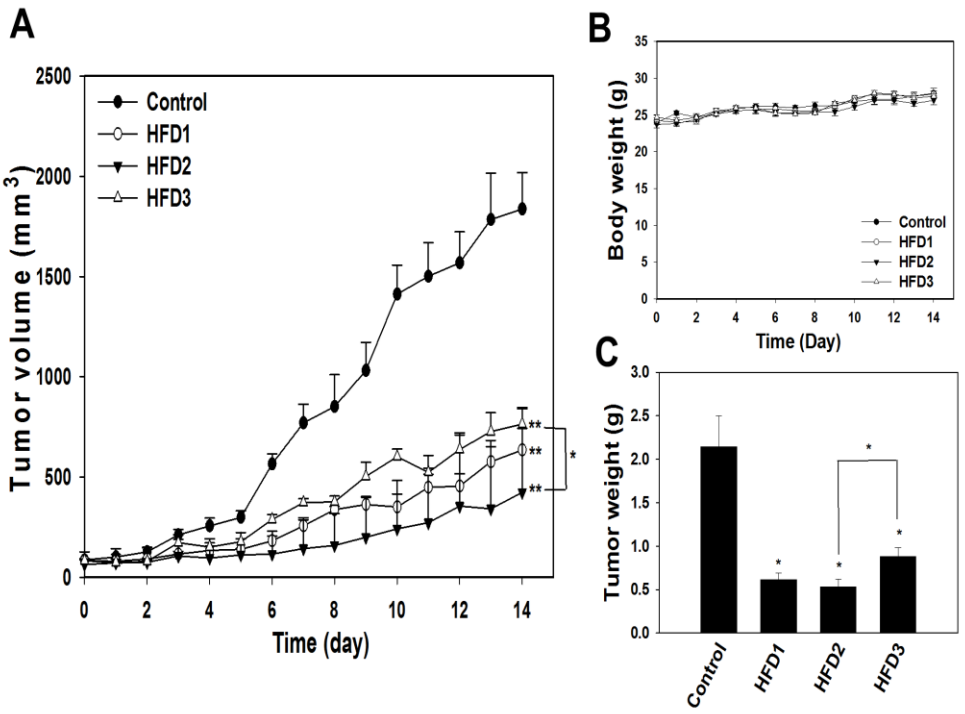

Figure 4.8. *In vivo* tumor growth inhibition test of HFDs in SCC7 inoculated mice. (A) Tumor volumes of control (●) or after oral administration of HFD1 (○), HFD2 (▼) and HFD3 (Δ) at a dose of 10 mg/kg/day (B) Body weight changes (C) Isolated tumor mass after 14 days (n= 7). Data are the mean ± standard error of mean. *p<0.05 vs. the control group, **p<0.001 vs. the control group

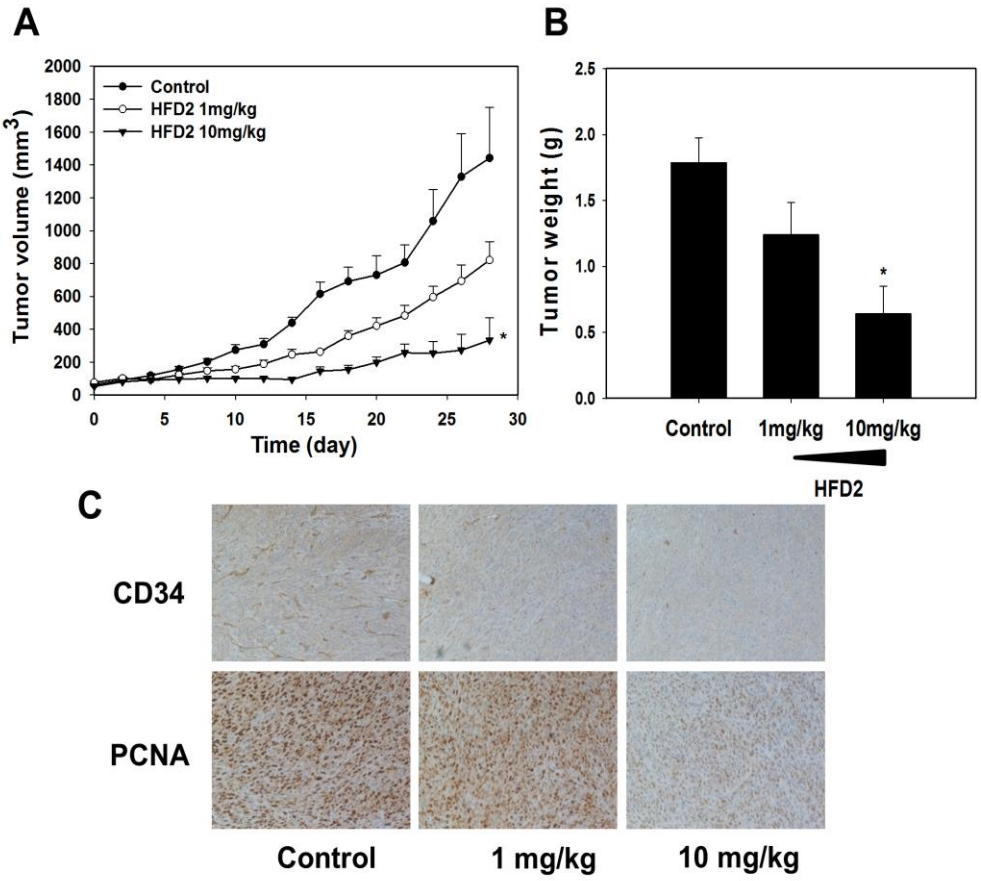

Figure 4.9. The anti-cancer effect of HFD2 in MDA-MB231 human breast carcinoma xenograft model (n= 7) (A) Tumor growth curves for control (●), HFD2 (○; 1 mg/kg/day, ▼; 10 mg/kg/day). (B) Isolated tumor weight (C) Immunohistochemistry with CD34, PCNA of tumor tissue (×200). The administration of HFD2 (1 mg/kg/day and 10 mg/kg/day) decreased the number of CD34 positive blood vessels 69.4 % and 82 %, respectively. The error bar represents S.E. *p<0.05 vs. the control group

4.3.5. Comparison between HFD and SFD for development of small and synthetic heparin mimics

Anticancer effects of HFDs were studied in various models. However, heparin fragment based drug development is hard because of heterogeneous in heparin structure. To overcome the current problem of heparin based drug development, suramin fragment and deoxycholic acid conjugate (SFD) could be an alternative (**Figure 4.10**). Small heparin fragment or heparin fragment mimics would interact with VEGF because the heparin binding domain of VEGF is suitable for small heparin fragment (**Figure 4.11**). After synthesis of SFD, the binding affinity to VEGF was measured by using computer simulation and surface plasmon resonance (SPR).

4.4. Discussion

Glycosaminoglycans are linear polysaccharides which have molecular masses of about 2×10^4 Da. They also hold a large number of water molecules in their molecular structure and occupy enormous hydrodynamic space [22]. Heparin and heparan sulfates, which are biologically important polysaccharides, have molecular weight greater than 10 kDa. Given the importance of protein-glycosaminoglycan interactions, small size of polysaccharides and oligosaccharide fragments are important biomaterials for drug design. $VEGF_{165}$ is an important tumor-related growth factor in cancer research and its heparin-binding domain has been studied. The heparin-binding site on $VEGF_{165}$ consists of positively charged residues such as Arg123, Arg124, Arg145, Arg149 and Arg156 [6]. The size of the heparin-binding site of $VEGF_{165}$ is similar to the heparin-derived hexasaccharide site observed in basic fibroblast growth factor (bFGF). Considering heparin binding sites on growth factors, we expected that the heparin-binding domain of $VEGF_{165}$ will be suitable for heparin and heparin derivatives of a smaller size.

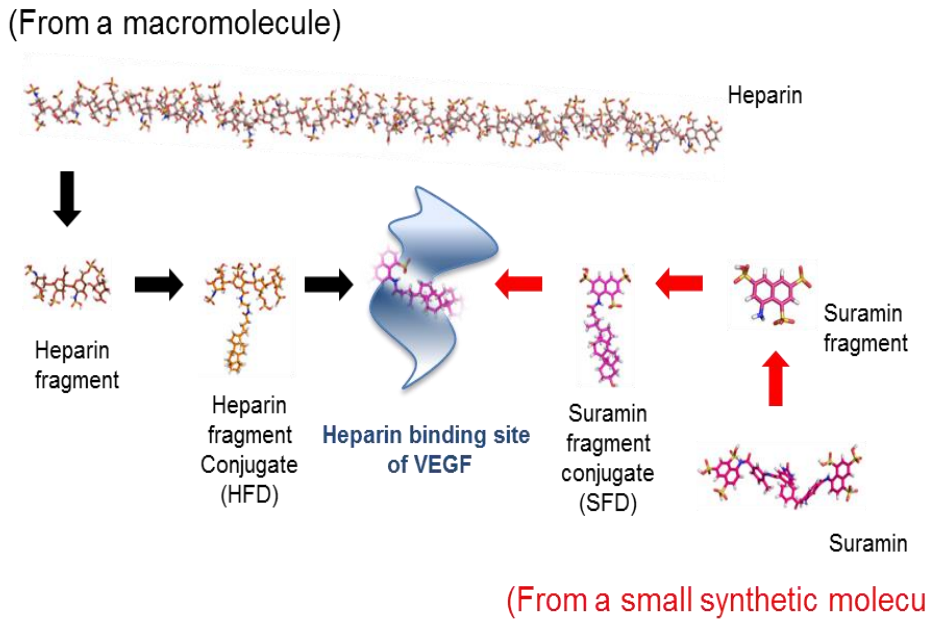

Figure 4.10. Scheme of drug development from suramin fragment and deoxycholic acid conjugate (SFD) as an heparin fragment conjugate mimics

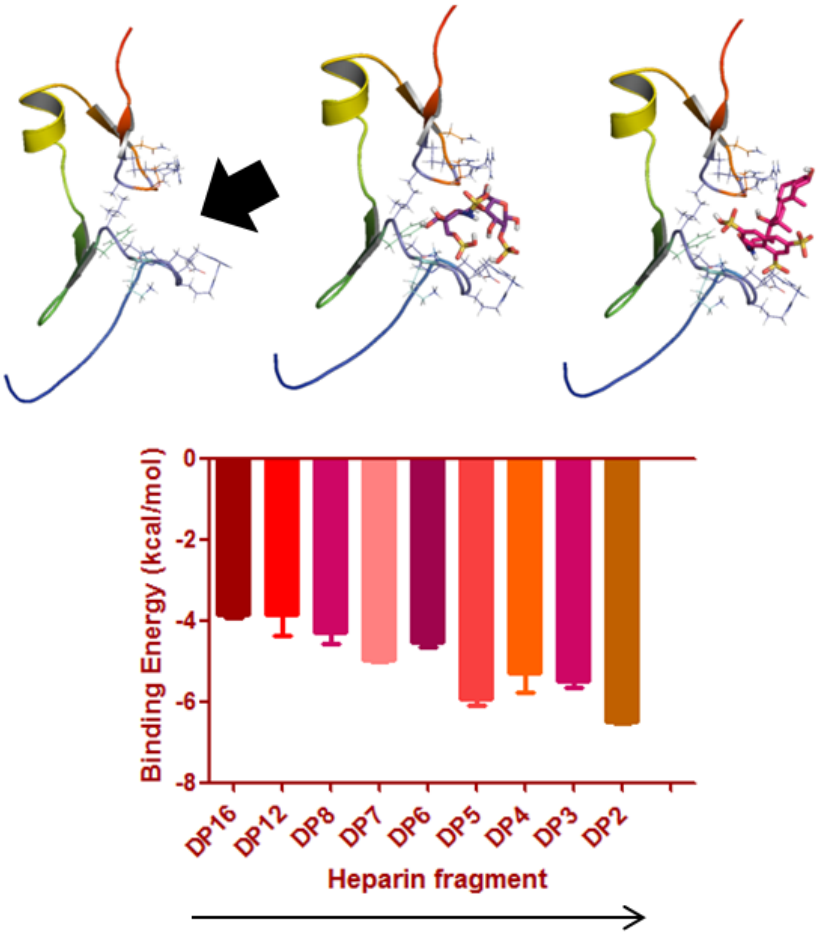

Figure 4.11. Docking score results in computer simulation using small heparin fragments with heparin binding domain of VEGF

The ability of heparin and LMWH to bind with $VEGF_{165}$ implies that they can act as antiangiogenic agents to interfere with growth factor mediated angiogenesis processes. Molar based SPR study showed similar binding affinities of UFH, LMWH and heparin fragment to $VEGF_{165}$. Therapeutic effects of heparin-based oligosaccharides also indicate that heparin needs a smaller molecular size ideal for optimum binding with $VEGF_{165}$. Considering the molecular weight of heparin, heparin fragments could be preferred because they have higher molar concentrations when they treated with the same amount. However, the anticoagulant effect of heparin fragments still existed although the molecular sizes of heparin were decreased.

The purpose of this experiment was to determine the optimum molecular size of heparin derivative for an orally available heparin based anti-cancer agent with minimized anticoagulant activity. We have already reported that DOCA conjugated heparin derivatives were orally available without anticoagulant activity. In the present experiment, to optimize the polysaccharide size, we prepared heparin fragments of different sizes by conjugating heparin fragments with DOCA molecules. They showed different molecular sizes but the conjugated DOCA amounts were maintained according to the NMR peak analysis. In this study, LHD and HFDs did not present any significant toxic effects on the cells and showed size-dependent anti-angiogenesis effects related to $VEGF_{165}$ inhibition. This means that the DOCA conjugated heparin fragments are not toxic and might not directly inhibit tumor cells by cytotoxic effect. HFDs inhibited the proliferation and migration of vascular endothelial cells at 100 μg/mL in vitro experiments. In particular, HFD2 showed improved effects in the $VEGF_{165}$-accelerated tubular formation assay by preventing microvessel formation of HUVECs more than other HFDs.

We also confirmed the $VEGF_{165}$ inhibition effects of HFDs in vivo murine tumor graft model using SCC7 cells and human tumor graft model using MDA-MB231 cells. In our previous studies, we described the anti-angiogenesis effect of LHD and also reported the bile acid transporter mediated drug delivery system using DOCA. Here, we proved that the molecular size of LMWH could be controlled to heparin binding site of VEGF and optimized for growth factor

inhibition. In animal study, HFDs were orally administered to SCC7 tumor bearing mouse at 10 mg/kg/day, HFD2 was determined as the therapeutic material with the proper molecular size to inhibit angiogenesis processes. Using MDA-MB231 human breast carcinoma, we also confirmed the tumor growth inhibitory effect of HFD2 as a drug candidate with the optimized molecular size.

VEGF, bFGF and other scatter factors have been reported to be dependent on the mechanics of heparin and heparan sulfate related to angiogenesis process [33-35]. The crystallographic structures of proteins in the presence of heparin have been determined by X-ray crystallography, providing the information about the proper molecular size of heparin for protein binding, basic fibroblast growth factor (Pentasaccharide), acidic fibroblast growth factor (Hexasaccharide), FGF1/FGFR2 (Decasaccharide) and hepatocyte growth factor (Pentasaccharide) [36-38]. The crystallographic structure of $VEGF_{165}$ with heparin or heparin conjugates has not been confirmed, but on the basis of our results, the heparin binding to VEGF could be optimized by small heparin fragments or heparin fragments conjugates such as HFD2 (Hexasaccharide).

4.5. Conclusion

The present study showed that the HFDs could have antiangiogenic effects by blocking the activity of $VEGF_{165}$ depending on its molecular size. For maximum angiogenesis inhibitory effect and low toxicity, HFD was synthesized using heparin fragments and DOCA. In several in vitro experiments, HFDs inhibited the angiogenic effect of $VEGF_{165}$ differently based on its average molecular weight. Among them, HFD2 could delay tumor growth significantly in both murine cancer and human breast carcinoma model. The results indicate that HFD2 could be an anticancer agent with an ideal molecular size.

References

[1] Linhardt RJ, Gunay NS. Production and chemical processing of low molecular weight heparins. Seminars in thrombosis and hemostasis. 1999;25 Suppl 3:5-16.
[2] Kakkar AK, Levine MN, Kadziola Z, Lemoine NR, Low V, Patel HK, et al. Low molecular weight heparin, therapy with dalteparin, and survival in advanced cancer: the fragmin advanced malignancy outcome study (FAMOUS). Journal of clinical oncology : official journal of the American Society of Clinical Oncology. 2004;22:1944-8.
[3] Harrop HA, Rider CC. Heparin and its derivatives bind to HIV-1 recombinant envelope glycoproteins, rather than to recombinant HIV-1 receptor, CD4. Glycobiology. 1998;8:131-7.
[4] Folkman J, Langer R, Linhardt RJ, Haudenschild C, Taylor S. Angiogenesis inhibition and tumor regression caused by heparin or a heparin fragment in the presence of cortisone. Science. 1983;221:719-25.
[5] Gaengel K, Betsholtz C. Endocytosis regulates VEGF signalling during angiogenesis. Nature cell biology. 2013;15:233-5.
[6] Fairbrother WJ, Champe MA, Christinger HW, Keyt BA, Starovasnik MA. Solution structure of the heparin-binding domain of vascular endothelial growth factor. Struct Fold Des. 1998;6:637-48.
[7] Coyne E. From heparin to heparin fractions and derivatives. Seminars in thrombosis and hemostasis. 1985;11:10-2.
[8] Linhardt RJ, Loganathan D, al-Hakim A, Wang HM, Walenga JM, Hoppensteadt D, et al. Oligosaccharide mapping of low molecular weight heparins: structure and activity differences. Journal of medicinal chemistry. 1990;33:1639-45.
[9] Planes A. Review of bemiparin sodium--a new second-generation low molecular weight heparin and its applications in venous thromboembolism. Expert opinion on pharmacotherapy. 2003;4:1551-61.
[10] Chapman TM, Goa KL. Bemiparin: a review of its use in the prevention of venous thromboembolism and treatment of deep vein thrombosis. Drugs.

2003;63:2357-77.
[11] Birkmeyer NJO, Finks JF, Carlin AM, Chengelis DL, Krause KR, Hawasli AA, et al. Comparative Effectiveness of Unfractionated and Low-Molecular-Weight Heparin for Prevention of Venous Thromboembolism Following Bariatric Surgery. Arch Surg-Chicago. 2012;147:994-8.
[12] Agnelli G, George DJ, Kakkar AK, Fisher W, Lassen MR, Mismetti P, et al. Semuloparin for Thromboprophylaxis in Patients Receiving Chemotherapy for Cancer. New Engl J Med. 2012;366:601-9.
[13] Viskov C, Just M, Laux V, Mourier P, Lorenz M. Description of the chemical and pharmacological characteristics of a new hemisynthetic ultra-low-molecular-weight heparin, AVE5026. Journal of thrombosis and haemostasis : JTH. 2009;7:1143-51.
[14] Walenga JM, Lyman GH. Evolution of heparin anticoagulants to ultra-low-molecular-weight heparins: a review of pharmacologic and clinical differences and applications in patients with cancer. Critical reviews in oncology/hematology. 2013;88:1-18.
[15] Zhao W, McCallum SA, Xiao Z, Zhang F, Linhardt RJ. Binding affinities of vascular endothelial growth factor (VEGF) for heparin-derived oligosaccharides. Bioscience reports.2012;32:71-81.
[16] Vignoli A, Marchetti M, Russo L, Cantalino E, Diani E, Bonacina G, et al. LMWH Bemiparin and ULMWH RO-14 Reduce the Endothelial Angiogenic Features Elicited by Leukemia, Lung Cancer, or Breast Cancer Cells. Cancer Invest. 2011;29:153-61.
[17] Kakkar VV, Balibrea JL, Martinez-Gonzalez J, Prandoni P, Group CS. Extended prophylaxis with bemiparin for the prevention of venous thromboembolism after abdominal or pelvic surgery for cancer: the CANBESURE randomized study. Journal of thrombosis and haemostasis : JTH. 2010;8:1223-9.
[18] Lee E, Kim YS, Bae SM, Kim SK, Jin S, Chung SW, et al. Polyproline-type helical-structured low-molecular weight heparin (LMWH)-taurocholate conjugate as a new angiogenesis inhibitor. International journal of cancer Journal international du cancer. 2009;124:2755-65.

[19] Ferro V, Dredge K, Liu L, Hammond E, Bytheway I, Li C, et al. PI-88 and novel heparan sulfate mimetics inhibit angiogenesis. Seminars in thrombosis and hemostasis. 2007;33:557-68.
[20] Mousa SA, Feng X, Xie J, Du Y, Hua Y, He H, et al. Synthetic oligosaccharide stimulates and stabilizes angiogenesis: structure-function relationships and potential mechanisms. Journal of cardiovascular pharmacology. 2006;48:6-13.
[21] Cole CL, Hansen SU, Barath M, Rushton G, Gardiner JM, Avizienyte E, et al. Synthetic heparan sulfate oligosaccharides inhibit endothelial cell functions essential for angiogenesis. PloS one. 2010;5:e11644.
[22] Imberty A, Lortat-Jacob H, Perez S. Structural view of glycosaminoglycan-protein interactions. Carbohydrate research. 2007;342:430-9.
[23] Lee Y, Kim SH, Byun Y. Oral delivery of new heparin derivatives in rats. Pharmaceutical research. 2000;17:1259-64.
[24] Al-Hilal TA, Park J, Alam F, Chung SW, Park JW, Kim K, et al. Oligomeric bile acid-mediated oral delivery of low molecular weight heparin. Journal of controlled release : official journal of the Controlled Release Society. 2014;175:17-24.
[25] Lee DY, Lee SW, Kim SK, Lee M, Chang HW, Moon HT, et al. Antiangiogenic activity of orally absorbable heparin derivative in different types of cancer cells. Pharmaceutical research. 2009;26:2667-76.
[26] Kim SK, Lee DY, Lee E, Lee YK, Kim CY, Moon HT, et al. Absorption study of deoxycholic acid-heparin conjugate as a new form of oral anti-coagulant. Journal of controlled release : official journal of the Controlled Release Society. 2007;120:4-10.
[27] Kim SK, Vaishali B, Lee E, Lee S, Lee YK, Kumar TS, et al. Oral delivery of chemical conjugates of heparin and deoxycholic acid in aqueous formulation. Thrombosis research. 2006;117:419-27.
[28] Park JW, Jeon OC, Kim SK, Al-Hilal TA, Lim KM, Moon HT, et al. Pharmacokinetic evaluation of an oral tablet form of low-molecular-weight heparin and deoxycholic acid conjugate as a novel oral anticoagulant. Thrombosis and haemostasis. 2011;105:1060-71.

[29] Park K, Kim YS, Lee GY, Nam JO, Lee SK, Park RW, et al. Antiangiogenic effect of bile acid acylated heparin derivative. Pharmaceutical research. 2007;24:176-85.
[30] Park JW, Jeon OC, Kim SK, Al-Hilal TA, Jin SJ, Moon HT, et al. High antiangiogenic and low anticoagulant efficacy of orally active low molecular weight heparin derivatives. Journal of controlled release : official journal of the Controlled Release Society. 2010;148:317-26.
[31] Cho KJ, Moon HT, Park GE, Jeon OC, Byun Y, Lee YK. Preparation of sodium deoxycholate (DOC) conjugated heparin derivatives for inhibition of angiogenesis and cancer cell growth. Bioconjugate chemistry. 2008;19:1346-51.
[32] Lee DY, Kim SK, Kim YS, Son DH, Nam JH, Kim IS, et al. Suppression of angiogenesis and tumor growth by orally active deoxycholic acid-heparin conjugate. Journal of controlled release : official journal of the Controlled Release Society. 2007;118:310-7.
[33] Jayson GC, Gallagher JT. Heparin oligosaccharides: inhibitors of the biological activity of bFGF on Caco-2 cells. British journal of cancer. 1997;75:9-16.
[34] Tessler S, Rockwell P, Hicklin D, Cohen T, Levi BZ, Witte L, et al. Heparin modulates the interaction of $VEGF_{165}$ with soluble and cell associated flk-1 receptors. The Journal of biological chemistry.1994;269:12456-61.
[35] Soker S, Goldstaub D, Svahn CM, Vlodavsky I, Levi BZ, Neufeld G. Variations in the size and sulfation of heparin modulate the effect of heparin on the binding of $VEGF_{165}$ to its receptors. Biochemical and biophysical research communications. 1994;203:1339-47.
[36] Faham S, Hileman RE, Fromm JR, Linhardt RJ, Rees DC. Heparin structure and interactions with basic fibroblast growth factor. Science. 1996;271:1116-20.
[37] DiGabriele AD, Lax I, Chen DI, Svahn CM, Jaye M, Schlessinger J, et al. Structure of a heparin-linked biologically active dimer of fibroblast growth factor. Nature. 1998;393:812-7.
[38] Pellegrini L, Burke DF, von Delft F, Mulloy B, Blundell TL. Crystal structure of fibroblast growth factor receptor ectodomain bound to ligand and heparin. Nature. 2000;407:1029-34.

[39] Lee Y, Nam JH, Shin HC, Byun Y. Conjugation of low-molecular-weight heparin and deoxycholic acid for the development of a new oral anticoagulant agent. Circulation. 2001;104:3116-20.

Chapter: 5

Chemically modified heparin with suramin fragment for enhanced antiangiogenic effect

5.1. Introduction

Since angiogenesis is a fundamental process for tumor growth and metastasis by the formation of new blood vessels from preexisted blood vessels, anti-angiogenesis has been established as a crucial strategy for cancer treatment [1, 2]. A number of angiogenic growth factors and cytokines have been studied as potential therapeutic targets for pharmacological intervention of angiogenesis [3, 4]. Among angiogenic growth factors, vascular endothelial growth factor (VEGF) plays a key role in both normal and pathological angiogenesis [5]. One of the unique characteristics of VEGF is that it contains a heparin-binding domain (HBD) in its molecular structure related to its biological functions [6].

Heparin is highly sulfated polysaccharides which bind to a variety of growth factors including vascular endothelial growth factor $_{165}$ ($VEGF_{165}$) via its heparin-binding domain [7, 8]. Several studies have shown the inhibitory effects of heparin and heparin derivatives on tumor angiogenesis through their targeting of angiogenic growth factors [9-11]. Chemically modified heparin conjugates have advantages in diminished the risk of bleeding, as well as their features of preventing angiogenesis and metastasis [10, 12].

Recent studies have indicated that the clinical use of heparins and low molecular weight heparins (LMWH; Avg. 4-5 kDa) could be extended to patients with cancer, as its systemically applied anticoagulant effect is useful for pharmacologic prevention of unwanted blood coagulation [13-15]. However, The FDA-approved heparins are not suitable as anticancer agents because of their physiological functions as below [16]. Heparin is a strong anticoagulant agent that has been used clinically for decades, but its anticancer effect is not strong enough to

apply for clinical uses [17]. Thus, to be able to use heparin as an anti-angiogenesis agent for anticancer therapy, it is necessary that heparin has an enhanced therapeutic effect and a lower risk of hemorrhage [10, 18].

On the other hand, suramin which was developed by Bayer, is a hydrophilic polysulfonated naphthylurea and can bind to HBD of proteins like heparins [19-21]. Several studies using suramin and suramin fragment have proposed that suramin binds to HBD in a variety of proteins [22, 23]. Suramin inhibits the activities of various growth factors including human fibroblast growth factor (hFGF), platelet-derived growth factor (PDGF), epidermal growth factor (EGF) and transforming growth factor-beta (TGF-β), thus it is considered to possess potent antitumor activity [24-27]. However, suramin possesses toxic properties, several suramin analogues have been developed to overcome its side-effects [28-30].

In this context, it may be important to understand the structural interactions between heparin and HBD in different kinds of proteins, which could lead to rational design of a carbohydrate-derived drug [31]. The highly anionic nature of heparin and suramin suggests that their binding with the positively charged HBD is charge-based in nature. HBD in proteins are characterized by the presence of clusters of positively charged basic amino acids such as arginine and lysine which form ion pairs with defined negatively charged sulfonate groups of heparin and suramin [6, 32, 33]. Elucidation of the structure activity relationship has revealed that suramin, suramin derivatives or suramin fragment can have defined molecular structures such as sulfonate groups that interact with the heparin binding domain of proteins at high affinity [34, 35].

In our previous studies, we developed several heparin and heparin fragment conjugates using bile acids for oral delivery [11, 36-39]. We also synthesized an orally active antiangiogenic heparin by conjugating several bile acids and making a charge complex [40]. However, the introduction of such the hydrophobic bile acid can cause disruption of the hydrogen bonding interaction of heparin and allow hydrophobic molecules to be solubilized in water by forming self-assemble micelles. This changed property of heparin could increase toxicities in vivo and cause accumulation problem [41].

Here, we introduce a newly developed a low molecular weight heparin and suramin fragment conjugate (LHsura) with enhanced binding affinity with the heparin binding domain of $VEGF_{165}$ which results in inhibition of angiogenesis in tumors. In the present study, considering the molecular structure of suramin and HBD, we hypothesized that the conjugation of suramin to LMWH could increase the binding affinity of heparin to the growth factors including VEGF with lower toxicity and anticoagulant effect. LHsura would inhibit tumor growth possibly by blocking $VEGF_{165}$ that has a clear heparin binding site in the body. To clarify the hypothesis, we investigated their structural interactions using biophysical techniques, including computer simulation and surface plasmon resonance (SPR). Then, we evaluated the therapeutic effect of LHsura through both in vitro HUVEC tubular formation assay and *in vivo* tumor growth inhibition test.

5.2. Materials and methods

5.2.1. Materials

LMWH (nadroparin, average molecular weight 4.5 kDa, produced by deaminative cleavage with nitrous acid) was obtained from the Nanjing King-Friend Biochemical Pharmaceutical Company Ltd. (Nanjing, China). 1-ethyl-3-(3-dimethylaminopropyl)carbodiimide (EDAC), toluidine blue, suramin sodium salt and formamide were purchased from Sigma chemical Co. (St. Louis, MO, USA). Suramin fragment (disodium 8-amino-1,3,6-naphthalenetrisulfonate) was obtained from TCI (Tokyo Chemical Industry co., Japan). Coatest anti-Factor Xa assay kits were purchased from Chromogenix (Milano, Italy). Recombinant vascular endothelial growth $factor_{165}$ was obtained from Peprotech (Rocky Hills, NJ). A SPR sensor chip CM5 was purchased from GE Healthcare (Uppsala, Sweden). Matrigel was obtained from BD Bioscience.

5.2.2. Synthesis and characterization

LMWH (Avg. M.W. 4.5 kDa) was dialyzed in distilled water for 2 days using a membrane of MWCO 1,000 Da. The LMWH solution was then filtered and freeze-dried. The white powder of LMWH (200 mg) was dissolved in formamide (20 mL) at 50 ℃. Suramin fragment (8-amino-1,3,6-naphthalenetrisulfonate) and EDAC were added and agitated for 5 min. The feed mole ratio of LMWH, suramin fragment and EDAC was 1:30:60. This reaction was started at 30 ℃ without light and then, the reaction condition was thoroughly sustained for 6 h. The final solution was precipitated in acetone. Unreacted EDAC and suramin fragment were removed by dialysis in distilled water using a membrane of MWCO 2,000 Da. The final product was then filtered and freeze-dried. The purity was evaluated by thin-layer chromatography and UV/Vis analysis. The synthesized LMWH conjugate was characterized using proton nuclear magnetic resonance (^{1}H NMR) and UV/VIS spectroscopy. The chemical conjugation ratio of heparin and suramin fragment was confirmed through UV/Vis analysis using simply mixed heparin and suramin fragment solution of different molecular ratios. Suramin fragment exhibited a peak at 354 nm and LHsura showed a shifted peak at 305 nm.

5.2.3. Factor Xa and cell viability assay

Anticoagulant activity was carried out using Coatest anti-FXa chromogenic assay. Briefly, LHsura solution (100 μL) was mixed with 100 μL of antithrombin III (ATIII) solution and incubated at 37℃ for 3 min according to the manufacturer's instructions. after that, 100 μL of Factor Xa (FXa) and the substrate (200 μL) were added and then, incubated exactly for 3 min. Anti-FXa activities of materials were calculated from the absorbance at 405 nm using UV/Vis spectrometer (n=3). The cell toxicities of materials were evaluated by using HUVEC (human umbilical vein endothelial cell). The cells were seeded in a 96 well plate with 100 μL of supplemented EGM-MV2 medium. After treatment at different concentrations, the cells were incubated at 37℃ for 4 h. To measure the number of live HUVECs, 10

μL of CCK-8 solution was added and then, further incubated for 1 h. Cell viability was expressed using a microplate fluorescence reader as a ratio of absorbance (450 nm) between the values from treated and untreated groups (n=6).

5.2.4. Surface plasmon resonance (SPR)

Binding affinities of LMWH and LHsura to the heparin binding domain of $VEGF_{165}$ were measured using surface plasmon resonance on a BIAcore T100 (GE Healthcare, Uppsala, Sweden). Samples were prepared at concentrations ranging from 1 to 0.0078 μM in HEPES buffer (0.05 M) which was also used as a running buffer. Recombinant human heparin binding domain of $VEGF_{165}$ was immobilized onto a sensor chip CM5 and the measurement was performed at a flow rate of 20 μL/min. The affinity analysis of data was performed using BIAcore T100 evaluation software.

5.2.5. Computer simulation

The solution structure of the heparin binding domain of $VEGF_{165}$ (protein data bank [PDB] code, 2VGH) was reported. The structures of materials were created using ChemBioDraw Ultra 11.0 and ChemBio3D Ultra 11.0 (Cambridge Soft, CA) and the 3D coordinates of the heparin binding domain was converted using the AutoDockTools package [42]. For the docking study, the grid was centered at the arginine rich-heparin binding site of the protein. The molecular docking simulation was carried out using the AutoDock Vina 1.0.3 program with default parameters [43]. Illustrations of the 3D model were generated and visualized using the PyMOL program. Arginine was shown in blue and other positive amino acids (Histidine and lysine) were shown in deep blue color.

5.2.6. Endothelial tubular formation assay

100 μl of growth factor reduced Matrigel was added to a 96-well plate and incubated for 30 min at 37℃. HUVECs (4×10^4 cells/well) were cultured in a final volume of 100 μl of EBM medium containing $VEGF_{165}$ (20 ng/mL) alone or mixed with LMWH or LHsura. After 6 h of incubation, calcein-AM was treated. The

vessel formation was observed and the number of completed vessels was counted (n=4).

5.2.7. Cell proliferation assay

HUVECs were seeded at a density of 1×10^3 cells per well in 100 μL of M199 medium (2 % Fetal bovine serum). LHsura was incubated with $VEGF_{165}$ (10 ng/mL) at 37 ℃ for 72 h, and the media including LHsura and VEGF were refreshed every day. On day 3, 10 μL of CCK-8 solution was added to each well. After 1h incubation, absorbance was measured at 450 nm using a microplate fluorescence reader (n=6).

5.2.8. Wound healing assay

The HUVECs were cultured in a 24-well plate in EGM-MV2 media. After the cells reached confluence, the plate were wounded with a pipet chip by creating a groove in the center of well and incubated further in M199 medium (FBS 1 %) for 1 h. LHsura was added into each well and incubated with $VEGF_{165}$ (10 ng/mL) . After 24 h, the medium was removed and the cells were fixed with 4 % paraformaldehyde. They were gently washed twice with PBS, and stained with 0.001 % toluidine blue (n=5).

5.2.9. Tumor growth inhibition test

All procedures for animal experiment were approved by the Committee on the Use and Care on Animals according to the regulations of the Institutional Animal Ethics Committee of the Seoul National University animal care facility. SCC7 (murine squamous cell carcinoma) cells were cultured in DMEM high glucose medium supplemented with 10 % (v/v) FBS, and then the cells were injected subcutaneously into C3H/HeN mice (1×10^6 cells/60 μL). A week later, mice were administrated intravenously 10 mg/kg/day of LMWH or LHsura for 2 weeks. Tumor volumes were measured and calculated ($a2 \times b \times 0.52$, where a = width, and b = length). After sacrifice, isolated tumor masses were also measured and tumor tissues were histologically evaluated by staining with anti-CD34

antibodies. Microvascular density (MVD) was evaluated by counting in five areas at 200 ×.

5.2.10. Statistical analysis

We analyzed the results by comparing the means of groups in in vitro and in vivo experiments using one-way analyses of variance (ANOVA) followed by Bonferroni's post-hoc tests using sigmaplot 12. P-values less than 0.05 were considered to be statistically significant.

5.3. Results

5.3.1. Synthesis and characterization

Heparin-protein interactions are dependent upon the electrostatic forces between the sulfonate group and polysaccharide sequence in the molecular structure of heparin. In order to maintain the highly anionic nature of heparin and suramin, we conjugated suramin fragment (8-amino-1,3,6-naphthalenetrisulfonate) to the carboxyl group of LMWH using EDAC/NHS coupling reaction (**Figure 5.1**). In the 1H NMR spectrum of LHsura, which is the chemical conjugate of LMWH and suramin fragment, the suramin fragment peaks in the range of 7.6-8.8 ppm indicated the successful introduction of the fragment moiety to LMWH. The chemical conjugation ratio of heparin and suramin fragment was measured by UV/Vis analysis at 354 and 305 nm; the peak of conjugated fragment appeared at 305 nm. The maximum coupling ratio of LMWH and suramin fragment was about 3.3 ± 0.2.

5.3.2. Binding affinity study using SPR and computer simulation

The binding affinity of LHsura to HBD of $VEGF_{165}$ was measured using surface plasmon resonance (SPR), and LMWH was used as the control. After immobilizing $VEGF_{165}$ on the CM5 chip, LHsura was injected at different concentrations ranging from 1 to 0.0078 μM and subsequently the affinity analysis was performed using BIAcore T100 evaluation software with default parameters. As a result, LHsura (KD = 84 nM) had a higher binding affinity than LMWH (KD =

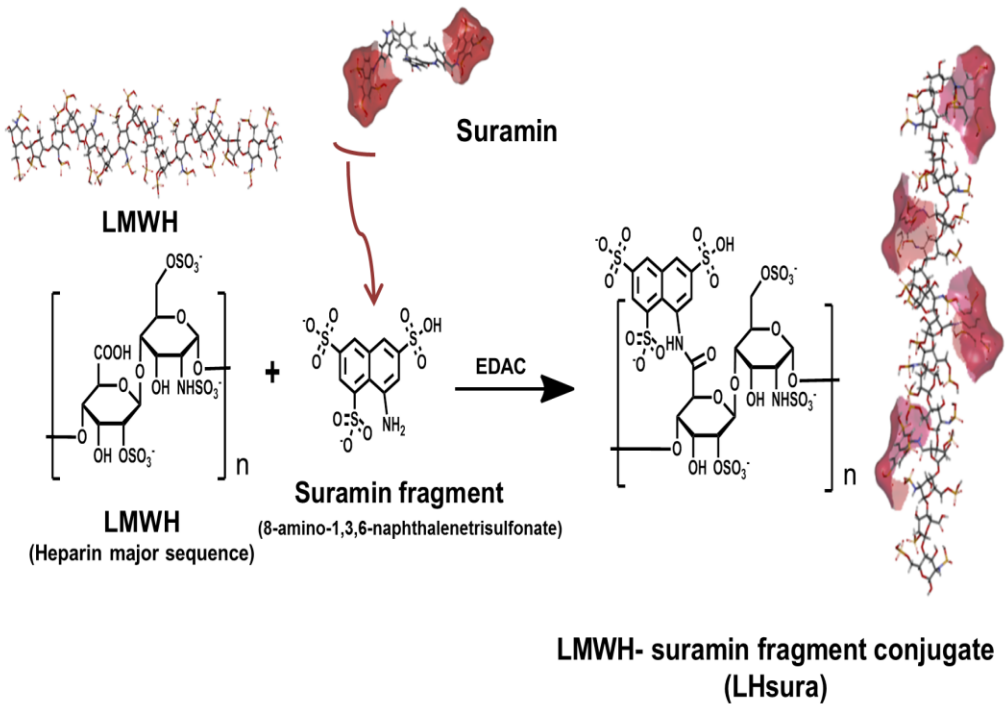

Figure 5.1. Schematic synthesis protocol and molecular structures showing low molecular weight heparin (LMWH), suramin, suramin fragment and low molecular weight heparin-suramin fragment conjugate (LHsura). LMWH was conjugated with suramin fragment to enhance its binding with the heparin binding domain of $VEGF_{165}$.

401 nM) (**Figure 5.2**). The KD value of LHsura showed a high affinity for HBD of $VEGF_{165}$ after suramin fragment conjugation. In the docking simulation result, the minimum internal energy levels for heparin or LHsura oligosaccharide were -4.5 and -5.7 kcal/mol, respectively. This means that LHsura has a higher binding affinity to HBD of VEGF than heparin.

5.3.3. Anti-FXa and cell viability assays

The anticoagulant activity of LHsura was evaluated by Anti-FXa activity and the results showed significantly decreased such activity in the presence of suramin fragment (**Figure 5.3**). This means that LHsura has lower risk of hemorrhage for anticancer therapy. We tested cell viability using the CCK-8 assay with HUVECs (doubling time is 30 h) after LHsura treatment. LHsura did not affect cell viability in high concentrations (up to 1 mg/mL). On the other hand, suramin and suramin fragment were toxic at high concentrations (0.2 - 1 mg/mL) even for short-term treatment (**Figure 5.3**). So, suramin and suramin fragment were excluded from further experiments because of their toxic effect.

5.3.4. Inhibition effect of LHsura on $VEGF_{165}$-mediated angiogenesis

Anti-angiogenic efficacy of LHsura was evaluated using $VEGF_{165}$-accelerating angiogenesis conditions. In $VEGF_{165}$ inducing HUVEC tubular formation assay, the endothelial cells were cultured on a gelled basement membrane matrix in fasting EBM medium. The tubular formation inhibitory effects of LMWH and LHsura at 50 μg/mL showed 21.2% and 46.4%, respectively (**Figure 5.4**). The tubular formation inhibitory effect of LHsura was increased to 78.6% at 200 μg/mL.

The effect of LHsura on the inhibition of the proliferations of HUVECs was also evaluated by counting the final cell number using CCK assay. VEGF-accelerating HUVEC cell proliferation was restricted after LHsura treatment at 100 and 400 μg/mL (**Figure 5.5**). In $VEGF_{165}$-induced wound healing assay, LHsura inhibited the migration of HUVECs by blocking the activity of $VEGF_{165}$. The percentage of the healed area in treated group were 35.8% at 10 μg/mL and 18.6% at 250 μg/mL, on the other hand, that in the $VEGF_{165}$ treated the control group was

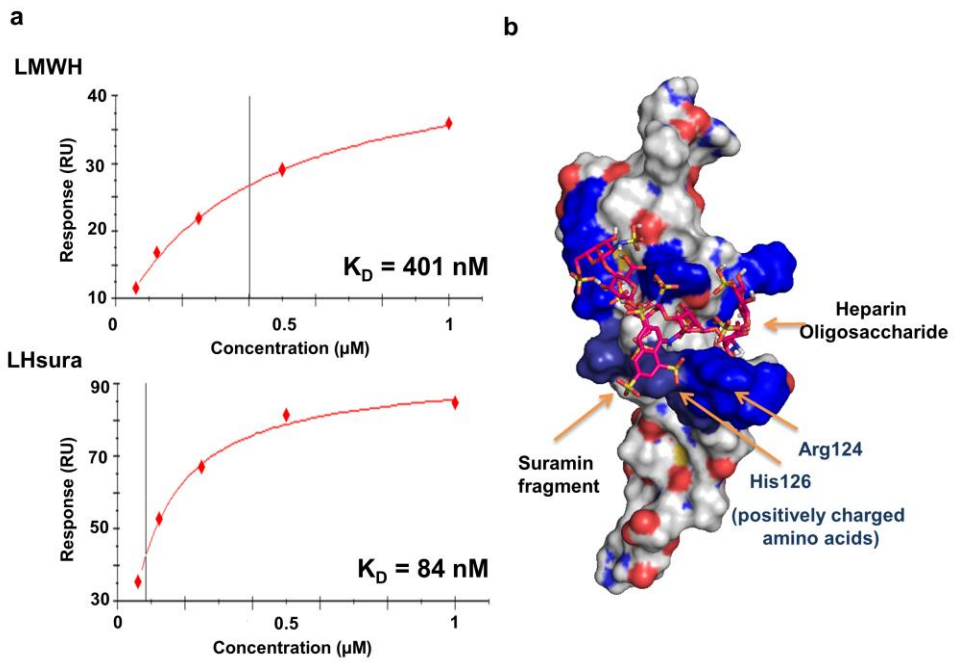

Figure 5.2. (a) The dissociation rate constants (K_D) of LMWH or LHsura with the heparin binding domain of $VEGF_{165}$ were measured using surface plasmon resonance (SPR). (b) In silico molecular docking of LHsura fragment (Dp 6) within the heparin binding site of $VEGF_{165}$. LHsura oligosaccharide fits into the molecular space consist of a lot of arginines. Arginine was shown in blue and other positive amino acids (histidine and lysine) were shown in deep blue.

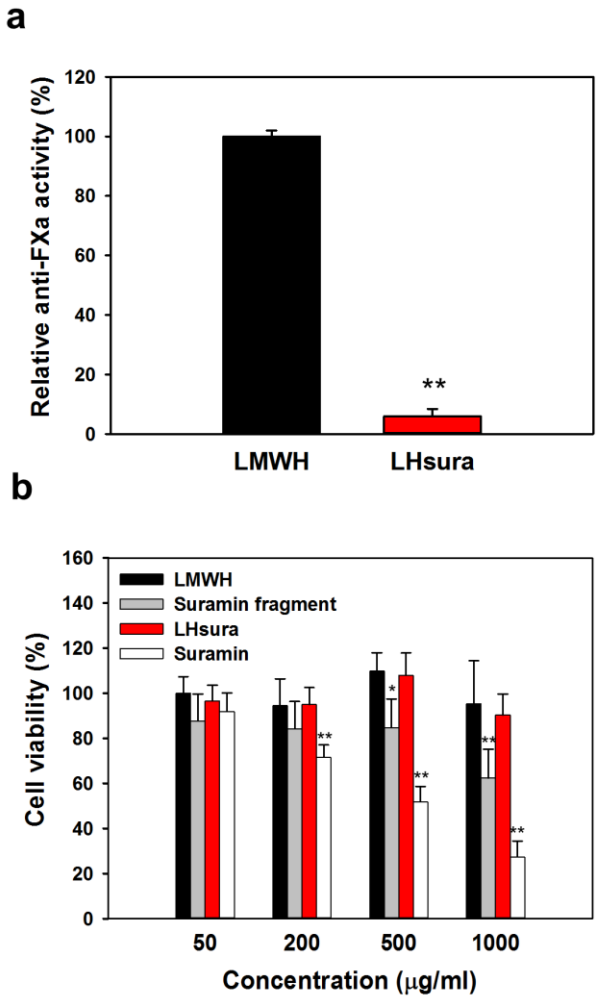

Figure 5.3. (a) Relative anticoagulant activities (anti-FXa) of LMWH and LHsura (n=3) (b) In vitro cell viability assay against human umbilical vein endothelial cell (HUVEC) (n=6). The data are plotted as mean ± standard deviation. *p<0.05 vs the control group, **p<0.001 vs the control group.

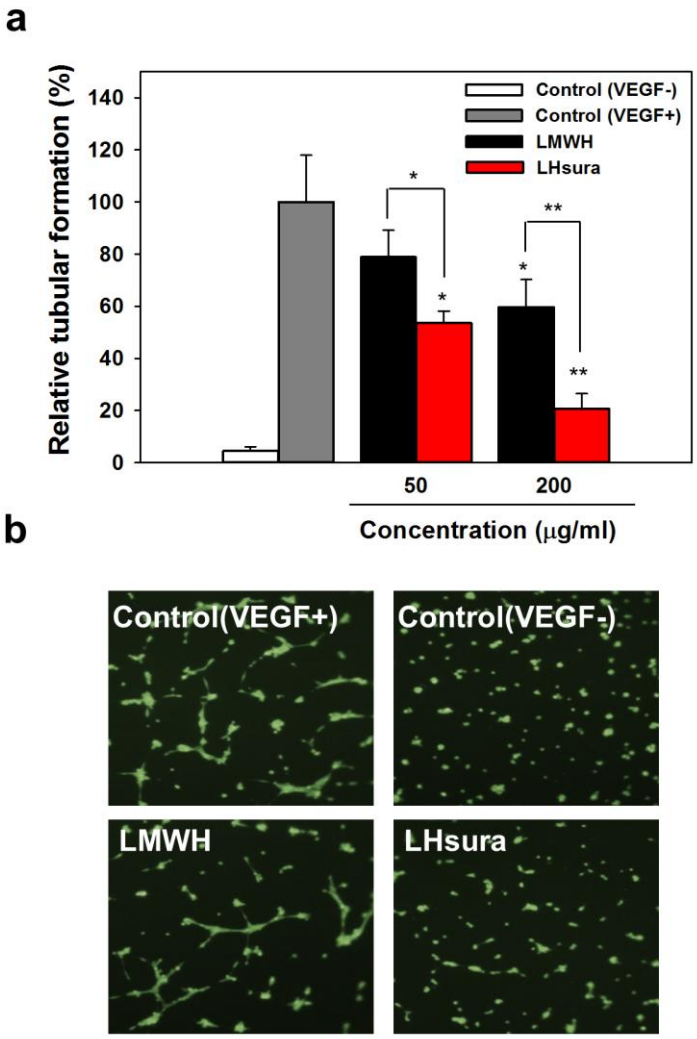

Figure 5.4. Tubular formation assay with $VEGF_{165}$ in HUVECs (a) Analysis of tubular formation was carried out by counting the number of connected vessels (n=4). (b) Representative microphotographs of HUVEC morphogenesis (100×). Calcein AM was added to visualize the vessels. *p<0.05 vs the control group, **p<0.001 vs the control group.

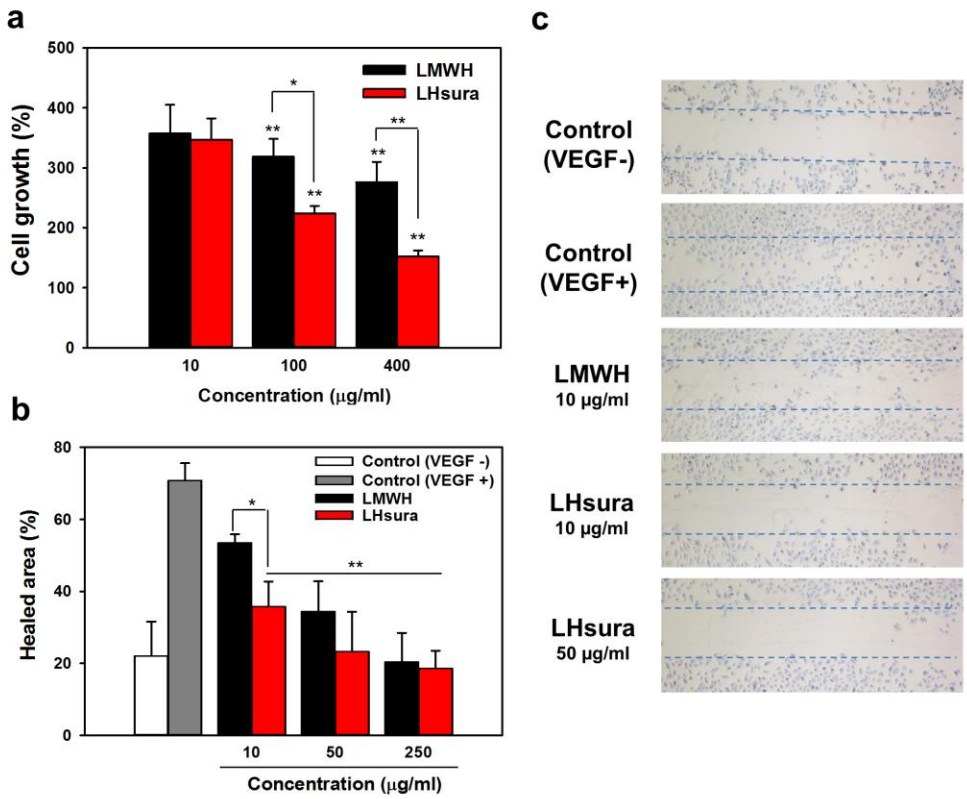

Figure 5.5. (a) Inhibitory effects of LMWH and LHsura on $VEGF_{165}$-induced endothelial cell proliferation. The cell proliferation after 72hr incubation was evaluated using CCK assay compared with $VEGF_{165}$ untreated group (100%) (n=6). (b) LHsura inhibits $VEGF_{165}$-stimulated endothelial cell migration into the wound. The wound area was measured after 24 h. Each bar indicates the mean ± SD (n=5). **p*<0.05 vs the control group, ***p*<0.001 vs the control group.

70.8% (22.1% in $VEGF_{165}$ untreated group).

5.3.5. *In Vivo* inhibition effect of LHsura on tumor growth

The anticancer effect of LHsura was investigated in a tumor graft model using SCC7 cells. LHsura was administrated to mice for 2 weeks and it was found to exhibit therapeutic potentials in SCC7 cancer models. Tumor growth rates were reduced by 26.1% in the LMWH-treated group and 61.4% for the LHsura-treated group, compared to the the control group (**Figure 5.6**). This result confirmed the antiangiogenesis effect of LHsura via $VEGF_{165}$ inhibition in a cancer model without loss of body weight. We confirmed the blood vessel formation inhibitory effect of LHsura in tumor by tissue analysis. To determine the anti-$VEGF_{165}$ effect on angiogenesis, tumor tissue sections were stained with anti-CD34 antibody after the animal experiments and then visualized under a microscope. Treatment with LHsura decreased the number of CD34 positive blood vessels by 79.2% compared with that of the the control group.

5.4. Discussion

Heparin binding domains are important in several biological functions, and found in various growth factors which interact with heparin and heparan sulfate. Inhibition of the heparin binding domain of VEGF using heparin conjugate has therapeutic potential to target the other heparin binding growth factors. Enhanced inhibition to heparin binding domain growth factors could be a key to solving many current problems existing in the current anticancer therapy.

There are several clinically approved LMWHs for patients in healthcare therapeutics. Low molecular weight heparins (average molecular weight of 4-5 kDa) are generally prepared from unfractionated heparin (12 kDa) by different manufacturing methods. Among the various LMWHs, tinzaparin (5 kDa) is uniquely produced by enzymatic beta eliminative cleavage with heparinase, whereas all the other LMWHs are isolated by acid or alkaline depolymerization

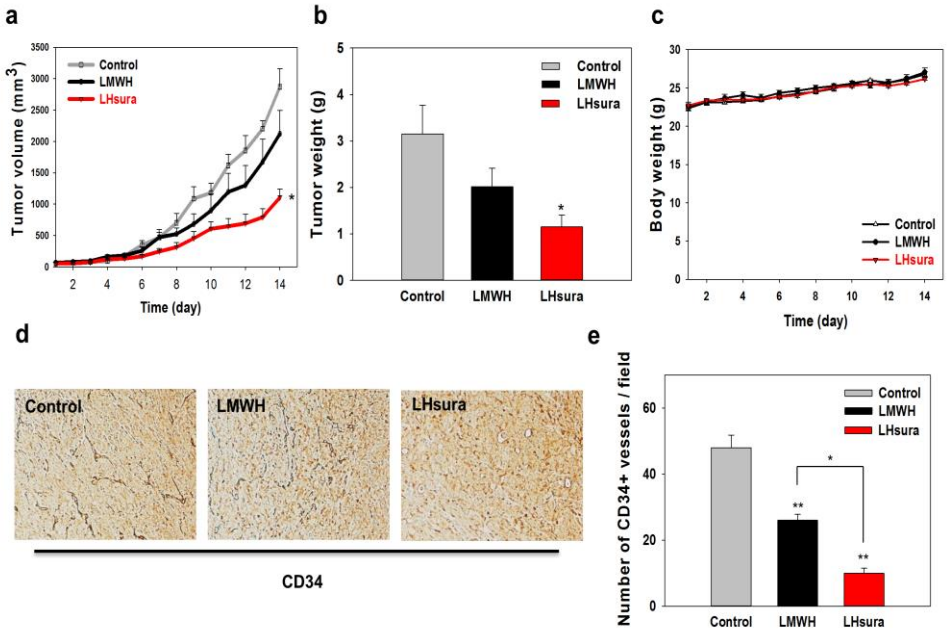

Figure 5.6. Tumor growth inhibition effect of LHsura in SCC7 inoculated mice (n=6) (a) Tumor volume change in LMWH or LHsura treated mice compared with control (saline treated) (b) Isolated tumor mass after 14 days (c) Body weight changes (d) Immunohistochemistry of experimental tumor tissue with CD34 (200×) (e) The number of CD34 positive blood vessels. Data are the mean ± standard error of mean. *p<0.05 vs the control group, **p<0.001 vs the control group.

[44]. For example, nadroparin (4.5 kDa) is synthesized through deaminative clevage with nitrous acid from heparin.

The present study demonstrates that conjugation using LMWH (nadroparin) and a suramin fragment, two negatively charged materials that can both bind with HBD of growth factors, shows antiangiogenic effects. Arginines of HBD form stable and strong electrostastic interactions with sulfonate groups of heparin and suramin. The molecular structure of heparin binding domain of $VEGF_{165}$ was reported and heparin oligosaccharide fits into the molecular space of HBD of $VEGF_{165}$. The negative charge of sulfonate groups of heparin and suramin could electrostatically bind to the positive amino acids in HBD, thereby inducing high binding affinity between heparin oligosaccharide and its binding site. The effect of suramin fragment on the integrity of heparin would be low because their characteristics are not different.

Both low anticoagulant activity and cell cytotoxicity are important factors for drug development of heparin as an anti-angiogenesis agent. The low anticoagulant activity of LHsura means that LHsura has lower risk of hemorrhage for anticancer therapy. Anti-angiogenesis compounds should inhibit growth factor-mediated endothelial cell angiogenesis without any toxicity.

To prove the anticancer effect of LHsura, the anti-angiogenic efficacy of LHsura was evaluated in several $VEGF_{165}$-accelerating angiogenesis experiments. At first, in the Matrigel plug assay, the results showed varying responses to $VEGF_{165}$ and heparins (data not shown). However, in the endothelial tubular formation, after LHsura and VEGF treatment, LHsura inhibited the capillary-like structure formation of endothelial cells. LHsura also inhibited the migration and proliferation of HUVECs by blocking the activity of $VEGF_{165}$. These findings thus strengthened the notion that suramin fragment conjugated heparin could be optimized to inhibit the angiogenesis process mediated by $VEGF_{165}$.

Given the importance of protein-glycosaminoglycan interactions, polysaccharide conjugates or derivatives are potential therapeutic biomaterials in drug design. $VEGF_{165}$ is an important growth factor in cancer-related studies, and its heparin-binding domain has already been studied. Among heparin binding growth

factors, $VEGF_{165}$ has unique 55-residue carboxy-terminal heparin-binding fragments; conversely, $VEGF_{110}$ and $VEGF_{121}$ lack the heparin-binding sequences, therefore they do not bind significantly to heparin [8]. The ability of LHsura to bind with $VEGF_{165}$ implies that they can act as antiangiogenic agents to interfere with the process of angiogenesis process. The SPR and computer simulation studies illustrated the molecular binding affinities of LHsura to $VEGF_{165}$.

The antiangiogenesis effect of LHsura via $VEGF_{165}$ inhibition showed the tumor inhibitory effect without any sign of toxicity in animal study. SCC7 cells which had significantly higher expression of VEGF were used for the xenografted animal model [38]. After isolation of tumor, we evaluated the microvascular density which has been considered a useful prognostic indicator in patients with most types of cancer. The relationship between MVD and angiogenesis dependence of a tumor is controversial [45-47]. The outcome of MVD analysis could be influenced by a number of factors and histochemical procedure. Nevertheless, MVD determined in primary tumors is associated with angiogenesis, and LHsura decreased the number of microscopically visualized blood vessels following histochemical staining with anti-CD34 antibodies in a SCC7 cancer model. These results demonstrate that LHsura is a suitable candidate for development as an angiogenesis inhibitor with low toxicity. Apart from $VEGF_{165}$, other proteins with heparin binding domain in the tumor could have been also affected by LHsura treatment. Having a high therapeutic potential to target other growth factors with angiogenesis-modifying properties is one advantage of LHsura development because LHsura consists of two molecules, both of which can bind to HBD.

5.5. Conclusion

In $VEGF_{165}$-mediated endothelial cell angiogenesis inhibition experiments and tumor inhibition test, LHsura is suitable as an angiogenesis inhibitor with low toxicity. This indicates that LHsura has an optimized molecular structure for binding with $VEGF_{165}$. Owing to its angiogenesis inhibitory effect, LHsura inhibited tumor

growth in SCC7 murine model. These findings indicate that LHsura could be an anticancer candidate by its $VEGF_{165}$ inhibition effect.

References

[1] Brem S, Brem H, Folkman J, Finkelstein D, Patz A. Prolonged tumor dormancy by prevention of neovascularization in the vitreous. Cancer research. 1976;36:2807-12.

[2] Parangi S, Dietrich W, Christofori G, Lander ES, Hanahan D. Tumor suppressor loci on mouse chromosomes 9 and 16 are lost at distinct stages of tumorigenesis in a transgenic model of islet cell carcinoma. Cancer research. 1995;55:6071-6.

[3] Folkman J, Langer R, Linhardt RJ, Haudenschild C, Taylor S. Angiogenesis inhibition and tumor regression caused by heparin or a heparin fragment in the presence of cortisone. Science. 1983;221:719-25.

[4] Smorenburg SM, Van Noorden CJ. The complex effects of heparins on cancer progression and metastasis in experimental studies. Pharmacological reviews. 2001;53:93-105.

[5] Gaengel K, Betsholtz C. Endocytosis regulates VEGF signalling during angiogenesis. Nature cell biology.2013;15:233-5.

[6] Munoz EM, Linhardt RJ. Heparin-binding domains in vascular biology. Arteriosclerosis, thrombosis, and vascular biology. 2004;24:1549-57.

[7] Harrop HA, Rider CC. Heparin and its derivatives bind to HIV-1 recombinant envelope glycoproteins, rather than to recombinant HIV-1 receptor, CD4. Glycobiology. 1998;8:131-7.

[8] Fairbrother WJ, Champe MA, Christinger HW, Keyt BA, Starovasnik MA. Solution structure of the heparin-binding domain of vascular endothelial growth factor. Struct Fold Des. 1998;6:637-48.

[9] Ferro V, Dredge K, Liu L, Hammond E, Bytheway I, Li C, et al. PI-88 and novel heparan sulfate mimetics inhibit angiogenesis. Seminars in thrombosis and

hemostasis. 2007;33:557-68.
[10] Lee E, Kim YS, Bae SM, Kim SK, Jin S, Chung SW, et al. Polyproline-type helical-structured low-molecular weight heparin (LMWH)-taurocholate conjugate as a new angiogenesis inhibitor. International journal of cancer Journal international du cancer. 2009;124:2755-65.
[11] Park J, Jeong JH, Al-Hilal TA, Kim JY, Byun Y. Size Controlled Heparin Fragment-Deoxycholic Acid Conjugate Showed Anticancer Property by Inhibiting $VEGF_{165}$. Bioconjugate chemistry. 2015;26:932-40.
[12] Yin W, Zhang J, Jiang Y, Juan S. Combination therapy with low molecular weight heparin and Adriamycin results in decreased breast cancer cell metastasis in CH mice. Experimental and therapeutic medicine.2014;8:1213-8.
[13] Pelzer U, Opitz B, Deutschinoff G, Stauch M, Reitzig PC, Hahnfeld S, et al. Efficacy of Prophylactic Low-Molecular Weight Heparin for Ambulatory Patients With Advanced Pancreatic Cancer: Outcomes From the CONKO-004 Trial. Journal of clinical oncology : official journal of the American Society of Clinical Oncology. 2015;33:2028-34.
[14] Agnelli G, George DJ, Kakkar AK, Fisher W, Lassen MR, Mismetti P, et al. Semuloparin for thromboprophylaxis in patients receiving chemotherapy for cancer. The New England journal of medicine. 2012;366:601-9.
[15] Franchini M, Bonfanti C, Lippi G. Cancer-associated thrombosis: investigating the role of new oral anticoagulants. Thrombosis research.2015;135:777-81.
[16] Kamphuisen PW, Beyer-Westendorf J. Bleeding complications during anticoagulant treatment in patients with cancer. Thrombosis research. 2014;133 Suppl 2:S49-55.
[17] Sideras K, Schaefer PL, Okuno SH, Sloan JA, Kutteh L, Fitch TR, et al. Low-molecular-weight heparin in patients with advanced cancer: a phase 3 clinical trial. Mayo Clinic proceedings. 2006;81:758-67.
[18] Park JW, Jeon OC, Kim SK, Al-Hilal TA, Jin SJ, Moon HT, et al. High antiangiogenic and low anticoagulant efficacy of orally active low molecular weight heparin derivatives. Journal of controlled release : official journal of the Controlled Release Society.2010;148:317-26.

[19] Middaugh CR, Mach H, Burke CJ, Volkin DB, Dabora JM, Tsai PK, et al. Nature of the interaction of growth factors with suramin. Biochemistry. 1992;31:9016-24.
[20] Marks RM, Lu H, Sundaresan R, Toida T, Suzuki A, Imanari T, et al. Probing the interaction of dengue virus envelope protein with heparin: assessment of glycosaminoglycan-derived inhibitors. Journal of medicinal chemistry. 2001;44:2178-87.
[21] Takano S, Gately S, Neville ME, Herblin WF, Gross JL, Engelhard H, et al. Suramin, an anticancer and angiosuppressive agent, inhibits endothelial cell binding of basic fibroblast growth factor, migration, proliferation, and induction of urokinase-type plasminogen activator. Cancer research. 1994;54:2654-60.
[22] Kathir KM, Kumar TK, Yu C. Understanding the mechanism of the antimitogenic activity of suramin. Biochemistry. 2006;45:899-906.
[23] Song S, Wientjes MG, Gan Y, Au JL. Fibroblast growth factors: an epigenetic mechanism of broad spectrum resistance to anticancer drugs. Proceedings of the National Academy of Sciences of the United States of America. 2000;97:8658-63.
[24] Little PJ, Rostam MA, Piva TJ, Getachew R, Kamato D, Guidone D, et al. Suramin inhibits PDGF-stimulated receptor phosphorylation, proteoglycan synthesis and glycosaminoglycan hyperelongation in human vascular smooth muscle cells. The Journal of pharmacy and pharmacology. 2013;65:1055-63.
[25] Warn R, Harvey P, Warn A, Foley-Comer A, Heldin P, Versnel M, et al. HGF/SF induces mesothelial cell migration and proliferation by autocrine and paracrine pathways. Experimental cell research. 2001;267:258-66.
[26] Botta M, Manetti F, Corelli F. Fibroblast growth factors and their inhibitors. Current pharmaceutical design. 2000;6:1897-924.
[27] Wang LL, Li JJ, Zheng ZB, Liu HY, Du GJ, Li S. Antitumor activities of a novel indolin-2-ketone compound, Z24: more potent inhibition on bFGF-induced angiogenesis and bcl-2 over-expressing cancer cells. European journal of pharmacology. 2004;502:1-10.
[28] Tayel A, Ebrahim MA, Ibrahim AS, El-Gayar AM, Al-Gayyar MM. Cytotoxic effects of suramin against HepG2 cells through activation of intrinsic apoptotic

pathway. J BUON. 2014;19:1048-54.
[29] Li H, Li H, Qu H, Zhao M, Yuan B, Cao M, et al. Suramin inhibits cell proliferation in ovarian and cervical cancer by downregulating heparanase expression. Cancer Cell Int. 2015;15:52.
[30] Ullmann H, Meis S, Hongwiset D, Marzian C, Wiese M, Nickel P, et al. Synthesis and structure-activity relationships of suramin-derived P2Y11 receptor antagonists with nanomolar potency. Journal of medicinal chemistry. 2005;48:7040-8.
[31] Imberty A, Lortat-Jacob H, Perez S. Structural view of glycosaminoglycan-protein interactions. Carbohydrate research.2007;342:430-9.
[32] Rusnati M, Tulipano G, Urbinati C, Tanghetti E, Giuliani R, Giacca M, et al. The basic domain in HIV-1 Tat protein as a target for polysulfonated heparin-mimicking extracellular Tat antagonists. Journal of Biological Chemistry. 1998;273:16027-37.
[33] Chen HL, Her SY, Huang KC, Cheng HT, Wu CW, Wu SC, et al. Identification of a heparin binding peptide from the Japanese encephalitis virus envelope protein. Biopolymers. 2010;94:331-8.
[34] Ganesh VK, Muthuvel SK, Smith SA, Kotwal GJ, Murthy KH. Structural basis for antagonism by suramin of heparin binding to vaccinia complement protein. Biochemistry. 2005;44:10757-65.
[35] Lozano RM, Jimenez M, Santoro J, Rico M, Gimenez-Gallego G. Solution structure of acidic fibroblast growth factor bound to 1,3, 6-naphthalenetrisulfonate: a minimal model for the anti-tumoral action of suramins and suradistas. J Mol Biol. 1998;281:899-915.
[36] Al-Hilal TA, Park J, Alam F, Chung SW, Park JW, Kim K, et al. Oligomeric bile acid-mediated oral delivery of low molecular weight heparin. Journal of controlled release : official journal of the Controlled Release Society. 2014;175:17-24.
[37] Al-Hilal TA, Alam F, Park JW, Kim K, Kwon IC, Ryu GH, et al. Prevention effect of orally active heparin conjugate on cancer-associated thrombosis. Journal of controlled release : official journal of the Controlled Release Society. 2014.

[38] Lee DY, Lee SW, Kim SK, Lee M, Chang HW, Moon HT, et al. Antiangiogenic activity of orally absorbable heparin derivative in different types of cancer cells. Pharmaceutical research. 2009;26:2667-76.
[39] Park K, Lee GY, Kim YS, Yu M, Park RW, Kim IS, et al. Heparin-deoxycholic acid chemical conjugate as an anticancer drug carrier and its antitumor activity. Journal of controlled release : official journal of the Controlled Release Society. 2006;114:300-6.
[40] Alam F, Al-Hilal TA, Chung SW, Seo D, Mahmud F, Kim HS, et al. Oral delivery of a potent anti-angiogenic heparin conjugate by chemical conjugation and physical complexation using deoxycholic acid. Biomaterials. 2014;35:6543-52.
[41] Alam F, Chung SW, Hwang SR, Kim JY, Park J, Moon HT, et al. Preliminary safety evaluation of a taurocholate-conjugated low-molecular-weight heparin derivative (LHT7): a potent angiogenesis inhibitor. Journal of applied toxicology : JAT. 2014.
[42] Sanner MF. Python: a programming language for software integration and development. Journal of molecular graphics & modelling. 1999;17:57-61.
[43] Trott O, Olson AJ. AutoDock Vina: improving the speed and accuracy of docking with a new scoring function, efficient optimization, and multithreading. Journal of computational chemistry. 2010;31:455-61.
[44] Ingle RG, Agarwal AS. A world of low molecular weight heparins (LMWHs) enoxaparin as a promising moiety--a review. Carbohydr Polym. 2014;106:148-53.
[45] Nico B, Benagiano V, Mangieri D, Maruotti N, Vacca A, Ribatti D. Evaluation of microvascular density in tumors: pro and contra. Histol Histopathol. 2008;23:601-7.
[46] Zhao YY, Xue C, Jiang W, Zhao HY, Huang Y, Feenstra K, et al. Predictive value of intratumoral microvascular density in patients with advanced non-small cell lung cancer receiving chemotherapy plus bevacizumab. J Thorac Oncol. 2012;7:71-5.
[47] Willett CG, Boucher Y, di Tomaso E, Duda DG, Munn LL, Tong RT, et al. Direct evidence that the VEGF-specific antibody bevacizumab has antivascular effects in human rectal cancer. Nat Med. 2004;10:145-7.

Chapter: 6

Heparin conjugate based nanocomplex using PEG- protamine conjugate for anticancer therapy

6.1. Introduction

Cancer is the fetal disease to human with abnormal cell growth and uncontrolled metastasis. It requires and induces the angiogenesis process with activation or upregulation of angiogenesis inducers [1]. The action of growth factors triggers a number of physiological and pathological processes in the tumor and tumor-related environment [2]. A variety of proteins including growth factors, growth factor receptors and chemokines involve these processes [3, 4]. In particular, there are a lot of tumor-related growth factors which have heparin binding domain in their structure [5-7].

Heparin, low molecular weight heparins, fucoidan, hyaluronic acid, chitosan and their derivatives have been studied as potent anti-cancer polysaccharides [8-10]. There are a lot of suitable candidates for angiogenesis inhibitors with low toxicity [11, 12]. However, anticancer polysaccharides do not have specific mechanism to be delivery to the tumor site in the body. For a better anticancer therapy, anticancer related polysaccharides including heparin derivatives and conjugates need to have tumor targeting effect using a nanocarrier.

Anti-cancer therapy using polysaccharide is facing several challenges including tumor-targeting, low efficacy and toxicity [13]. Current polysaccharide research could find new therapeutic targets such as blood vessels in tumor related environment. Because of the characteristics of the microenvironment around tumor and angiogenetic process, it was available to develop new delivery systems for tumor targeting [14]. A polysaccharide based nanocomplex would work effectively for tumor targeting using enhanced permeability and retention (EPR) effect.

For the delivery of anti-cancer polysaccharides and their derivatives to the tumor site, protamine complex carrier could be an attractive approach to optimize

the therapeutic effect of biomaterials. Protamine is a low molecular weight peptide (Average M.W: 4500 Da) rich in basic arginine residues. Approximately 67% of the amino acid composition of protamine is arginine, and the positive charge of protamine helps to form a stable nanocomplex with heparin and other polysaccharides through electrostatic interactions

To use protamine-based nanocomplex for anti-cancer therapy, what is needed is a chemical modification to increase the clinical advantages of nanocomplex while minimizing the adverse effects of nanocomplex and anti-cancer materials. The PEG system has been considered to be effective model with potential applications in anticancer related research [15-17]. PEG-protamine could be a key material to increase the targeting effect of anticancer related polysaccharides, gene and protein formulating a nanocomplex [18, 19].

The purpose of this study is on using PEG (10 kDa)-protamine for tumor targeting effect with potential implications for polysaccharide-based anticancer therapy. To accomplish this purpose, we designed polysaccharide-based nanocomplexes having safe and effective properties. In previous studies, we developed several anti-tumoral heparin conjugates like LHsura, LHT7, LHD and VHD. They have been stuied that they are potent angiogenesis inhibitors for their modulation of several growth factors [8, 20]. In the case of protamine, PEG (10 kda) was conjugated to the N-terminal of the molecular structure of peptide. We developed a new PEG-protamine based nanocomplex system using PEG-protamine. We evaluated the physical and chemical characteristics of PEG-protamine, and LHsura/PEG-protamine complex was made. The targeting effect of nanocomplex was proved in tumor-bearing animal model. Finally, PEG-protamine delivery system with anti-cancer polysaccharide could be a promising anticancer therapy based on its safety and targeting effect.

6.2. Materials and methods

6.2.1. Materials

LMWH (nadroparin, average molecular weight 4.5 kDa, produced by

deaminative cleavage with nitrous acid) was obtained from the Nanjing King-Friend Biochemical Pharmaceutical Company Ltd. (Nanjing, China). Heparin, Deoxycholic acid (DOCA), Dextran-FITC, N-hydroxylsuccinimide (NHS), protamine sulfate and 1-ethyl-3-(3-dimethylaminopropyl)carbodiimide (EDAC) were purchased from Sigma chemical Co. (St. Louis, MO, USA). N,N-dimethylformide (DMF) was purchased from Merck (Darmstadt, Germany). Suramin fragment (disodium 8-amino-1,3,6-naphthalenetrisulfonate) was obtained from TCI (Tokyo Chemical Industry co., Japan). PEG-SVA (10,000 Da) was purchased from Sunbio Inc. (South Korea). Acetone was purchased from Daejung Chemicals and Metals Co. (Shiheung, South Korea). Fetal bovine serum was obtained from GIBCO (Grand Island, NY, USA).

6.2.2. Synthesis and characterization of PEG-protamine

Protamine sulfate (Avg. M.W. 4.5 kDa) was dissolved in borate buffer (pH 8.5) at 5 mg/ml concentration. Methoxy poly (ethylene glycol) succinimidyl valerate (mPEG-SVA, 10kDa, Sunbio Inc.) was dissolved in DMF. The DMF solution with PEG was added to the protamine solution slowly. The solution was stirred for 24h. Additionally, the same amount of mPEG-SVA in DMF was added to the mixed solution again considering the rapid hydrolysis of SVA group in mPEG, and then stirred for 24 h again. The total feed mole ratio of protamine and mPEG-SVA was 1:10. Remained PEG was removed by repeated precipitation using acetone-methanol mixture. The product was dissolved in distilled water, then freeze-dried.

The synthesized PEG-protamine conjugate was characterized using proton nuclear magnetic resonance (^{1}H NMR, JEOL JNM-LA, Japan) and MALDI-TOF mass spectrometry. The conjugation ratio of PEG-protamine was determined using the integration values of PEG (3.7 ppm) and protamine (1.8, 1.5 and 0.8 ppm) peaks, compared with the peaks in PEG and protamine mixtures. NMR spectra were recorded at 500 MHz using D_2O as solvent (Sigma).

6.2.3. Formulation of PEG-protamin Based Nanocomplex

PEG-protamine nanocomplexes were prepared by mixing of polysaccharides and PEG-protamine in solution state. To generate the nanocomplex, at first, PEG-protamine was dissolved in normal saline (0.5 mg/mL concentration). Polysaccharides including LHsura were also prepared at 0.5-2 mg/mL concentration. The PEG-protamine solution was slowly dropped in the stirred polysaccharide solution and then kept at room temperature for 10 min.

6.2.4. Characterization of PEG-protamine based nanocomplex

After the formulation of nanocomplex, the size and zeta potential of PEG-protamine based nanocomplexes with various polysaccharides derivatves were measured by Dynamic Light Scattering instrument (ELS-8000, Japan). We also used transmission electron microscopy (200 kV, Japan) to detect the appearance of nanocomplex. Stability was tested in normal saline and saline with 20% fetal bovine serum (FBS) for 120 h. The primary amine in N-terminal of protamin was checked by trinitrobenzene sulfonate (TNBS) assay.

The molecular structure of protamine was obtained from the structure of protamine-DNA complex 1 (protein data bank [PDB] code, 2AWR). In the case of heparin conjugate, we draw the energy minimized structure of the polysaccharide using chemBioDraw Ultra 12.0 and ChemBio3D Ultra 12.0 (Cambridge Soft, CA).

6.2.5. *In vivo* tumor inhibition and targeting study

SCC7 (murine squamous cell carcinoma) cells were cultured in DMEM high glucose medium supplemented with 10% (v/v) FBS, and then the cells were injected subcutaneously into Balb/c nude mice (1×10^7 cells/60 μL). After 12 days, cy5 conjugated LHsura and PEG protamine nanocomplex was injected via the tail vein of mice. Images of mice, dissected tumors and organs were obtained using Optical Imaging System.

Tumor inhibition study was conducted using SCC7. All procedures for animal experiment were approved by the Committee on the Use and Care on Animals according to the regulations of the Institutional Animal Ethics Committee

of the Seoul National University animal care facility. SCC7 (murine squamous cell carcinoma) cells were cultured in DMEM high glucose medium supplemented with 10 % (v/v) FBS, and then the cells were injected subcutaneously into C3H/HeN mice (1×10^6 cells/60 μL). On day 5, the mice were administrated intravenously 10 mg/kg/3 day of LHsura for 2 weeks. Tumor volumes were measured and calculated ($a^2 \times b \times 0.52$, where a = width, and b = length). Before sacrifice, dextran-FITC was injected via the tail vein of mice. After sacrifice, isolated tumor masses were also measured, and tumor tissues were histologically evaluated by H&E staining.

6.2.6. Statistical analysis

We analyzed the results by comparing the means of groups in in vitro and in vivo experiments using one-way analyses of variance (ANOVA) followed by Bonferroni's post-hoc tests using sigmaplot 12. P-values less than 0.05 were considered to be statistically significant.

6.3. Results

6.3.1. Characterization of PEG-protamine

PEG (10 kDa)-protamine was synthesized and characterized for polysaccharide-based anticancer therapy (**Figure 6.1**). At first, the total feed mole ratio of protamine and mPEG-SVA was 1:10 considering hydrolysis of mPEG-SVA in the reaction. PEGThe final conjugation ratio of PEG-protamine was determined using the integration values in NMR compared with the peaks in PEG and protamine mixtures, and it was approximately 0.85. The primary amine in N-terminal of protamine was measured by TNBSA assay. The number of primary amine in protamine was 0.9 before conjugation. After synthesis, the number was decreased to approximately 0.1 (**Figure 6.2)**. The MALDI-TOF MS results showed shifted peaks from the peaks of protamine (**Figure 6.3)**.

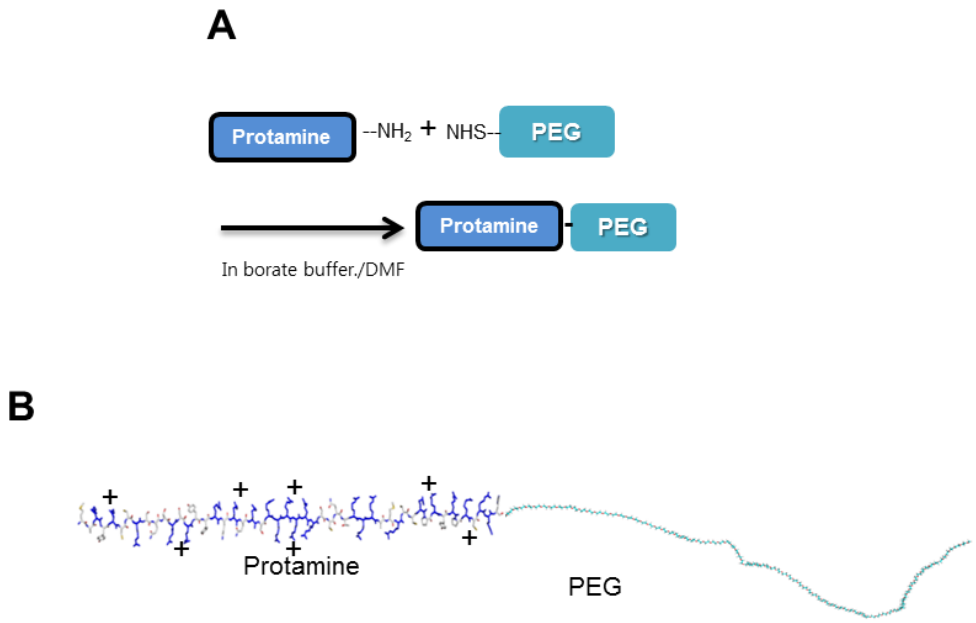

Figure 6.1. (A) Chemical reaction scheme for synthesis of PEG-protamine (B) The molecular structure of PEG-protamine

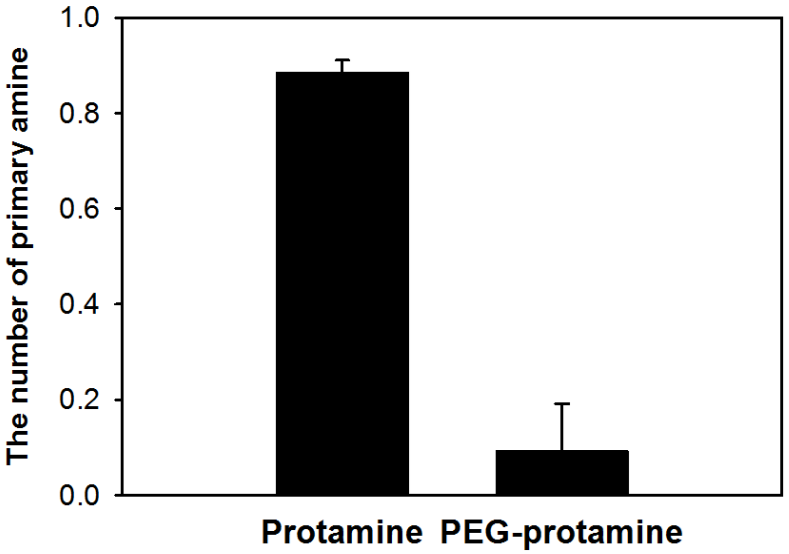

Figure 6.2. The number of primary amine in N-terminal of protamine was decreased after synthesis.

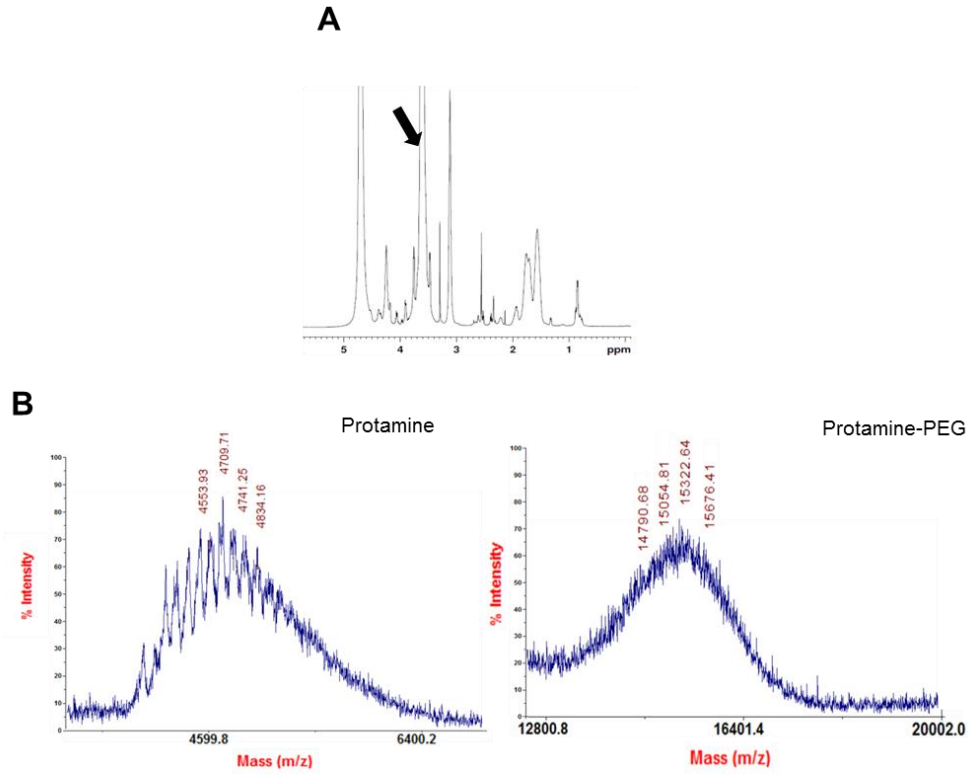

Figure 6.3. (A) ^{1}H NMR data of PEG-protamine (B) The measured molecular weight of PEG-protamine by using MALDI-TOF MS

6.3.2. Formation of nanocomplex using PEG-protamine

PEG-protamine based nanocomplexes with various polysaccharides were prepared by mixing two solutions (**Figure 6.4**). Two kind of differently charged nanocomplexes were made depending on surface materials. When we control the molecular size of polysaccharide, the average size of nanocomplex was also changed (**Figure 6.5**). It means that the size of nanocomplex based on PEG-protamine could be controlled intentionally.

There are several kinds of heparin derivatives and conjugates which have anticancer property including LMWH-suramine fragment, LMWH-DOCA, LMWH-taurocholic acid conjugates. They have shown significant anticancer effects in many experiments. PEG-protamine could mix them and generate different stable nanocomplexes. The size of each nanocomplex was measured. Especially, among polysaccharides, LMWH-suramine fragment conjugate (LHsura) showed stable nanocomplex without toxicity (**Figure 6.6**). Stable nanocomplexes with LHsura and PEG-protamine could be generated by the charge-to-charge interaction. The size of LHsura and PEG-protamine was also measured with different ratios.

PEG coated nanocomplexes showed differences. Especially, PEG-protamine could provide molecular protection against enzyme and immune system. The effect of PEG changed the morphology of nanocomplexes which visualized by transmission electron microscope (**Figure 6.7**). The picture indicated a moderate surface coating of flexible hydrophilic PEG on the nanocomplex.

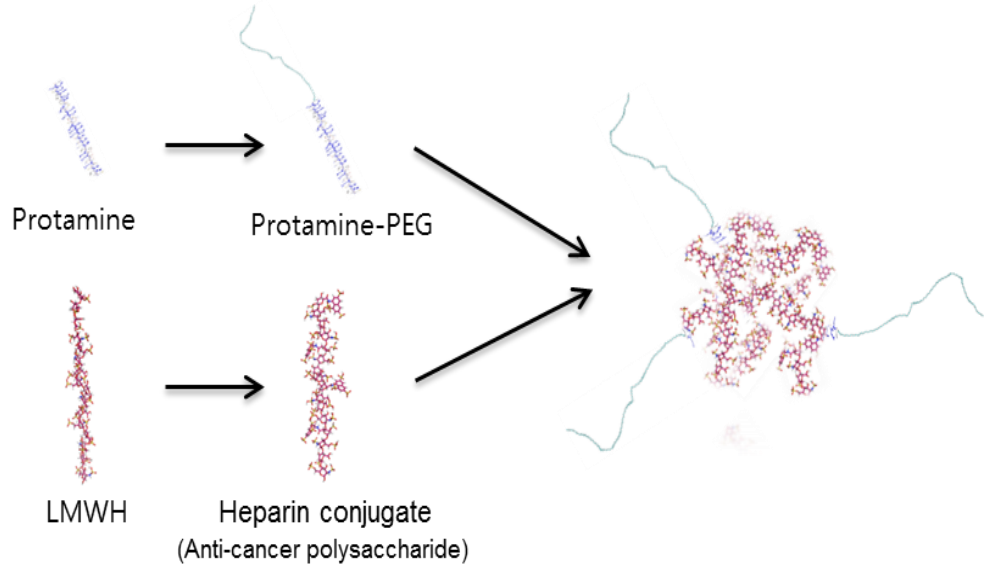

Figure 6.4. Molecular scheme of formulation of PEG-protamine based nanocomplex. It could bind with heparin or anticancer polysaccharides, and formed stable nanocomplex.

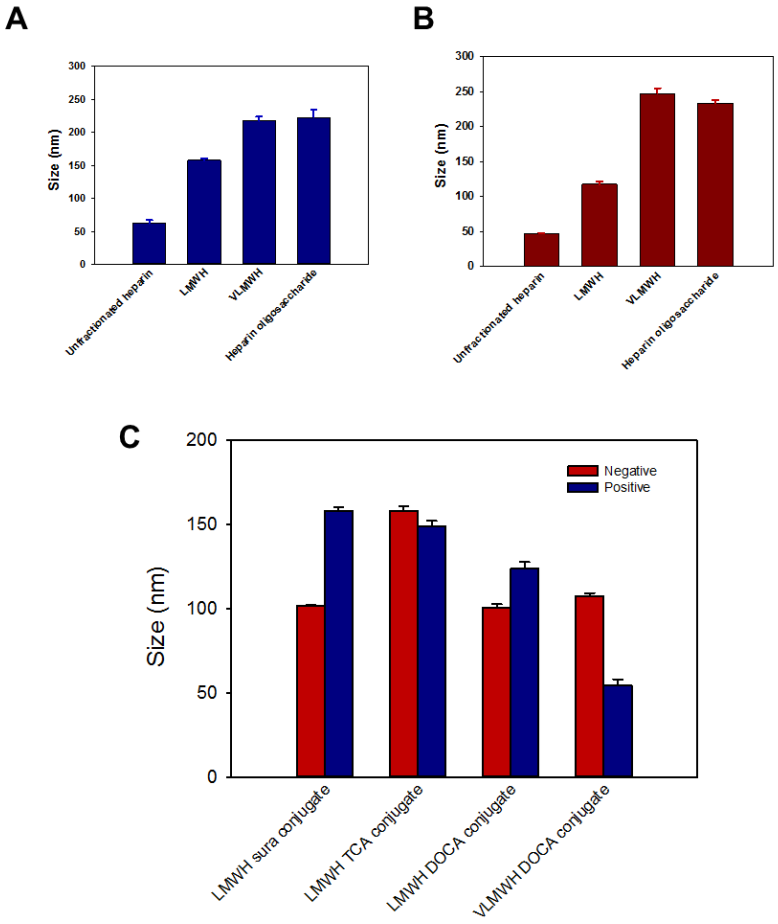

Figure 6.5. (A) The average molecular size of positively charged nanocomplex with various size of heparin. The size of nanocomplex could be changed by control of the size of polysaccharides. (B) The average molecular size of negatively charged nanocomplex with various size of heparin. (C) Nanocomplex formulation with different kind of anticancer polysaccharides

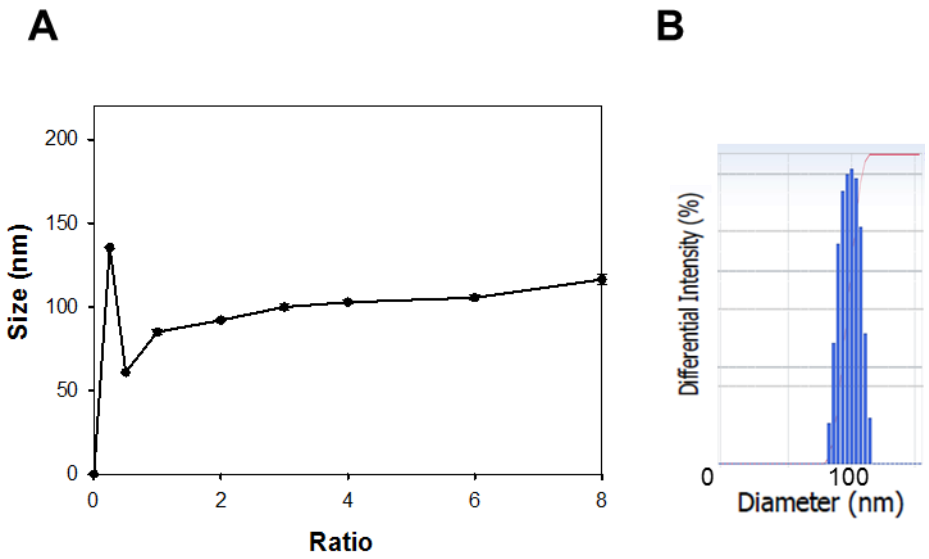

Figure 6.6. (A) The average size of negatively charged nanocomplex with anticancer polysaccharide named LHsura with different ratio (B) The molecular size distribution of the nanocomplex.

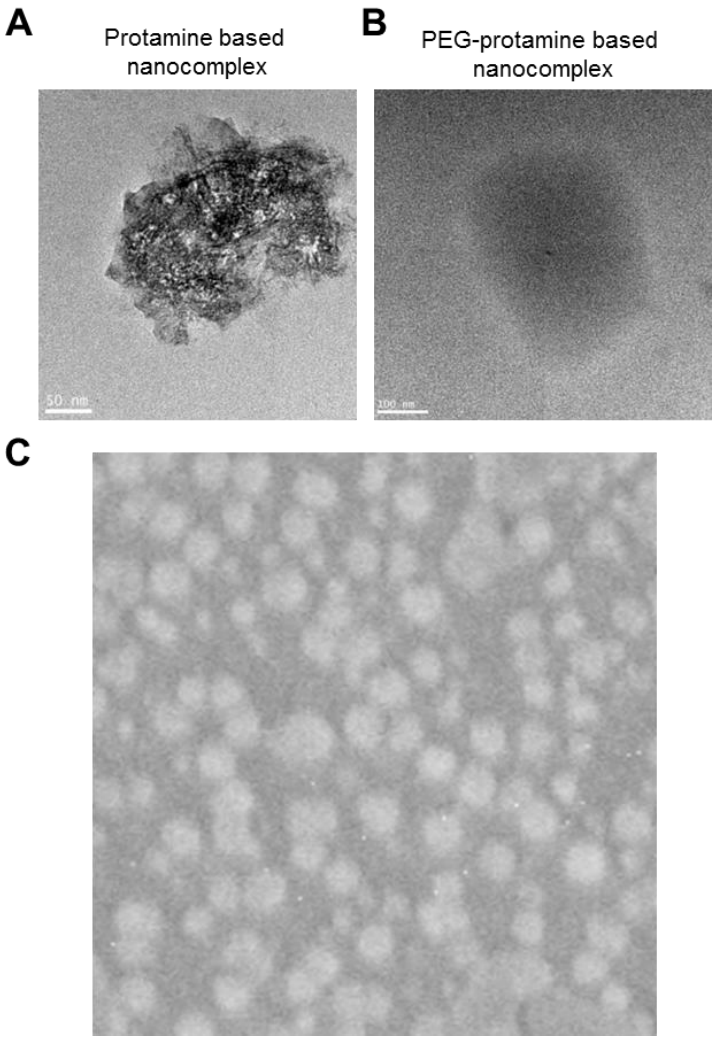

Figure 6.7. (A) TEM image of protamine or PEG-protamine based nanocomplex. The shielding effect of PEG changed the image of the nanocomplex. (B) SEM image of PEG-protamine based nanocomplex.

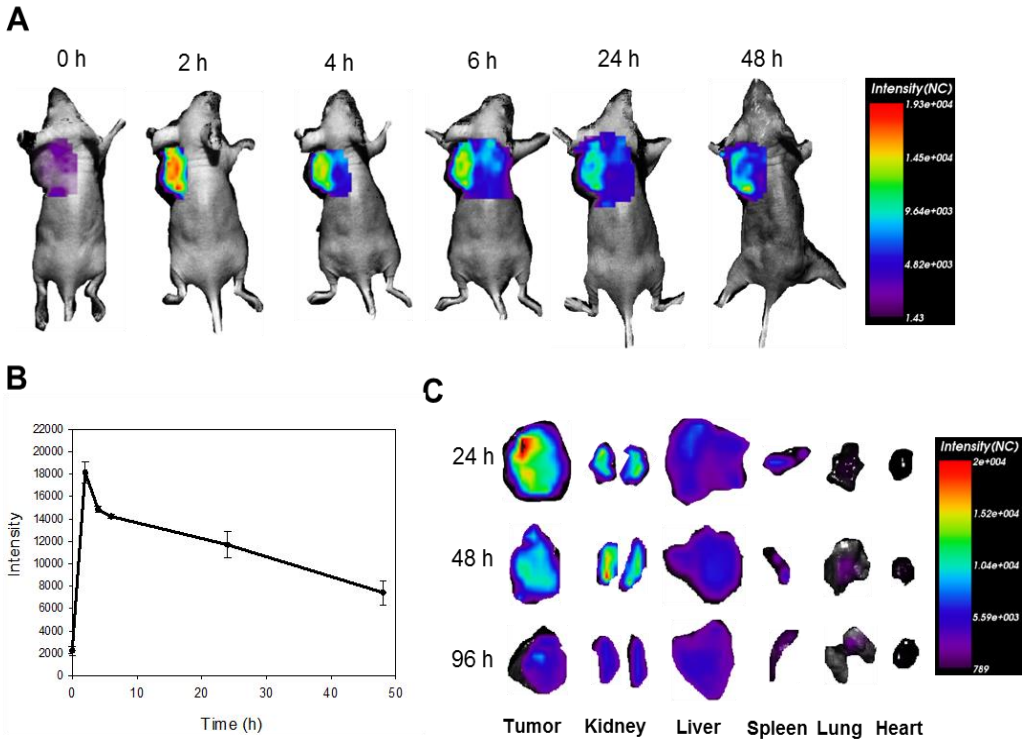

Figure 6.8. (A) The tumor targeting image of PEG-protamine based nanocomplex (LSPP)-cy5 in tumor bearing mice (B) Intensity of cy5 in nanocomplex in tumor was measured (n=3) (C) Organ distribution image of PEG-nanocomplex

6.3.3. Anticancer and targeting effect PEG-protamine nanocomplex

To prove therapeutic and targeting effect of the complex, PEG-protamine based LHsura nanocomplex (LSPP) was injected to mice. In the image of SCC7 tumor bearing mice, intensity of cy5 in nanocomplex in tumor was increased and maintained (**Figure 6.8**). To compare it with other organs, mice were sacrificed. In the organ distribution image, tumor showed higher signal than other organs.

To use PEG-protamine in anticancer therapy, antitumor effect of PEG-protamine based nanocomplex (LSPP) in SCC7 tumor model was measured (**Figure 6.9**). The nanocomplex showed enhanced therapeutic effect without toxicity. The final tumor weight was decreased, and the body weight was maintained. In tissue analysis using H&E histological staining, no significant toxicity was detected (**Figure 6.10**). Accumulation of nanocomplex (LSPP) and the tissue distribution of the nanocomplex were measured after 2 and 24 h of injection (**Figure 6.11**).

6.4. Discussion

Anticancer therapy using polysaccharide is important because polysaccharide usually show remarkable safety and efficacy in therapy. Current polysaccharide research focused on finding new biomaterials and polysaccharides related anticancer and antinflamatory effects. When we use nanocomplex system with polysaccharide, we could figure out the chance for new drug development using functional polysaccharides. Protamine complex carrier could be an attractive approach to optimize the therapeutic effect of biomaterials. The positive charge of PEG conjugated protamine formed a stable nanocomplex with anticancer heparin conjugate (LSPP). PEG-protamine could be a key material for drug and polysaccharide delivery. The purpose of this study was on using PEG protamine for tumor targeting effect. For the study, we designed polysaccharide-based nanocomplexes delivery system. The system showed promising results with tumor related targeting effect.

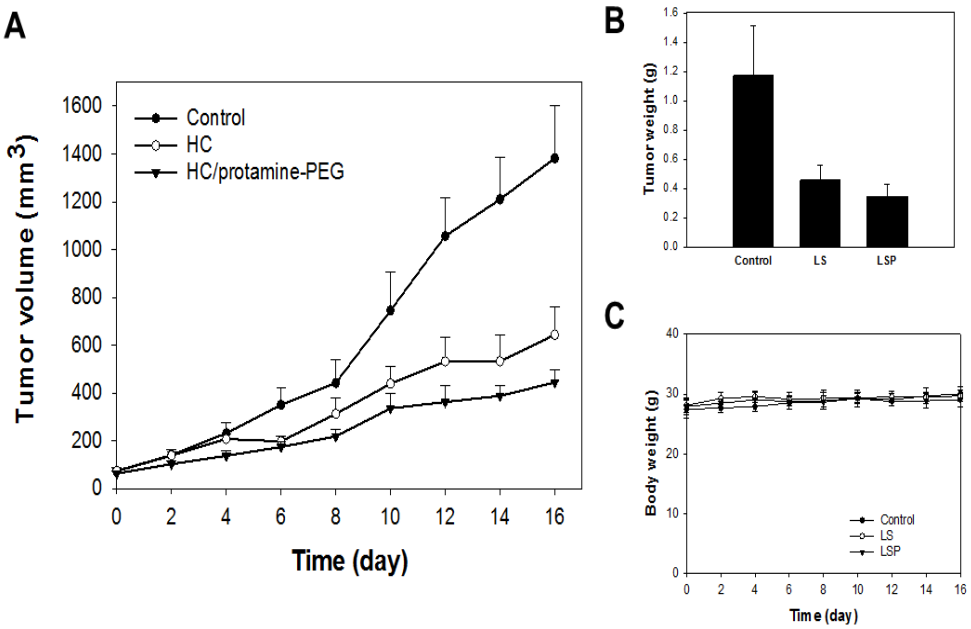

Figure 6.9. (A) Antitumor effect of PEG-protamine based nanocomplex (LSPP) in SCC7 tumor model (10 mg/kg/3day) (B) The final tumor weight was measured. (B) Isolated tumor mass after 16 days (C) Body weight change after administration

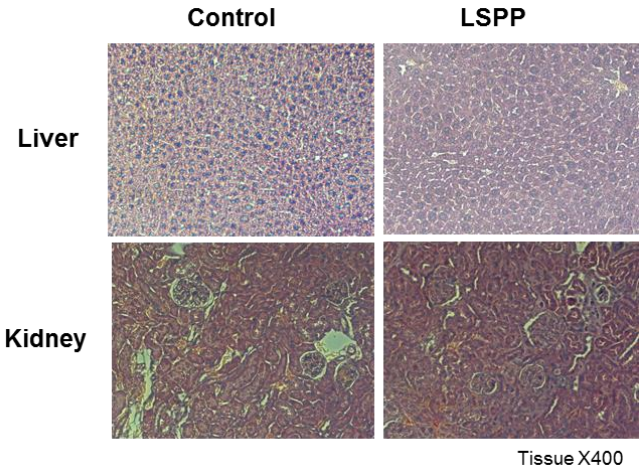

Figure 6.10. Tissue analysis using H&E histological staining after injection. No significant toxicity was detected.

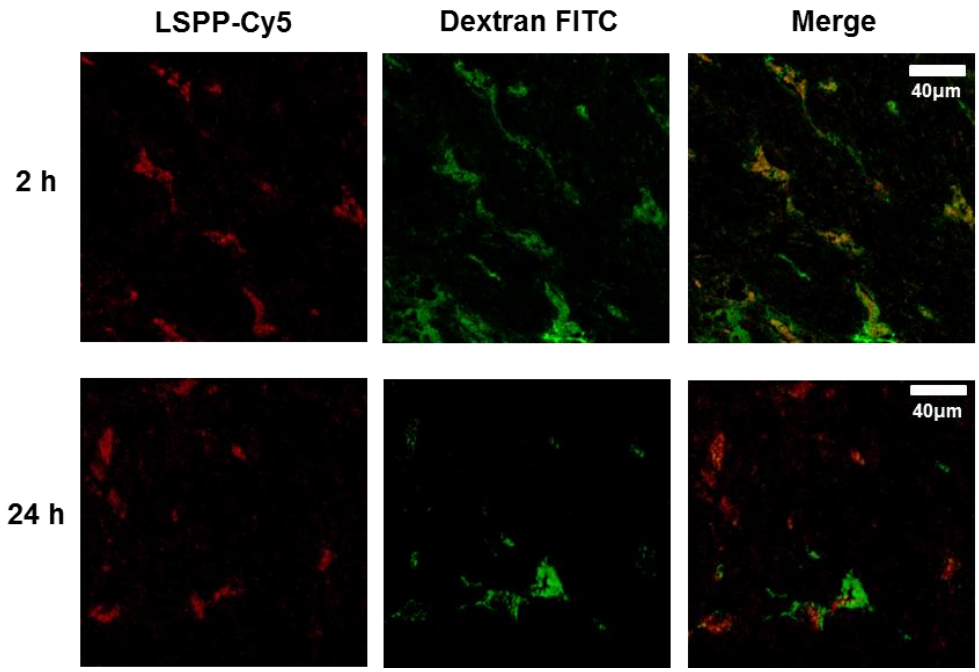

Figure 6.11. Accumulation of nanocomplex (LSPP) and the tissue distribution of the nanocomplex were measured after 2 and 24 h of injection. Dextran-FITC was injected to visualize blood vessels in tumor.

6.5. Conclusion

We developed a new nanocomplex using PEG based protamine for the tumor-targeting and anticancer effect. PEG-Protamine was effectively mixed with anticancer polysaccharides by charge-charge interaction. We also evaluated the tumor-targeting and therapeutic effects of new nanocomplex in tumor bearing animal model. In conclusion, PEG-protamine has potential to use for advanced drug delivery system.

References

[1] Folkman J. Tumor angiogenesis: therapeutic implications. The New England journal of medicine. 1971;285:1182-6.

[2] Kerbel R, Folkman J. Clinical translation of angiogenesis inhibitors. Nature reviews Cancer. 2002;2:727-39.

[3] Ferrara N. Vascular endothelial growth factor. Arteriosclerosis, thrombosis, and vascular biology. 2009;29:789-91.

[4] Brem S, Brem H, Folkman J, Finkelstein D, Patz A. Prolonged tumor dormancy by prevention of neovascularization in the vitreous. Cancer research. 1976;36:2807-12.

[5] Tessler S, Rockwell P, Hicklin D, Cohen T, Levi BZ, Witte L, et al. Heparin modulates the interaction of VEGF165 with soluble and cell associated flk-1 receptors. The Journal of biological chemistry. 1994;269:12456-61.

[6] Pellegrini L, Burke DF, von Delft F, Mulloy B, Blundell TL. Crystal structure of fibroblast growth factor receptor ectodomain bound to ligand and heparin. Nature. 2000;407:1029-34.

[7] Moreira IS, Fernandes PA, Ramos MJ. Vascular endothelial growth factor (VEGF) inhibition--a critical review. Anti-cancer agents in medicinal chemistry. 2007;7:223-45.

[8] Lee E, Kim YS, Bae SM, Kim SK, Jin S, Chung SW, et al. Polyproline-type helical-structured low-molecular weight heparin (LMWH)-taurocholate conjugate as a new angiogenesis inhibitor. International journal of cancer Journal international du cancer. 2009;124:2755-65.

[9] Sideras K, Schaefer PL, Okuno SH, Sloan JA, Kutteh L, Fitch TR, et al. Low-molecular-weight heparin in patients with advanced cancer: a phase 3 clinical trial. Mayo Clinic proceedings. 2006;81:758-67.

[10] Kakkar AK, Levine MN, Kadziola Z, Lemoine NR, Low V, Patel HK, et al. Low molecular weight heparin, therapy with dalteparin, and survival in advanced cancer: the fragmin advanced malignancy outcome study (FAMOUS). Journal of clinical oncology : official journal of the American Society of Clinical Oncology. 2004;22:1944-8.

[11] Park J, Jeong JH, Al-Hilal TA, Kim JY, Byun Y. Size Controlled Heparin Fragment-Deoxycholic Acid Conjugate Showed Anticancer Property by Inhibiting VEGF165. Bioconjugate chemistry. 2015;26:932-40.

[12] Adulnirath A, Chung SW, Park J, Hwang SR, Kim JY, Yang VC, et al. Cyclic RGDyk-conjugated LMWH-taurocholate derivative as a targeting angiogenesis inhibitor. Journal of Controlled Release. 2012;164:8-16.

[13] Alam F, Chung SW, Hwang SR, Kim JY, Park J, Moon HT, et al. Preliminary safety evaluation of a taurocholate-conjugated low-molecular-weight heparin derivative (LHT7): a potent angiogenesis inhibitor. Journal of applied toxicology : JAT. 2014.

[14] Danhier F, Feron O, Preat V. To exploit the tumor microenvironment: Passive and active tumor targeting of nanocarriers for anti-cancer drug delivery. Journal of controlled release : official journal of the Controlled Release Society. 2010;148:135-46.

[15] Mattison KW, Dubin PL, Brittain IJ. Complex formation between bovine serum albumin and strong polyelectrolytes: Effect of polymer charge density. J Phys Chem B. 1998;102:3830-6.

[16] Dragan S, Cristea M, Luca C, Simionescu BC. Polyelectrolyte complexes .1. Synthesis and characterization of some insoluble polyanion-polycation complexes. J

Polym Sci Pol Chem. 1996;34:3485-94.
[17] Masayuki Ishihara SK, Megumi Takikawa, Yasutaka Mori, Shingo Nakamura, Masanori Fujita. Low-Molecular-Weight Heparin and Protamine-Based Polyelectrolyte Nano Complexes for Protein Delivery. J Biomat and Nanobiotech. 2011;2:500-9.
[18] Patra CR, Bhattacharya R, Wang E, Katarya A, Lau JS, Dutta S, et al. Targeted delivery of gemcitabine to pancreatic adenocarcinoma using cetuximab as a targeting agent. Cancer Res.2008;68:1970-8.
[19] Ran S, Downes A, Thorpe PE. Increased exposure of anionic phospholipids on the surface of tumor blood vessels. Cancer Res. 2002;62:6132-40.
[20] Chung SW, Lee M, Bae SM, Park J, Jeon OC, Lee HS, et al. Potentiation of anti-angiogenic activity of heparin by blocking the ATIII-interacting pentasaccharide unit and increasing net anionic charge. Biomaterials. 2012;33:9070-9.
[21] Denuziere A, Ferrier D, Damour O, Domard A. Chitosan-chondroitin sulfate and chitosan-hyaluronate polyelectrolyte complexes: biological properties. Biomaterials. 1998;19:1275-85.
[22] Hashimoto M, Koyama Y, Sato T. In vitro gene delivery by pDNA/chitosan complexes coated with anionic PEG derivatives that have a sugar side chain. Chem Let. 2008;37:266-7.
[23] Boddohi S, Moore N, Johnson PA, Kipper MJ. Polysaccharide-based polyelectrolyte complex nanoparticles from chitosan, heparin, and hyaluronan. Biomacromolecules. 2009;10:1402-9.
[24] Liang JF, Song H, Li YT, Yang VC. A novel heparin/protamine-based pro-drug type delivery system for proteases drugs. J Pharm Sci. 2000;89:664-73.
[25] Park YJ, Liang JF, Song H, Li YT, Naik S, Yang VC. ATTEMPTS: a heparin/protamine-based triggered release system for the delivery of enzyme drugs without associated side-effects. Adv Drug Deliv Rev.2003;55:251-65.
[26] Kemp MM, Linhardt RJ. Heparin-based nanoparticles. Wiley Interdiscip Rev Nanomed Nanobiotechnol. 2010;2:77-87.
[27] Rossmann P, Matousovic K, Horacek V. Protamine-heparin aggregates. Their

fine structure, histochemistry, and renal deposition. Virchows Arch B Cell Pathol Incl Mol Pathol. 1982;40:81-98.

[28] Mori Y, Nakamura S, Kishimoto S, Kawakami M, Suzuki S, Matsui T, et al. Preparation and characterization of low-molecular-weight heparin/protamine nanoparticles (LMW-H/P NPs) as FGF-2 carrier. Int J Nanomed. (2010);5:147-55.

[29] Nichols JW, Bae YH. Odyssey of a cancer nanoparticle: from injection site to site of action. Nano today. 2012;7:606-18.

[30] Moghimi SM, Hunter AC, Murray JC. Long-circulating and target-specific nanoparticles: theory to practice. Pharmacol Rev. 2001;53:283-318.

[31] Wang J, Lu Z, Gao Y, Wientjes MG, Au JL. Improving delivery and efficacy of nanomedicines in solid tumors: role of tumor priming. Nanomedicine (Lond). 2011;6:1605-20.

Chapter: 7

Summary

Biomaterials including heparin could be chemically modified and improved for biopharmaceutics. In general, there are a few biomaterials which are used clinically to patients without chemical modification. The study on design, synthesis and therapeutic evaluation of biofunctional conjugates using heparin showed several strategies to overcome current problems related to the development of new drug and delivery system. In particular, the anticancer effects and oral delivery of heparin and heparin conjugates were intensively studied using various heparin conjugates (**Figure 7.1**).

Oral delivery of heparin and heparin based nanocomplex was evaluated in many ways. Heparin and LMWHs have been the drug of choice for the treatment or the prevention of thromboembolic disease. There are clinically approved LMWHs on the market, and each of them has been prepared by using different methods. Enoxaparin which prepared by alkaline depolymerization has reducing sugar moiety at the end of polysaccharide. In this study, tetraDOCA was conjugated at the end of enoxaparin via chemical glycosylation reaction to synthesize orally available heparin. The end-specific conjugation is important for polysaccharide drug development due to its heterogeneity. End-specific activity of LMWHs was also confirmed by using Benedict's reagent. The conjugate was characterized in different methods such as NMR, sulfuric acid assay, anti-FXa assay and nitrous acid depolymerization. Chemical glycosylation of enoxaparin with TetraDOCA increased the bioavailability of the orally non-absorbable enoxaparin in rats. We have also shown that orally active enoxaTD could have therapeutic effects in DVT and bleeding animal models.

Newly developed heparin and bile acid based nanocomplex showed promising results related to oral delivery. Oral nanocomplexes using heparin and bile acids were designed, and their efficacy and toxicity were tested. This study proved that orally available heparin and nanocomplex could be designed. Finally,

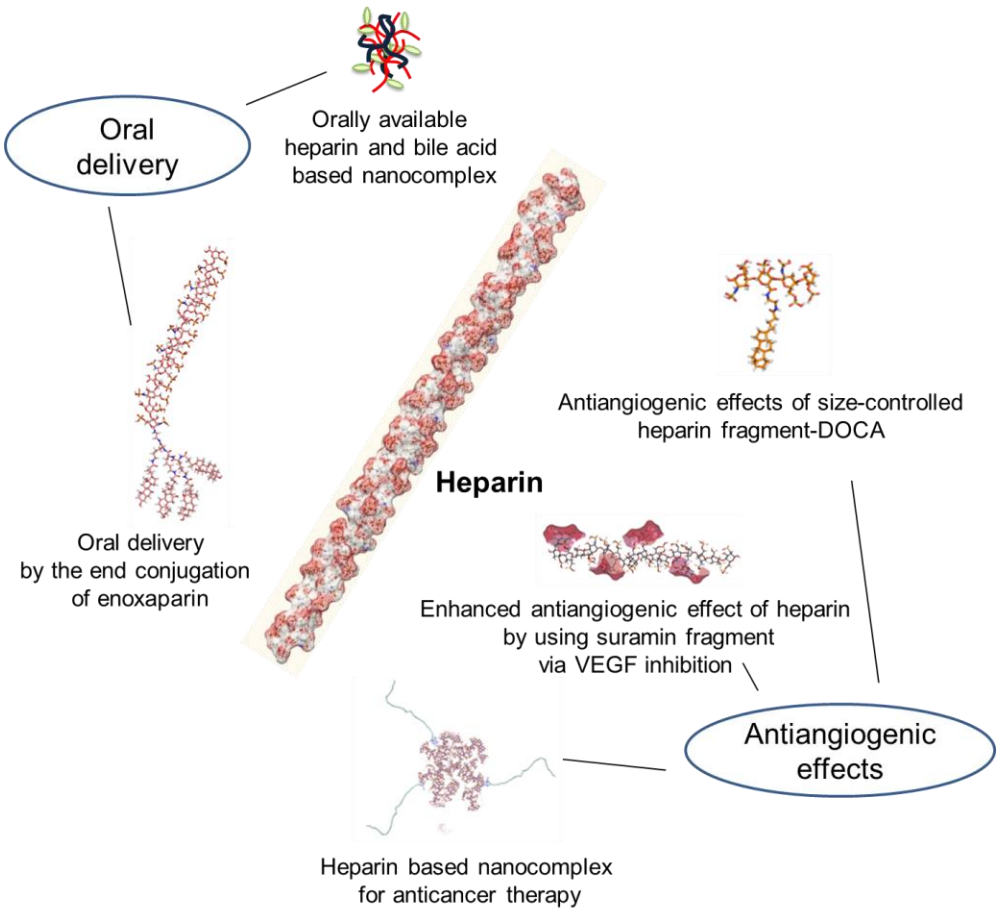

Figure 7.1. Summary of the study on design and therapeutic evaluation of heparin based bioconjugate and nanocomplex

considering the importance of oral nanoparticle and heparin, the absorption mechanism of oral nanocomplex was conducted. Based on the clinical demand for orally available nanocomplex, their usefulness was also evaluated. Using heparin and bile acid conjugate, we designed nano-sized heparin based nanocomplex (100-150 nm). Bile acid conjugated nanocomplex showed low cytotoxicity and effective binding to bile acid transporters in cells. In animal study, nanocomplexes were detected in the ileum and they stayed in the epithelial cells for 1-3 days. Orally available heparin based conjugates and nanocomplexes showed therapeutic potential associated with new drug development and delivery system.

These synthetic bioconjugates using heparins showed potentials to solve several problems related to the use of heparin in anticancer therapy. Heparins have been prescribed for patients to prevent deep vein thrombosis or pulmonary embolism. However, clinical applications of LMWH for anticancer therapy have been restricted due to its anticoagulant effect and insufficient therapeutic efficacy. The antiangiogenic effect of heparin has been drawing attention because heparins are able to bind to the heparin binding domain in growth factors. In this study, we synthesized heparin fragments and deoxycholic acid conjugated heparin fragments to search for the optimal size-controlled conjugate that will inhibit the angiogenic effect of $VEGF_{165}$. Heparin fragment-deoxycholic acid conjugates were also able to have antiangiogenic effects depending on its molecular size. We have also shown that the HFDs could have an enhanced therapeutic effect *in vitro* and *in vivo* consequent to the molecular size control. HFDs have significant antiangiogenic effects by blocking the angiogenic activity of $VEGF_{165}$ depending on its molecular size. Among them, HFD2 was a promising candidate for oral angiogenesis inhibitor. These results suggest that size-controlled synthesis is necessary for heparin-based drug development.

To overcome limitations and enhance the antiangiogenic efficacy of heparin, suramin fragments was conjugated to it. Suramin fragment has a binding affinity to the heparin-binding domain of proteins. The conjugation of suramin fragments to LMWH enhanced the antiangiogenic effect of LMWH by increasing the binding affinity to $VEGF_{165}$, while decreasing its anticoagulant activity. The chemical

conjugate of LMWH and suramin fragments (LHsura) showed a substantial inhibitory effect on $VEGF_{165}$-mediated cell proliferation, migration, and tube formation of HUVECs without significant cytotoxicity *in vitro*. Finally, we confirmed the anticancer effect of LHsura in a SCC7-bearing mouse model. Moreover, we increased the anticancer effect of LHsura by using PEG-protamine. PEG-protamine successfully generated a stable nanocomplex with LHsura, and the nanocomplex showed tumor-targeting effect in animal model.

Finally, in this study, design and therapeutic evaluation of heparin conjugates were discussed with the current challenges associated with the development of new drugs. Based on the unmet clinical need for an ideal anticancer agent, various attempts using heparin have been made to develop a new antiangiogenic agent in this study. The development of heparin conjugated for antiangiogenic therapy was with drug delivery system. Chemical conjugation and formulation with heparin showed therapeutic potential for new oral or antiangiogenic agents by using heparin. Recent advances in biotechnology and bioconjugate associated with heparin were discussed in the context of current progression states in drug delivery and development.

Supporting Chapter:

Design, synthesis and therapeutic evaluation of polyacrylic acid-tetraDOCA conjugate for hyperlipidemia therapy

S.1. Introduction

Hyperlipidemia is a major risk factor for atherosclerosis and cardiovascular diseases [1-3]. Hyperlipidemia includes hypercholesterolemia and hypertriglyceridemia, which showed to increase levels of cholesterol and triglycerides in the blood. Recently, the inhibition of cholesterol homeostasis and intestinal absorption of bile acids has attracted attention as a pharmacological target for the hypocholesterolemic effect, which is necessary for the treatment of hypercholesterolaemia [4]. The regulation of cholesterol and bile acid homeostasis is important, because about 50 percent of cholesterol is eliminated from the body by converting into bile acid [5]. Bile acids, which are synthesized from cholesterol in the liver and the released from the gallbladder into the small intestine, are constantly reabsorbed and recycled in the enterohepatic circulation [6, 7].

Cholesterol-derived amphipathic bile acids are released from the bile duct, and more than 90% of released bile acids are then reabsorbed in the ileum by the apical sodium-dependent bile acid transporter (ASBT, also known as SLC10A2) [8]. For this reason, ASBT is considered a pharmaceutical target for the treatment of hypercholesterolaemia, cholestatic liver diseases and type 2 diabetes [9, 10]. Small synthetic ASBT inhibitors have shown considerably lower plasma cholesterol levels in animal models [11, 12]. Moreover, ASBT inhibitors have shown to increase the conversion of hepatic cholesterol into bile acids in the liver when they inhibit the recycle of bile acid in the enterohepatic circulation [13].

Bile acid analogues, which are small hydrophobic synthetic molecules with steroid nucleus or non-steroid structure, have considerable therapeutic potential related to the biological function of bile acid [14, 15]. In recent years, the development of bile acid analogues has been showing progress in regards of the

molecular structure of bile acids and the bile acid-binding domains of bile acid transporter and receptor [16-18]. They have bile acid-similar structures to fit into a tight bile acid binding pocket of the targets [16]. Obeticholic acid and synthetic bile acid receptor agonists are also currently being investigated in phase II and phase III trials in patient [19-21]. Because of the small molecular size and hydrophobicity of bile acid mimics, they are usually absorbed in the GI tract and inhibit the bile acid receptors or transporters which exist in the intestine, liver, bile duct and kidney [16]. However, bile acid receptors control a number of fundamental pathways in the liver and physiological process including energy metabolism, glucose homeostasis, and inflammation; these are essential for normal living and digesting [22-28]. These various bile acid receptor actions could complicate bile acid based drug development and cause unexpected effects in a long term drug administration [16].

Unlike bile acid receptors in the liver, bile acid transporters in the ileum are much more attractive pharmaceutical targets. When the therapeutic materials focus on the bile acid in the ileum, extensive drug metabolism and receptor interaction can be avoided. That is why GlaxoSmithKline recently tried to develop a synthetic non-absorbable ASBT inhibitor for the treatment of type 2 diabetes [29, 30]. Current drug development strategy based on the use of bile acid prefers to inhibit the transporters in the distal ileum which is the primary site of ASBT.

Conjugating a polymer could be an attractive approach to optimize the physical and chemical properties of biomaterials and make them useful materials as therapeutic agents [31-34]. Minimizing the systemic side effects and developing non-systemic bile acid based polymer targeting the bile acid transporter in the ileum will provide a promising strategy for drug development [4, 35, 36]. Here, we introduce a novel ASBT inhibitor using non-absorbable hydrophilic polymer and oligomeric bile acid which has a high affinity to ASBT. In our previous study, we developed bile acid-based oligomers which showed selectivity for ASBT using multiple deoxycholic acids [37-39].

In this study, we designed and confirmed the activity of polyacrylic acid-tetraDOCA conjugate (PATD) as a bile acid transporter inhibitor. We also evaluated the therapeutic effect of PATD in a preclinical animal model of hyperlipidemia. This

study could be discussed in terms of first macromolecule-based drug development for ASBT inhibition using a polymer and natural bile acids.

S.2. Materials and methods

S.2.1. Materials

Deoxycholic acid (DOCA), N-hydroxylsuccinimide (NHS), 1-ethyl-3-(3-dimethylaminopropyl)carbodiimide (EDAC), ethylene-diamine, fluoresceinamine and polyacrylic acid (PAA) were purchased from Sigma chemical Co. (St. Louis, MO, USA). Anhydrous dimethyl sulfoxide (DMSO) and acetone were obtained from Daejung Chemicals and Metals Co. (Shiheung, South Korea). Polyethylene polyoxypropylene block copolymer (poloxamer) was purchased from BASF (Ludwigshafen, Germany) and caprylocaproyl macrogolglyceride (Labrasol®) was obtained from Gattefossé (Lyon, France). Cell counting kit (CCK-8) was perchased from Dojindo molecular technologics. All chemicals were used without further purification.

S.2.2. Synthesis of PATDs

PATDs were synthesized by coupling reaction of polyacrylic acid and tetraDOCA, as shown in **Figure S.1**. Polyacrylic acid (average molecular weight, 100 kDa) was reacted with tetraDOCA in DMF/FA solution for 12 h using 1-ethyl-3-(3-dimethylaminopropyl)carbodiimide (EDAC) and N-hydroxylsuccinimide (NHS). The feed molecular ratio of reaction was described in table 8.1. Unreacted EDAC, NHS and tetraDOCA were removed by dialysis for 48 h in methanol/water solution using a membrane of MWCO 8,000 Da and then confirmed by TLC.

TetraDOCA was synthesized following the procedure described in the previous study [37]. Briefly, lysine dimer, Boc-CH3O-Lys(Lys(Boc)2) was synthesized using lysine peptides in DMF and then purified. Using lysine dimer, lysine trimer was synthesized and purified by column chromatography (10% MeOH/MC as an eluent). In other batch, DOCA was activated using the DCC/NHS coupling method [40]. After a deprotection process, lysine trimer was reacted with

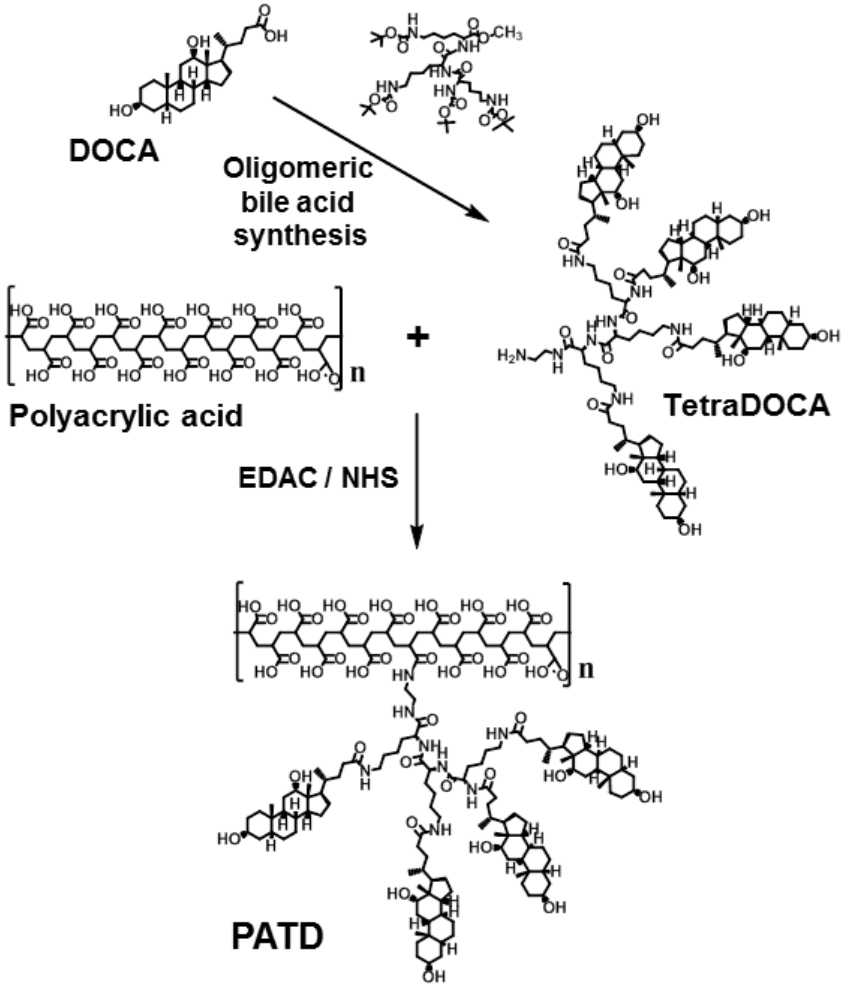

Figure S.1. Schematic synthesis protocol and molecular structures showing polyacrylic acid, tetraDOCA and polyacrylic acid-tetraDOCA conjugate (PATD).

activated DOCA-NHS. To introduce an amine group to tetraDOCA-lysine peptide conjugate, the conjugate reacted with EDA for 48 h, and purified by column chromatography. The final compound which named tetraDOCA, was confirmed by TLC and MALDI-TOF (Voyager-DE STR Biospectrometry Workstation, Applied Biosystems Inc.).

S.2.3. Characterization of PATD

The average conjugated ratios of tetraDOCA to polyacrylic acid were determined by the sulfuric acid method which was introduced in previous study [41]. Briefly, polyacrylic acid, polyacrylic acid-tetraDOCA mixtures and polyacrylic acid-tetraDOCA conjugates were dissolved in water (140 μL) and mixed with sulfuric acid solution (360 μL) at 70 °C for 30 min and then cooled. The absorbance was measured at 420 nm using UV/Vis spectrometer, and the conjugation ratio was calculated. Then, we measured the binding affinities of a bile acid (taurocholic acid; TCA), polyacrylic acid, and PATD to ASBT using BIAcore T100 (GE Healthcare, Uppsala, Sweden). In surface plasmon resonance (SPR) study, the samples were prepared at concentrations ranging from 1 to 0.0078 μM and the running solution was 2 % DMSO containing HEPES buffer supplemented with 150 mM NaCl. Recombinant human ASBT was immobilized onto a sensor chip CM5 using DMSO, EDAC and NHS, then measurements were performed at a flow rate of 20 μL/min. Biacore T100 Evaluation software was used to calculate the affinity of samples to ASBT as described in **Table S.1**.

S.2.4. Molecular dynamic simulation

The crystal structure of ASBT (protein data bank [PDB] code, 3ZUX and 3ZUY) was already reported [42]. The molecular structure of ASBT (3ZUX) without the bound taurocholic acid (TCA) and lipid molecules was used for the docking and dynamic simulation. The molecular docking simulation was performed using the AutoDock Vina 1.0.3 program with default parameters [43]. Illustrations of the 3D model were generated and visualized using the PyMol program. Molecular dynamic simulations were performed using Discovery Studio 3.0 with

Table S.1. Synthesis, characterization and dissociation rate constants (K_D) of polyacrylic acid-tetraDOCA conjugate (PATD) using sulfuric acid and SPR study

materials	conjugation ratio [a]	feed mole ratio (TetraDOCA)	feed mole ratio (EDAC/ NHS)	avg. M.W. (kDa)	K_D (nM)[b] to ASBT
TCA	-	-	-	0.5	120.7
PATD1	1.10 ± 0.03	3	20	102	39.1
PATD3	3.24 ± 0.04	10	50	106	1.5

Results are the means ± standard deviation

[a] Conjugation ratio of tetraDOCA and polyacrylic acid(1) measured using sulfuric acid assay

[b] Calculated by SPR software

the CHARMm (Chemistry at HARvard Molecular Mechanics) forcefield [44]. Briefly, ASBT complex was generated and solvated with the water molecules in an explicit spherical boundary condition. Each simulation was carried out by Standard Dynamics Cascade protocol of Discovery Studio 3.0 which consists of minimization, equilibrium and run steps. Constant temperature and constant-volume ensemble (NVT) was selected. The molecular movements of polyacrlylic acid and tetraDOCA were recorded every 500 ns. Molecular dynamic simulation steps were carried out in the Generalized Born with a simple SWitching (GBSW) implicit solvent model for application of the solvent (water) effect.

S.2.5. Binding and viability study using ASBT overexpressed MDCK cell

Madin-Darby canine kidney (MDCK) cell line obtained from the Korea Cell Bank (Korea) and was transfected using SLC10A2 (sodium/bile acid co-transporter family) human cDNA open reading frame (ORF) clone and Lipofectamine 2000® [37]. ASBT over-expressed MDCK cells were cultured in DMEM high glucose medium (GIBCO, Invitrogen, CA, USA) supplemented with 10% (v/v) FBS (GIBCO, Invitrogen, CA, USA) and penicillin–streptomycin. To evaluate cellular binding of materials, fluorescence labeled polyacrylic acid and PATDs were synthesized and treated to the cells. Briefly, they were prepared by conjugation between the primary amine of fluoresceinamine and the carboxylic group of acrylic acid in water/DMF using EDAC/NHS. After synthesis, they were purified by dialysis in methanol/water solution using a membrane of MWCO 8,000 Da. MDCK-ASBT cells were incubated with fluorescence-labeled materials in sodium chloride (200 mM) containing HBSS medium at 37˚C for 1 h. After repeated washing steps, cells were fixed using 4% cold paraformaldehyde for 10 min. The nuclei were stained by Hoechst, and images were acquired with a confocal laser scanning microscopy (CLSM).

The viability of drug treated cells was measured by a cell counting kit (CCK-8). Cells suspended in 100 μL of DMEM high glucose medium were added into a 96-well culture plate and were incubated for 24 h. When cells reached

confluence, we treated cells with the synthesized materials at different concentrations (n=7). After 6 h, 10 μL of CCK solution was added into each well. The absorbance was measured at 450 nm wavelengths using a microplate reader after 1 h incubation.

S.2.6. Animal study using high-fat diet (HFD)

All procedures for animal experiments were approved by the Committee of the Use and Care on Animals according to the regulations of the Institutional Animal Ethics Committee of the Seoul National University animal care facility. To investigate the therapeutic potential of PATD, 7-week-old male C57BL/6 mice were obtained from Orient Bio Inc. (Seungnam, South Korea) and were acclimatized for 1 week. The mice were fed either a normal diet (ND) or an HFD (60% of kilocalories as fat, Research Diets) for 13 weeks [45]. HFD-fed animals were randomly assigned into three groups when we started PATD treatment (n=7). In the PATD treated group, PATD1 or PATD3 (10 mg/kg/day) in an oral formulation containing labrasol and Poloxamer 188 as solubilizers was orally administered to the mice. The mice were fasted for 4 h before administering PATDs.

S.2.7. Oil Red O staining

For oil red O staining, animals were sacrificed after the high-fat diet experiment. The left lateral lobe of liver was sliced and frozen. The samples were cut into 4-μm sections, and then affixed to microscope slides (n=5). The liver sections were stained in fresh oil red O for 10 min and rinsed in water. After the oil red O treatment, the sections were observed using a microscope (Eclipse TE2000S, Nikon, Japan) within 4 h and analyzed with Image J (NIH software).

S.2.8. Analysis of blood samples and oral glucose tolerance test

Blood (400 μl) was collected from mice after sacrifice (n=7). Plasma triglyceride (TG) and total cholesterol (TC) were measured using a FUJI DRI-CHEM3500 (FUJIFILM, Tokyo, Japan). The atherosclerotic index (AI) was calculated as (total cholesterol - high density lipoprotein cholesterol) / (high density

lipoprotein cholesterol). Oral glucose tolerance test (OGTT) was carried out to measure the glucose responsiveness on the last day of the high-fat diet experiment. Each group was fasted for 16 h before the oral treatment of glucose solution (2 g/kg). The blood glucose level in the blood was measured using glucometer (Super glucocard II) at 0, 15, 30, 45, 60, 75, 90, 120, 210 and 300 min after oral glucose treatment (n=7).

S.2.9. Statistical analysis

All results were analyzed by comparing the means of groups in in vitro and in vivo experiments using one-way analyses of variance (ANOVA) followed by Bonferroni's post-hoc tests using sigmaplot 12. P-values less than 0.05 were considered to be statistically significant.

S.3. Results

S.3.1. Synthesis and Characterization of Polyacrylic acid-tetraDOCA conjugate

ASBT inhibitors have been clinically explored as lipid-lowering agents for the treatment of hypercholesterolaemia, cholestatic liver diseases and type 2 diabetes mellitus [9]. Numerous small steroidal and non-steroidal compounds have been designed and synthesized for ASBT inhibition. In the presented study, we prepared novel ASBT inhibitors by conjugating polyacrylic acid with different ratios of tetraDOCA. TetraDOCA was chemically conjugated to polyacrylic acid by amide coupling reaction. The molecular structures of PATDs were shown in **Figure** 1 and characterization of these molecules was described in **table 8.1**. We designed to synthesize products which have conjugation ratio ranged from 1 to 5. After synthesis, the molecular coupling ratios of PATD1 and PATD3 were 1.1 and 3.2, respectively.

S.3.2. Computer Simulation of PATD and ASBT

The development of bile acid transporter inhibitors can be stimulated by the

revealing of the 3D structure of targets. The recently reported molecular structure of ASBT shows that bile acids fit into a tight pocket with the steroid nucleus in the ligand-binding domain of ASBT [16]. The overall space of the pocket allows simultaneous binding of 3 to 4 bile acid molecules to the hydrophobic groove of ASBT, thereby inducing high binding affinity between the tetramer of deoxycholic acid and ASBT (**Figure S.2**). The bile acid-binding cavity in ASBT is open to the cytoplasm and is approximately 1008 $Å^3$ in size, meaning it is much bigger than the size of a bile acid (150-250 $Å^3$) [42]. Therefore, it is necessary to use an oligomeic hydrophobic substrate, tetraDOCA, for strong ASBT binding. Computer docking simulation using polyacrylic acid fragment and tetraDOCA demonstrated that the molecular structure of polymer did not sterically hinder the binding of tetraDOCA to ASBT.

The binding interaction between PATD and ASBT is strong and more stable than the interaction of polyacrylic acid and ASBT. We also measured the interaction energy of the PATD-ASBT and polyacrylic acid-ASBT complex during the MD simulation (**Figure S.3**). In the docking structure, the conformation of tetraDOCA in ASBT did not change after MD simulation. The maintained interaction energy of complex also supported this finding, which indicated that tetrameric bile acid could form a stable binding pose in the binding pocket of bile acid transporter (**Figure S.4**). Recent studies have shown that the kinetics of drug–receptor binding could be important in drug discovery and development [46-48]. In our study, PATD not only showed a strong molecular interaction with ASBT in SPR, but also exhibited prolonged molecular dynamics in computer dynamic simulation. When tetraDOCA and ASBT interact via hydrophobic and hydrophilic interactions, the complex tends to be kinetically stable due to the strong hydrophobicity of the bile acid.

S.3.3. Cellular Binding of PATDs

At first, we transfected MDCK cells using the human ASBT gene (SLC10A2) to visualize the binding of PATD to ASBT on the cell surface in previous work [49]. ASBT over-expressed MDCK cells were incubated with fluorescence labeled polyacrylic acid, PATD1 or PATD3. Green fluorescein image

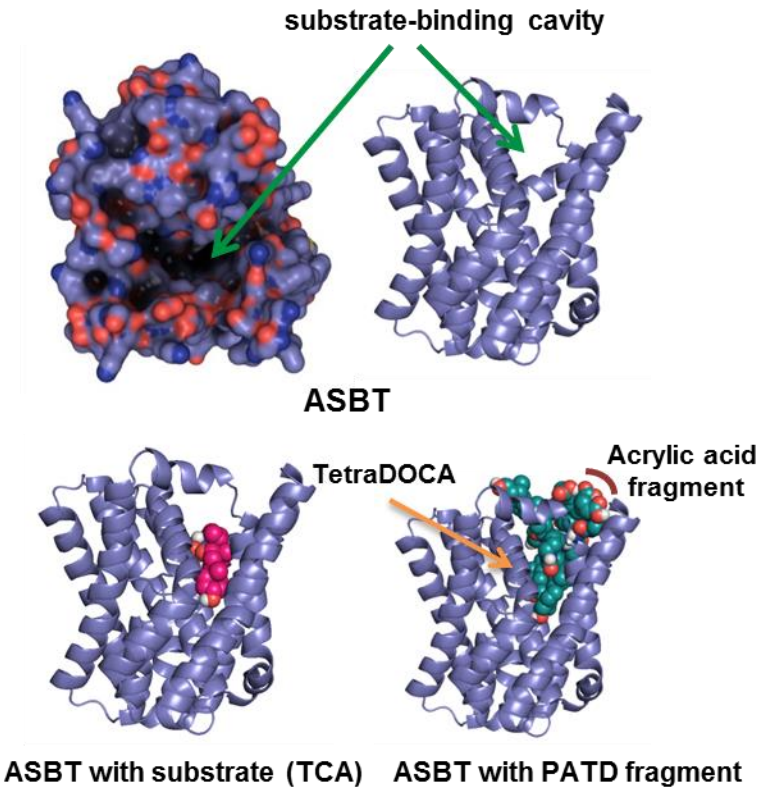

Figure S.2. *In silico* molecular docking of taurocholic acid (TCA) and polyacrylic acid-tetraDOCA conjugate (PATD) within the substrate-binding site of apical sodium-dependent bile acid transporter (ASBT) model. The substrate-binding cavity in ASBT is open to the cytoplasm.

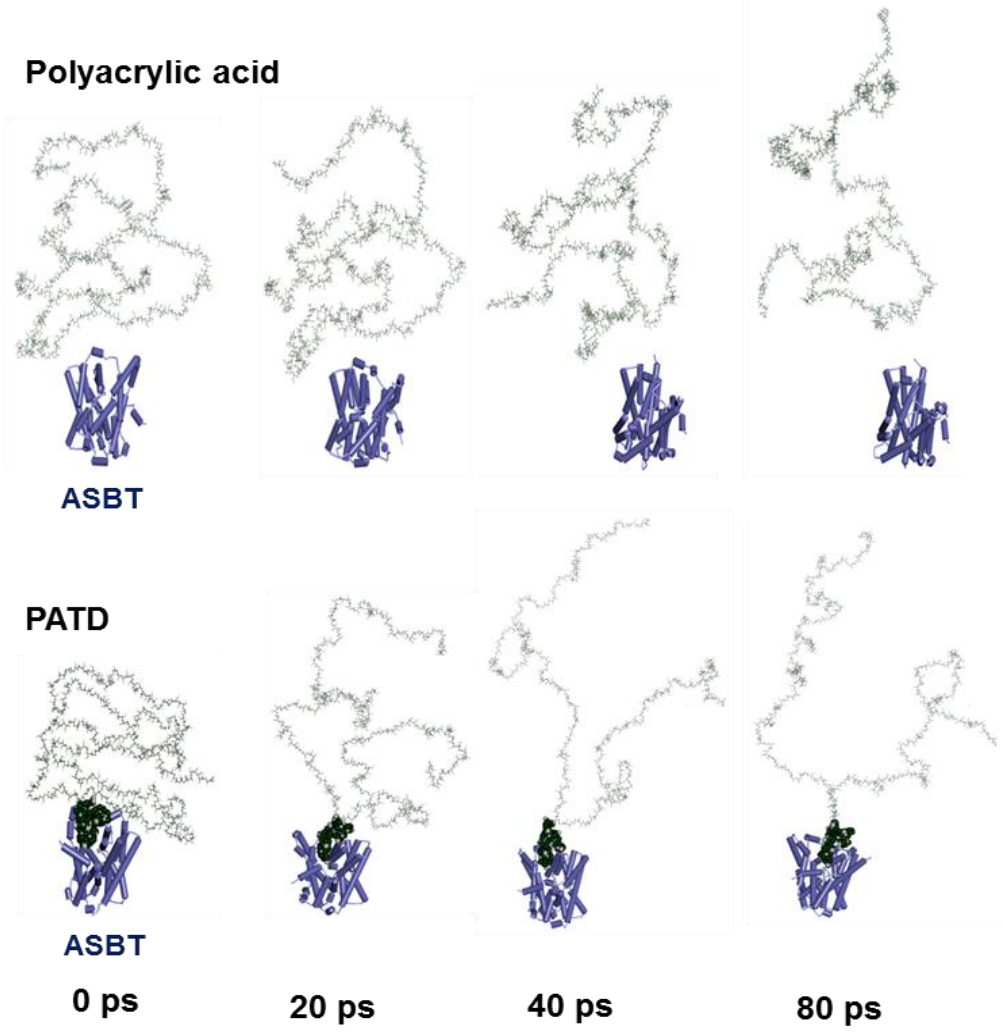

Figure S.3. Molecular dynamic simulation of polyacrylic acid, PATD, and ASBT for 80 ps

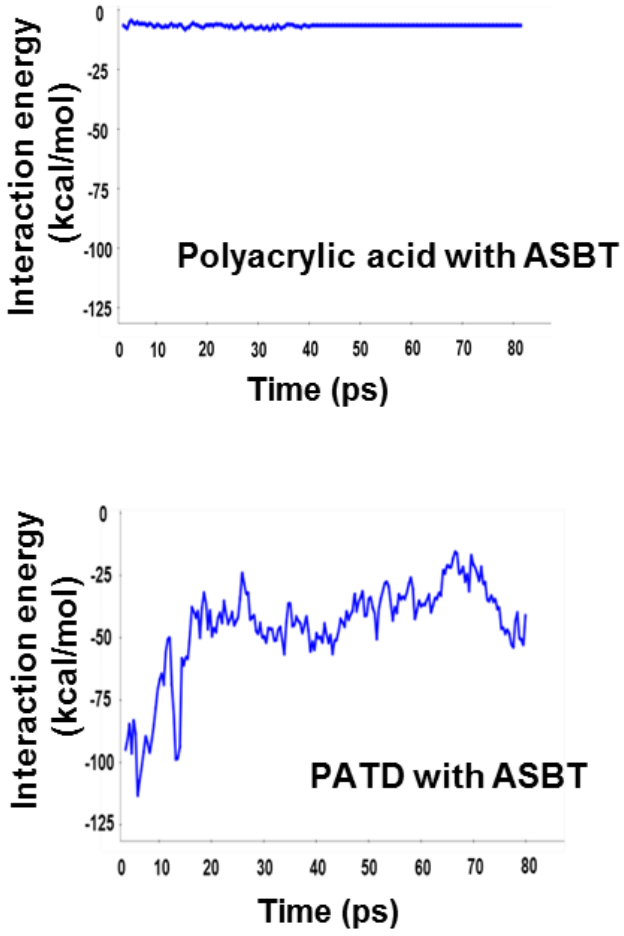

Figure S.4. Comparsion of the interaction energy between ASBT and polyacrylic acid or PATD. The binding interaction of PATD-ASBT complex was maintained during MD simulation.

was detected on the surface of MDCK cells, and fluorescence conjugated polyacrylic acid did not show any significant differences in MDCK-ASBT cells (**Figure S.5**). This demonstrated that over-expressed ASBT could react with PATD1 or PATD3 forming a PATD-ASBT complex, followed by the inhibition of ASBT activity. Molecular mechanism studies including co-localization and natural ligands inhibition test for tetraDOCA were conducted in previous study in detail [37, 49]. In addition, the viability test was carried out to check the toxicity of PATD1 or PATD3 on cells. The cell viability assay using CCK-8 confirmed no cytotoxicity when PATD1 or PATD3 was administered up to 400 μg/mL. Viability of MDCK cells was decreased by 8 percent at the maximum dose.

8.3.4. Animal Study using PATDs

We evaluated the therapeutic effect of PATD in vivo using HFD feeding, which when induced in animals, can cause obesity and leading to metabolic disorders. In the HFD-fed mice, hypercholesterolemia and hepatic fat accumulation were induced to evaluate the therapeutic effect of PATD. To evaluate the therapeutic effect of PATD1 and PATD3 in vivo, PATDs were administered to HFD fed mice. Feeding HFD increased the body weight gain in the control or PATD-treated group (**Figure S.6**). After 13 weeks, the body weights were increased by 154.2 ± 10.9 % (ND-feeding group), 260.8 ± 13.7 % (HFD-feeding group), 240.2 ± 15.6 % (HFD-feeding + PATD1 treatment) and 237.0 ± 13.1 % (HFD-feeding + PATD3 treatment).

PATD1 and PATD3 treatment reduced the body weight and liver weight gain in mice. In particular, the liver weight of the mice was significantly reduced by the treatment of PATDs (**Figure S.6**). In comparison to the liver weight of HFD-fed mice, the treatment with 10 mg/kg PATD1 or PATD3 per day for 9 weeks was resulted in a reduction of the liver weight by -27.3 % or -40.9 %, respectively. This result indicates that the reduced liver weight gain is related to the decreased body weight of the PATD treated group. PATD1 or PATD3 treatment: the reduced fat accumulation in the liver, which was visualized by oil red O staining. HFD-fed mice exhibited sufficient fat accumulation in Oil red O staining and the images showed a

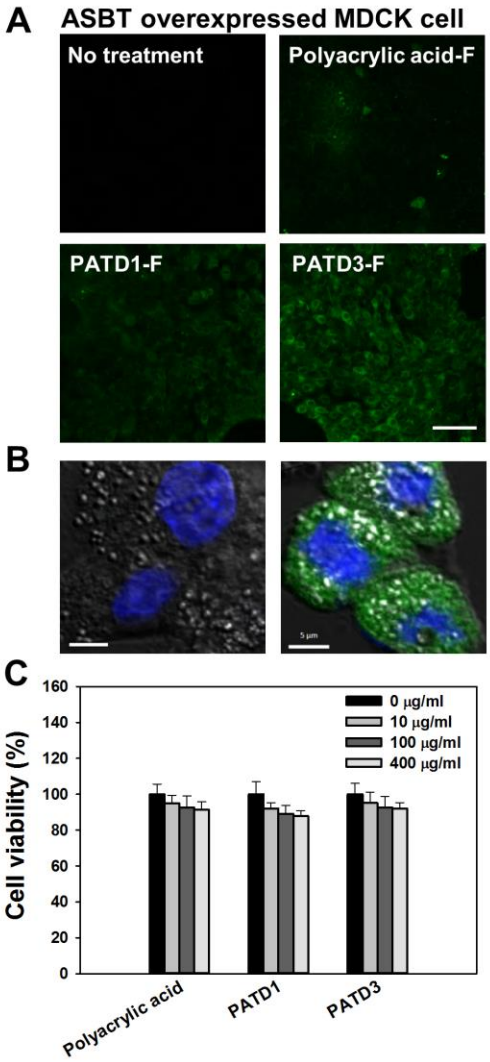

Figure S.5. (A) Comparison of cellular binding of polyacrylic acid and PATD in ASBT over-expressed MDCK cells (200×), Scale bar = 50 um (B) Representative confocal image of flourosence (F)-labeled materials in MDCK-ASBT cells was compared to that in the untreated cells (800×). Scale bar = 5 um (C) Cell viability was maintained in the presence of low or high dose of PATDs (n=7).

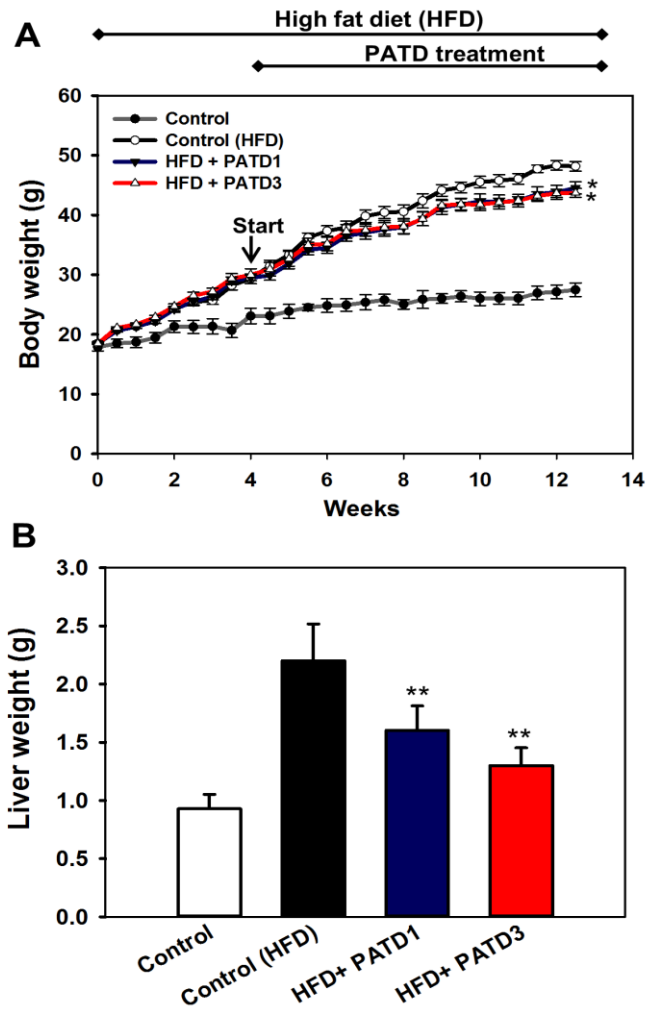

Figure S.6. Body wight and liver weight gain in high fat diet experiment model (A) The effect of PATD on body weight gain in mice. Male C57BL/6 mice were fed either a normal diet (ND) or a high-fat diet (HFD) for 13 weeks (n=7). For 9 weeks of diet feeding, PATD1 and PATD3 (10 mg/kg/day) were orally administered to mice after being fasted for 4 h (B) Changes in the liver weight. By reducing the weight of the liver, PATD inhibited body weight gain. *p<0.05 vs. the control group (HFD), **p<0.001 vs. the control group (HFD).

successful increase in hepatic fat accumulation in HFD-fed mice (**Figure S.7**). PATD treatment and inhibiting hepatic fat accumulation resulted in the inhibition of body weight gain. The amount of reduced fat accumulation in the liver verified the therapeutic effect of PATDs. In addition, PK and toxicity study for the ileum and blood concentration analysis was conducted (**Figure S.8**). PATD showed no toxicity and the low bioavailability.

Since cholesterol is balanced by entero-hepatic circulation through bile acid synthesis and reabsorption, the inhibition of bile acid re-uptake in the intestine decreases total cholesterol in the liver and the blood. In the result of the blood analysis, PATDs significantly decreased total cholesterol (TC) and triglyceride (TG) contents in the plasma (**Figure S.9**). Among the different risk factors for dyslipidemia, increase in LDL level appears to primarily indicate that high LDL concentrations promote atherosclerosis. The plasma level of low density cholesterol (LDL) was lower than that of the the control group, thereby decreasing the atherogenic index in the PATD3 treated group. High plasma level of LDL and hepatic fat accumulation has been associated with other metabolic abnormalities like glucose tolerance. Fasting glucose was monitored in the plasma and an oral glucose tolerance test (OGTT) was carried out on the last day of high-fat diet experiment (**Figure S.10**). In OGTT, the blood glucose level of HFD-fed group rapidly increased to 522 mg/dL within 15 min. In contrast, the blood glucose level of PATD3 group reached the highest concentration (419 mg/dL) after 15 min of glucose injection and then gradually decreased afterwards; showing that PATD treatment prevented a rapid increase of blood glucose level and decreased the glucose level rapidly.

S.4. Discussion

We designed to synthesize products which have conjugation ratio ranged from 1 to 5, then, the results showed that molecular coupling ratios of PATD1 and PATD3 were 1.1 and 3.2, respectively. Based on the conjugation, molecular

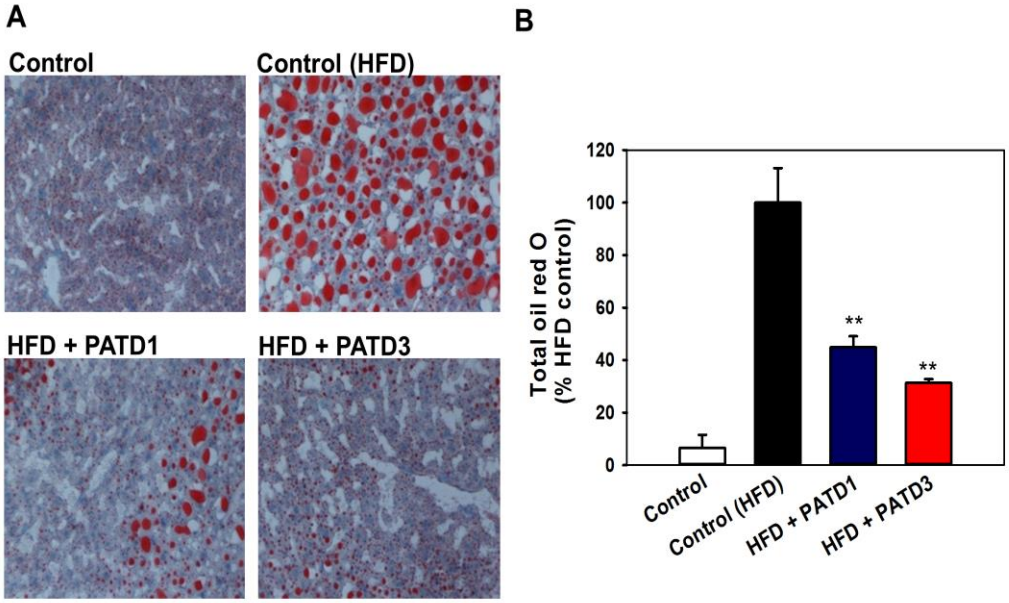

Figure S.7. Inhibition of liver fat accumulation by PATD (A) Oil red O staining of the liver in mice that were fed an ND, HFD or HFD with PATDs. PATD treatment significantly reduced fat accumulation in the liver (B) Analyses of oil red O staining with ImageJ software (n=5) *p<0.05 vs. the control group (HFD), **p<0.001 vs. the control group (HFD).

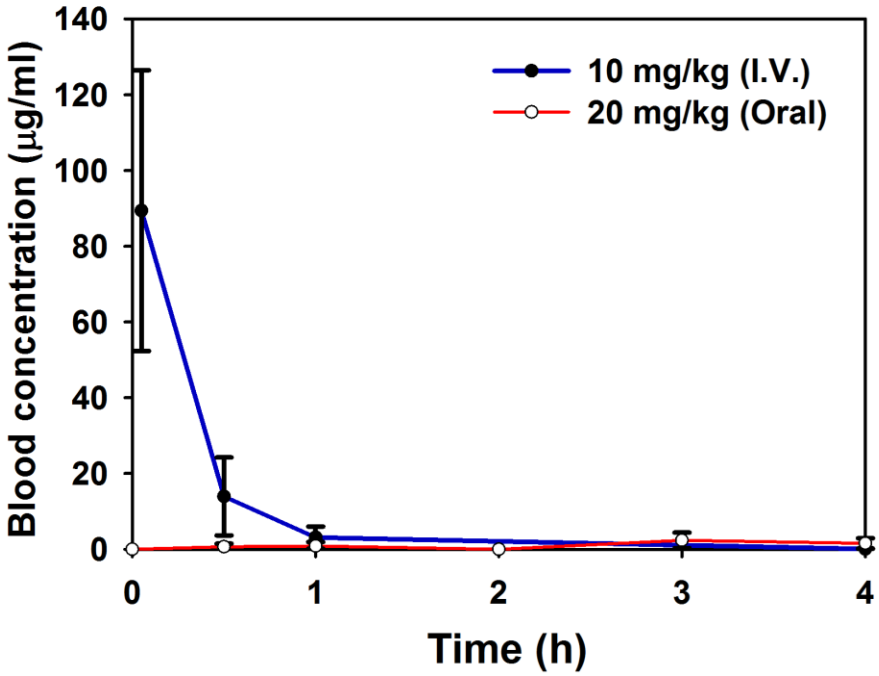

Figure S.8. PK study of PATD3 in rats

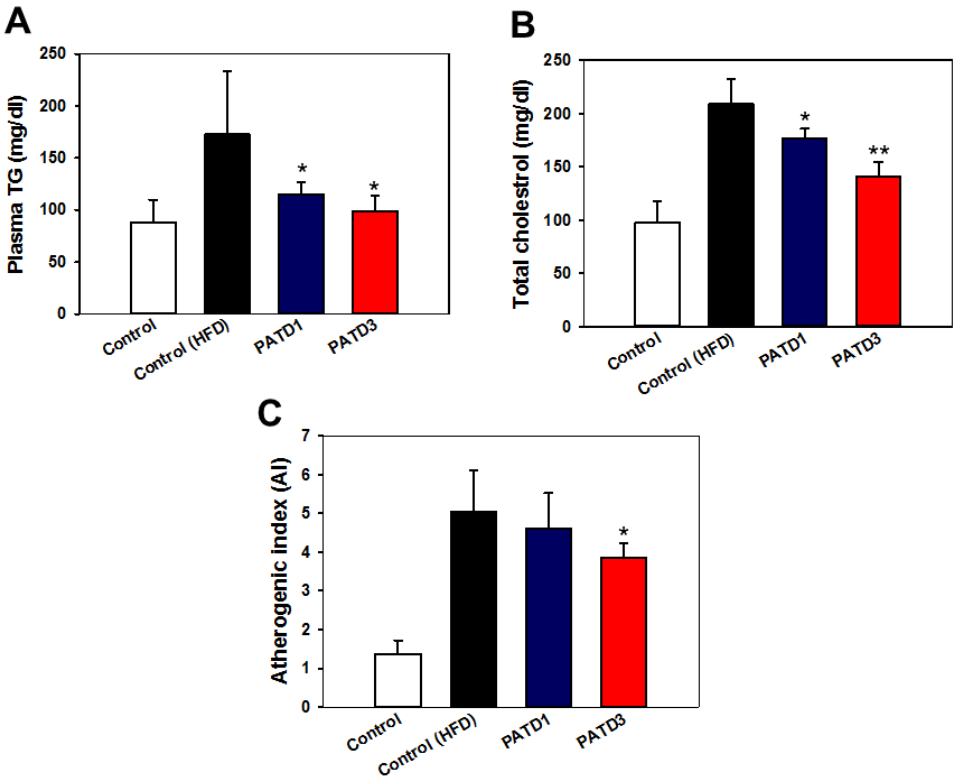

Figure S.9. The therapeutic effect of PATD in HFD-fed mice. (A) Plasma Triglyceride (TG) (B) Plasma Total cholesterol (TC) (C) Atherogenic index *p<0.05 vs. the control group (HFD), **p<0.001 vs. the control group (HFD).

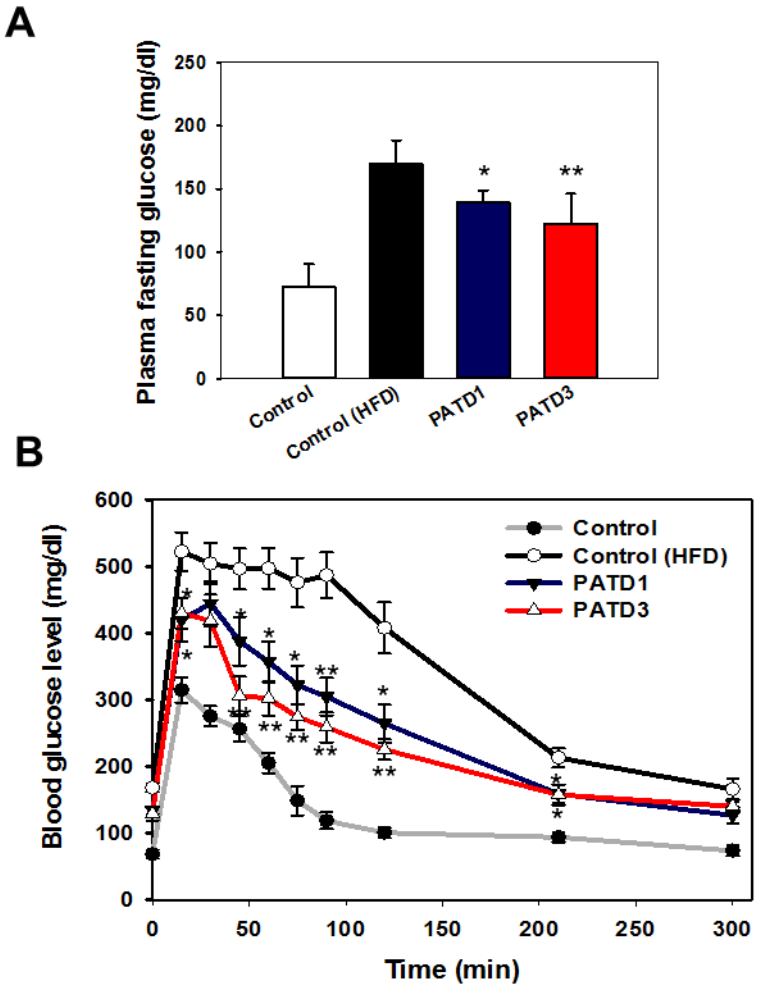

Figure S.10. (A) Plasma fasting glucose (B) Oral glucose tolerance test (OGTT) **p*<0.05 vs. the control group (HFD), ***p*<0.001 vs. the control group (HFD).

simulation was conducted. Molecular simulation plays an efficient role in the field of drug design and development by docking towards the active binding site of targets. We used a polyacrylic acid fragment for simulation due to its huge molecular size, and Autodock vina 1.0.3 calculated the energy of binding. The minimum internal binding energy of polyacrylic acid-tetraDOCA that the conjugate in ASBT was -9.2 kcal/mol, which indicated that tetraDOCA could bind to ASBT. The binding energy of taurocholic acid, deoxycholic acid, or other natural bile acid ranged between - 6.2 and -9.0 kcal/mol. Molecular dynamics (MD) simulation of PATD and ASBT was carried out using the Discovery Studio program and the CHARMM forcefield, which can describe biological macromolecules such as proteins, nucleic acids, and their ligands in aqueous environment. After simulation, PATDs were studied regarding the ASBT binding efficiency, as well as its cellular action and toxicity as ASBT inhibitors *in vitro* experiements. We also carried out a cell binding and viability assay to confirm the cellular action of PATD using ASBT overexpressed MDCK cell line. The results showed that PATD was safe and effective bioconjugate as an ASBT inhibitor. After that, we evaluated the therapeutic effect of PATD in vivo using HFD feeding, which when induced in animals, can cause obesity and leading to metabolic disorders. In the HFD-fed mice, hypercholesterolemia and hepatic fat accumulation were induced to evaluate the therapeutic effect of PATD. To evaluate the therapeutic effect of PATD1 and PATD3 in vivo, PATDs were administered to HFD fed mice. Feeding HFD increased the body weight gain in the control or PATD-treated group. These results demonstrate that PATD treatment on HFD animal group results in the inhibition of both hyperlipidemia and hepatic fat accumulation. Through this process we created, we were able to conclude that PATD can interact with ASBT in the ileum without toxicities.

8.5. Conclusion

We developed a new polymer based biomaterial for the inhibition of ASBT and manifesting hypocholesterolemic effect for the treatment of

hypercholesterolaemia. PATD effectively bound to ASBT in SPR and ASBT over-expressed MDCK cells without any cytotoxicity. We evaluated the therapeutic effect of PATD in a HFD-induced hyperlipidemia animal model, and the results showed that PATD3 prevented hyperlipidemia and hepatic fat accumulation. These findings, thus, strengthens the notion that bile acid and polymer based biomaterials can be utilized as potent ASBT inhibitors when interacting with their transporters.

References

[1] Ross R, Harker L. Hyperlipidemia and atherosclerosis. Science. 1976;193:1094-100.

[2] Drechsler M, Megens RT, van Zandvoort M, Weber C, Soehnlein O. Hyperlipidemia-triggered neutrophilia promotes early atherosclerosis. Circulation. 2010;122:1837-45.

[3] Hansson GK, Libby P. The immune response in atherosclerosis: a double-edged sword. Nature reviews Immunology. 2006;6:508-19.

[4] Zhou X, Levin EJ, Pan Y, McCoy JG, Sharma R, Kloss B, et al. Structural basis of the alternating-access mechanism in a bile acid transporter. Nature. 2014;505:569-73.

[5] Javitt NB. Bile acid synthesis from cholesterol: regulatory and auxiliary pathways. FASEB journal : official publication of the Federation of American Societies for Experimental Biology. 1994;8:1308-11.

[6] Hofmann AF. The enterohepatic circulation of bile acids in mammals: form and functions. Frontiers in bioscience. 2009;14:2584-98.

[7] Roberts MS, Magnusson BM, Burczynski FJ, Weiss M. Enterohepatic circulation: physiological, pharmacokinetic and clinical implications. Clinical pharmacokinetics. 2002;41:751-90.

[8] Xu G, Pan LX, Erickson SK, Forman BM, Shneider BL, Ananthanarayanan M, et al. Removal of the bile acid pool upregulates cholesterol 7alpha-hydroxylase by

deactivating FXR in rabbits. Journal of lipid research. 2002;43:45-50.
[9] Sakamoto S, Kusuhara H, Miyata K, Shimaoka H, Kanazu T, Matsuo Y, et al. Glucuronidation converting methyl 1-(3,4-dimethoxyphenyl)-3-(3-ethylvaleryl)-4-hydroxy-6,7,8-trimethoxy-2-naphthoat e (S-8921) to a potent apical sodium-dependent bile acid transporter inhibitor, resulting in a hypocholesterolemic action. The Journal of pharmacology and experimental therapeutics. 2007;322:610-8.
[10] Kobayashi M, Ikegami H, Fujisawa T, Nojima K, Kawabata Y, Noso S, et al. Prevention and treatment of obesity, insulin resistance, and diabetes by bile acid-binding resin. Diabetes. 2007;56:239-47.
[11] Lewis MC, Brieaddy LE, Root C. Effects of 2164U90 on ileal bile acid absorption and serum cholesterol in rats and mice. Journal of lipid research. 1995;36:1098-105.
[12] Bhat BG, Rapp SR, Beaudry JA, Napawan N, Butteiger DN, Hall KA, et al. Inhibition of ileal bile acid transport and reduced atherosclerosis in apoE-/- mice by SC-435. Journal of lipid research. 2003;44:1614-21.
[13] Root C, Smith CD, Sundseth SS, Pink HM, Wilson JG, Lewis MC. Ileal bile acid transporter inhibition, CYP7A1 induction, and antilipemic action of 264W94. Journal of lipid research. 2002;43:1320-30.
[14] Downes M, Verdecia MA, Roecker AJ, Hughes R, Hogenesch JB, Kast-Woelbern HR, et al. A chemical, genetic, and structural analysis of the nuclear bile acid receptor FXR. Molecular cell. 2003;11:1079-92.
[15] Hambruch E, Miyazaki-Anzai S, Hahn U, Matysik S, Boettcher A, Perovic-Ottstadt S, et al. Synthetic farnesoid X receptor agonists induce high-density lipoprotein-mediated transhepatic cholesterol efflux in mice and monkeys and prevent atherosclerosis in cholesteryl ester transfer protein transgenic low-density lipoprotein receptor (-/-) mice. The Journal of pharmacology and experimental therapeutics.2012;343:556-67.
[16] Schaap FG, Trauner M, Jansen PLM. Bile acid receptors as targets for drug development. Nat Rev Gastro Hepat. 2014;11:55-67.
[17] Pellicciari R, Fiorucci S, Camaioni E, Clerici C, Costantino G, Maloney PR, et al. 6alpha-ethyl-chenodeoxycholic acid (6-ECDCA), a potent and selective FXR

agonist endowed with anticholestatic activity. Journal of medicinal chemistry. 2002;45:3569-72.
[18] Pellicciari R, Gioiello A, Macchiarulo A, Thomas C, Rosatelli E, Natalini B, et al. Discovery of 6alpha-ethyl-23(S)-methylcholic acid (S-EMCA, INT-777) as a potent and selective agonist for the TGR5 receptor, a novel target for diabesity. Journal of medicinal chemistry. 2009;52:7958-61.
[19] Gracia-Sancho J, Hernandez-Gea V, Garcia-Pagan JC. Obeticholic acid: a new light in the shadows treating portal hypertension? Hepatology. 2014;59:2072-3.
[20] Mudaliar S, Henry RR, Sanyal AJ, Morrow L, Marschall HU, Kipnes M, et al. Efficacy and safety of the farnesoid X receptor agonist obeticholic acid in patients with type 2 diabetes and nonalcoholic fatty liver disease. Gastroenterology. 2013;145:574-82 e1.
[21] Abel U, Schluter T, Schulz A, Hambruch E, Steeneck C, Hornberger M, et al. Synthesis and pharmacological validation of a novel series of non-steroidal FXR agonists. Bioorganic & medicinal chemistry letters. 2010;20:4911-7.
[22] Claudel T, Staels B, Kuipers F. The Farnesoid X receptor: a molecular link between bile acid and lipid and glucose metabolism. Arteriosclerosis, thrombosis, and vascular biology. 2005;25:2020-30.
[23] Wang YD, Chen WD, Moore DD, Huang W. FXR: a metabolic regulator and cell protector. Cell research. 2008;18:1087-95.
[24] Pircher PC, Kitto JL, Petrowski ML, Tangirala RK, Bischoff ED, Schulman IG, et al. Farnesoid X receptor regulates bile acid-amino acid conjugation. The Journal of biological chemistry. 2003;278:27703-11.
[25] Watanabe M, Houten SM, Mataki C, Christoffolete MA, Kim BW, Sato H, et al. Bile acids induce energy expenditure by promoting intracellular thyroid hormone activation. Nature. 2006;439:484-9.
[26] Thomas C, Gioiello A, Noriega L, Strehle A, Oury J, Rizzo G, et al. TGR5-mediated bile acid sensing controls glucose homeostasis. Cell metabolism. 2009;10:167-77.
[27] Li T, Holmstrom SR, Kir S, Umetani M, Schmidt DR, Kliewer SA, et al. The G protein-coupled bile acid receptor, TGR5, stimulates gallbladder filling. Molecular

endocrinology. 2011;25:1066-71.
[28] Pols TW, Nomura M, Harach T, Lo Sasso G, Oosterveer MH, Thomas C, et al. TGR5 activation inhibits atherosclerosis by reducing macrophage inflammation and lipid loading. Cell metabolism. 2011;14:747-57.
[29] Wu Y, Aquino CJ, Cowan DJ, Anderson DL, Ambroso JL, Bishop MJ, et al. Discovery of a highly potent, nonabsorbable apical sodium-dependent bile acid transporter inhibitor (GSK2330672) for treatment of type 2 diabetes. Journal of medicinal chemistry. 2013;56:5094-114.
[30] Cowan DJ, Collins JL, Mitchell MB, Ray JA, Sutton PW, Sarjeant AA, et al. Enzymatic- and iridium-catalyzed asymmetric synthesis of a benzothiazepinylphosphonate bile acid transporter inhibitor. The Journal of organic chemistry. 2013;78:12726-34.
[31] Zhang Y, Chan HF, Leong KW. Advanced materials and processing for drug delivery: The past and the future. Advanced drug delivery reviews. 2013;65:104-20.
[32] Sedo J, Saiz-Poseu J, Busque F, Ruiz-Molina D. Catechol-Based Biomimetic Functional Materials. Adv Mater.2013;25:653-701.
[33] Lopez-Jaramillo FJ, Giron-Gonzalez MD, Salto-Gonzalez R, Hernandez-Mateo F, Santoyo-Gonzalez F. In vitro and in vivo evaluation of novel cross-linked saccharide based polymers as bile acid sequestrants. Molecules. 2015;20:3716-29.
[34] Park JK, Kim TH, Nam JP, Park S, Park Y, Jang MK, et al. Bile acid conjugated chitosan oligosaccharide nanoparticles for paclitaxel carrier. Macromol Res. 2014;22:310-7.
[35] Duan H, Ning M, Zou Q, Ye Y, Feng Y, Zhang L, et al. Discovery of intestinal targeted TGR5 agonists for the treatment of type 2 diabetes. Journal of medicinal chemistry. 2015.
[36] Sakanaka T, Inoue T, Yorifuji N, Iguchi M, Fujiwara K, Narabayashi K, et al. The effects of a TGR5 agonist and a dipeptidyl peptidase IV inhibitor on dextran sulfate sodium-induced colitis in mice. J Gastroenterol Hepatol. 2015;30 Suppl 1:60-5.
[37] Al-Hilal TA, Park J, Alam F, Chung SW, Park JW, Kim K, et al. Oligomeric bile acid-mediated oral delivery of low molecular weight heparin. Journal of

controlled release : official journal of the Controlled Release Society. 2014;175:17-24.
[38] Alam F, Al-Hilal TA, Chung SW, Seo D, Mahmud F, Kim HS, et al. Oral delivery of a potent anti-angiogenic heparin conjugate by chemical conjugation and physical complexation using deoxycholic acid. Biomaterials. 2014;35:6543-52.
[39] Al-Hilal TA, Alam F, Byun Y. Oral drug delivery systems using chemical conjugates or physical complexes. Advanced drug delivery reviews. 2013;65:845-64.
[40] Lee Y, Nam JH, Shin HC, Byun Y. Conjugation of low-molecular-weight heparin and deoxycholic acid for the development of a new oral anticoagulant agent. Circulation. 2001;104:3116-20.
[41] Nichifor M, Carpov A. Bile acids covalently bound to polysaccharides 1. Esters of bile acids with dextran. Eur Polym J. 1999;35:2125-9.
[42] Hu NJ, Iwata S, Cameron AD, Drew D. Crystal structure of a bacterial homologue of the bile acid sodium symporter ASBT. Nature. 2011;478:408-11.
[43] Trott O, Olson AJ. AutoDock Vina: improving the speed and accuracy of docking with a new scoring function, efficient optimization, and multithreading. Journal of computational chemistry. 2010;31:455-61.
[44] MacKerell AD. Developments in the CHARMM all-atom empirical energy function for biological molecules. Abstr Pap Am Chem S. 1998;216:U696-U.
[45] Kim YW, Kim YM, Yang YM, Kim TH, Hwang SJ, Lee JR, et al. Inhibition of SREBP-1c-mediated hepatic steatosis and oxidative stress by sauchinone, an AMPK-activating lignan in Saururus chinensis. Free Radical Bio Med. 2010;48:567-78.
[46] Lu H, Tonge PJ. Drug-target residence time: critical information for lead optimization. Current opinion in chemical biology. 2010;14:467-74.
[47] Copeland RA, Pompliano DL, Meek TD. Drug-target residence time and its implications for lead optimization. Nature reviews Drug discovery. 2006;5:730-9.
[48] Pan AC, Borhani DW, Dror RO, Shaw DE. Molecular determinants of drug-receptor binding kinetics. Drug discovery today. 2013;18:667-73.
[49] Al-Hilal TA, Chung SW, Alam F, Park J, Lee KE, Jeon H, et al. Functional

transformations of bile acid transporters induced by high-affinity macromolecules. Sci Rep. 2014;4:4163.

국문 초록

자연에 존재하는 수많은 치료효과를 가진 물질 중 그 자체로 약으로 쓰이는 경우는 매우 드물고, 물질구조를 유지한 상태로 신약으로 개발되는 예 또한 거의 없다. 대부분 스크리닝을 통해 최적의 다른 물질이 선택 및 개발되거나, 분자수식을 통하여 그 기능이 최적화된 뒤에 신약 후보물질로 선택된다. 이렇게 개발된 약물들은 약물전달시스템의 도움을 받거나 새로운 약학 조성물이 되어 최종적으로 사람에게 적용된다. 특히 분자수식을 통해 활성 물질의 특정 성질을 변경시키는 경우에 약물의 여러 가지 중대한 문제점들을 해결되기도 한다.

신약 개발에 있어서 바이오 의약품이 최근 주목을 받으면서 이러한 분자수식 기술과 약물 결합체 개발의 중요성은 커지고 있다. 유전자물질, 펩타이드 및 단백질 의약품의 경우 뛰어난 효능에도 불구하고 여러 생물학적 환경에서 치명적인 단점을 보이면서 쉽게 약으로 개발되지 못한다. 이와 비슷한 관점으로 헤파린과 같은 동물 유래 거대분자의 경우, 안전하면서도 뛰어난 효과에도 불구하고 약으로 널리 사용되기에는 여러 가지 단점을 지닌다. 또한 프로타민과 같이 양전하가 강력하고 생물학적 활용도가 높은 펩타이드는 헤파린의 해독제와 인슐린의 서방형 제제로 널리 사용되지만 그 이상 사용되기에는 한계가 있다.

생화학적 특성이 강한 헤파린은 다양한 분자수식 기술을 통해 항암제로 개발될 수 있다. 세포외 기질 구성물질 중 헤파란황산의 구조와 유사한 헤파린은 종양의 성장에 관련된 성장인자들과 결합할 수 있는 능력이 있어 그 항암효과를 주목받아 왔다. 하지만 강력한 항혈전효과를 가지고 있는 헤파린은 그 자체로 항암제로 사용될 수 없다. 이를 해결하기 위해 헤파린과 유사한 성질을 보이는 슈라민의 일부를 헤파린에 결합시킬 경우, 항암효과를 유지하면서 항혈전효과를 없앨 수 있다. 이러한 분자수식한 물질은 헤파린의 항암 특성이 강화되어서 항암제로써의 가치를 높이게 한다. 종양치료와 관련된 혈관표피성장인자에 대한 헤파린의 강화된 성질은 동물실험과 표면 플라스몬 공명 기술을 이용하여 증명되었다.

헤파린의 항암효과를 극대화시키기 위한 기술은 단순한 분자결합 기술 외에도 크기 조절을 통해서 이루어질 수 있다. 기존에 디옥시콜릭산과 같은 담즙산을 헤파린에 결합시킬 경우, 헤파린의 항혈전성을 제거하고 경구흡수의 능력을 향상시킬 수 있음이 보고되었다. 하지만 헤파린 기본적으로 다양성을 가지는 거대분자이며, 저분자량 헤파린조차 분자량이 4000 달톤이 넘는 큰 물질이다. 이는 표적인 혈관표피성장인자의 헤파린 결합부위보다 지나치게 크기 때문에, 표적 부위에 최적화되지 못했다는 단점을 지니고 있으며, 이는 낮은 효능과 예기치 못한 부작용으로 이어질 수 있다. 하지만 크기를 조절한

초저분자량 헤파린 결합체는 같은 양을 투여하였을 때 최적화된 효과를 보여주었다. 이러한 항암효과는 세포 실험과 동물 실험에서 같은 양이 투여되더라도 많은 분자 수로 인해 나타날 수 있다. 이러한 최적화된 크기의 헤파린 유도체는 표적에 적합한 항암제로 개발될 수 있을 것이다.

앞서 실험에서 헤파린에 담즙산을 결합시키는 일차적 목적은 경구화를 위한 것으로, 이는 담즙산 중합체를 이용하여 새로운 경구용 헤파린을 개발할 수 있음을 보여준다. 헤파린 중에 특히 에녹사파린의 경우, 분자 끝부분에 환원당 구조를 가지고 있어서 말단 특이적인 당화반응의 가능성을 보여준다. 일반적인 환원당에서 일어나는 반응을 가열과 지속적인 반응을 통해서 에녹사파린의 분자 말단 부분에 일어나게 할 수 있으며, 이는 베네딕트 반응을 이용하여 증명되었다. 이를 이용하여 말단 특이적인 경구용 헤파린 유도체를 생산해 낼 수 있으며, 담즙산 올리고머(4)를 이용하면 헤파린의 경구화도 가능하다. 이렇게 결합된 에녹사파린과 담즙산 올리고머 결합체는 변함없는 항혈전성을 각종 동물실험에서 보여주었다. 또한 이 결합체는 담즙산 수용체를 통하여 세포 내로 흡수됨이 세포실험에서 증명되었다.

거대분자 결합체의 연구는 약물전달시스템에서 새로운 나노 복합체 개발과 연결될 수 있다. 강력한 양전하를 띄고 있는 펩타이드인 프로타민은 음전하를 가지면서 항암효과를 보이는 다른 헤파린 유도체들과 안정한 나노 복합체를 형성할 수 있다. 이러한 나노복합체는 폴리에틸렌글라이콜과 결합된 프로타민을 이용하여 좀 더 안전하고 생체적합한 물질이 될 수 있다. 폴리에틸렌글라이콜과 결합된 프로타민과 항암효과를 지닌 헤파린-슈라민 결합체를 이용하여 새로운 나노결합체를 만들었고 이는 개선된 항암효과와 종양특이성을 보였다. 이러한 폴리에틸렌글라이콜 프로타민 결합체를 이용한 나노결합체는 다양한 물질을 종양으로 전달하는데 이용될 수 있을 것이다.

약물전달시스템에서 담즙산을 이용한 경구전달 기술은 지속적으로 발전하여 나노결합체를 경구로 전달할 수 있는 수준에 이르렀다. 기존에 담즙산을 이용한 펩타이드 및 거대분자 전달 기술은 발전을 거듭하여 앞서 기술한 바와 같이 결합체를 만들어서 경구로 흡수시킬 수 있다. 크기가 다소 큰 나노결합체 또한 경구로 전달될 수 있을 것으로 판단되어 실험해본 결과 나노결합체 또한 소장세포에 결합될 수 있음을 관찰하였다. 경구용 나노결합체는 그 안전성과 실용성 등에서 약물 및 유전자 전달기술 등과 결합될 경우 무한한 가치를 지닌다. 헤파린과 담즙산 그리고 프로타민을 이용하여 안정한 경구용 나노결합체를 만들 수 있으며 이는 세포실험에서 세포내로 담즙산수용체를 통해서 흡수될 수 있음이 증명되었다. 동물에 투여되었을 때도 장내 세포에서 지속적으로 존재하고 있는 결과를 보였으며 이는 장세포로 전달 가능한 새로운 약물전달시스템이 개발될 수 있음을 시사한다.

구조수식을 통한 새로운 결합체의 합성과 새로운 나노 결합체의 개발은 신약개발과 약물전달시스템에 있어서 매우 중요하다. 이번 연구에서 헤파린은 여러 분자수식을 통해 개선된 항암효과를 보였고, 그 분자크기 또한

최적화되었으며, 또한 말단 특이적인 결합으로 경구전달이 가능하게 합성되었다. 담즙산 올리고머는 헤파린의 경구흡수를 가능하게 하였고 복합아크릴산 결합체는 담즙산 수용체 억제제로서의 새로운 가능성을 보여주었다. 최종적으로 헤파린과 프로타민을 이용한 나노결합체는 약물전달기술에서 새로운 전달체로서의 개선된 효과를 보여주었고, 담즙산이 결합된 나노결합체는 신개념의 경구용 나노입자가 개발될 수 있음을 시사한다.